universität wien

MASTERARBEIT / MASTER'S THESIS

Titel der Masterarbeit / Title of the Master's Thesis

„Type I IFNs promote fungal persistence by modulation iron and zinc homeostasis in macrophages "

verfasst von / submitted by

Philipp Penninger BSc

angestrebter akademischer Grad / in partial fulfilment of the requirements for the degree of

Master of Science (MSc)

Wien 2019 / Vienna 2019

Studienkennzahl lt. Studienblatt / degree programme code as it appears on the student record sheet:	UA 066 834
Studienrichtung lt. Studienblatt / degree programme as it appears on the student record sheet:	Masterstudium Molekulare Biologie 2002
Betreut von / Supervisor:	ao. Univ.-Prof. Dipl.-Ing. Dr. Karl Kuchler

Table of contents

1. Summary

The opportunistic fungal pathogen *Candida glabrata* is frequently found in the human digestive tract. While usually unobtrusive, the fungus can lead to severe disseminated candidiasis in immune compromised patients (cancer, HIV, organ transplantation). These life-threatening infections still exhibit high mortality rates due to slow detection methods and high inherent multidrug resistance. The rise of nosocomial acquired Candida spp. infections present a high burden for the health system and require a broadened understanding of fungal pathogenesis.

Type I IFNs promote heightened fungal organ loads during *C. glabrata* infections; however, the exact molecular mechanism remains still elusive. Therefore, we investigated the impact of type I IFNs on Fe and Zn homeostasis in macrophages, owing to their pivotal regulatory functions. These homeostatic processes are tightly regulated, due to their importance for both the host and the fungal pathogen.

In this study, we show that type I IFN signaling obstructs macrophages in this important process by dysregulating key transcription factors implicated in trace metal homeostasis. The BACH1-Nrf2 axis, responsible for iron homeostasis, is altered by IFN-α and IFN-ß in a JAK1-dependent manner. Subsequently, type I IFNs hamper the redistribution of iron within infected macrophages, by iron transporter dysregulation (FPN1), ultimately driving fungal iron acquisition.

Further, the zinc intoxication process of *C. glabrata* inside macrophages is limited by type I IFNs. They modulate pathogen-specific zinc transporter expression (ZnT1, ZIP4 and ZIP14) and zinc binding proteins methallothionenin 1 and 2. Thereby, type I IFNs suppress MT1/2-dependent zinc intoxication leading to lowered fungal killing rates by immune cells. Ultimately, this promotes higher survival rates and fungal loads of *C. glabrata* during macrophage infections.

Additionally, our study shows the importance of iron acquisition for fungal fitness during infections. Fungal iron acquisition systems (Sit1 and Ftr1) are linked to fungal survival during macrophage and *in vivo* infections. Surprisingly, our data also supports the notion of a compensatory iron acquisition mechanism for *C. glabrata* Sit1, independent of exogenous fungal siderophore-uptake, and iron-acquisition independent functions during macrophage infections.

In conclusion, this study highlights the crucial role trace metals play during the infection course of *C. glabrata* and that type I IFNs promote fungal persistence, thereby displaying yet another deleterious effect on the host.

2. Zusammenfassung

Das opportunistische Pilzpathogen *Candida glabrata* kolonisiert häufig den Verdauungstrakt des Menschen und verursacht in immundefizienten Individuen (Krebserkrankung, HIV, Infektionen, Organtransplantate) lebensgefährliche systemische Infektionen. Diese sind, wegen langsamer Detektionsmöglichkeiten und der inherenten Resistenz des Pilzes gegen viele antimykotische Medikamente, mit einer hohen Todesrate von bis zu 40% verbunden. Viele Infektionen erfolgen während langer Krankenhausaufenthalte, deshalb ist es wichtig, mehr über diesen Krankheitserreger in Erfahrung zu bringen.

Typ I IFN beeinflussen die Bekämpfung von *C. glabrata* negativ, wobei der dafür verantwortliche molekulare Mechanismus nicht identifiziert werden konnte. Daher beschäftigt sich diese Arbeit mit den Auswirkungen von Type I IFN auf die Eisen- und Zinkhomeostase in Makrophagen. Diese Immunzellen, wichtig bei der Bekämpfung von Pilzinfektionen, regulieren die Homeostase von Spurenelementen, die sowohl vom Wirt als auch vom Pathogen gebraucht werden.

In dieser Studie konnten wir zeigen, dass Typ I IFN Makrophagen durch die Dysregulation der wichtigsten Transkriptionsfaktoren dabei hindern, diese Mechanismen auszuführen. Die BACH1-Nrf2 Axe, verantwortlich für Eisenhomeostase, wird durch IFN-α und IFN-ß über JAK1 beeinflusst. Folglich verhindern Typ I IFN die Relokalisation von Eisen in infizierten Makrophagen, durch Dysregulation von Transportern (FPN1), und ermöglichen so erhöhte Eisenaufnahme durch den Pilz.

Des Weiteren limitieren Typ I IFN den Zinkintoxikationsprozess, durch die Modulation von pathogen-spezifisch aktivierten Zinktransportern (ZnT1, ZIP4 und ZIP14) und den Zink-bindenden Proteinen Methallothionein 1 und 2. Dieser geschwächte Verteidigungsmechanismus von Makrophagen gegen *C. glabrata* ist ausschlaggebend für eine verringerte Elimination der Pilzzellen während Infektionen.

Zusätzlich zeigen wir die Wichtigkeit von Eisenaufnahmesystemen von *C. glabrata* (Sit1 und Ftr1) für die Fitness des Pilzes während Makrophagen- und *in vivo*-Infektionen. Überraschenderweise ist Sit1, während der Absenz von Ftr1, in die Xenosiderophore-unabhängige Acquirierung von Eisen involviert und hat Eisenaufnahme-unabhängige Eigenschaften während Infektionen von Makrophagen.

Zusammengefasst zeigt diese Arbeit die bedeutende Rolle von Eisen und Zink während *C. glabrata* Infektionen und die erhöhte Überlebensrate des Pilzes durch Dysregulierung dieser Spurenelemente durch Typ I IFN.

3. Introduction

3.1 Fungal infections

The impact of human fungal infections is often underappreciated, despite more than one billion superficial infections worldwide (Havlickova, Czaika and Friedrich, 2008; Bongomin *et al.*, 2017). Mild infections, like in the oral or vulvogenital tract, are very common and display a high burden for affected individuals (Bradford and Ravel, 2017). However, in immunocompromised patients (e.g. due to HIV, cancer, organ transplantation, old age and prolonged hospital stays), fungal infections can lead to life-threatening systemic invasions.

Although only a small fraction of the fungal kingdom is associated with invasive fungal infections, they claim approximately 1.5 million deaths per year worldwide (Brown *et al.*, 2012). The most common genera, which cause these infections, are Candida, Aspergillus, Cryptococcus and Pneumocystis. Thereby, a distinction is made between environmental fungi like Aspergillus or Cryptococcus, and human commensals like Candida spp., which reside on mucosal surfaces and the gastrointestinal tract (Malavia, Crawford and Wilson, 2017). These diverse traits determine microbial onset and route of entry.

For example, the environmental fungus Aspergillus enters the human body mostly by inhalation of spores, causing lung infections in COPD patients and susceptible individuals (Hope, Walsh and Denning, 2005). In contrast, Candida is transmitted by human-to-human contact, the earliest being mother-to-child (Hallen-Adams and Suhr, 2017). This route of transmission and the ability to form biofilms on medical equipment, like catheters, makes Candida spp. responsible for high numbers of nosocomial (hospital-acquired) blood stream infections (Wisplinghoff *et al.*, 2004; Kernien *et al.*, 2017). Strikingly, invasive fungal infections display high mortality rates of more than 50% in certain infected populations (Brown *et al.*, 2012).

3.2 *Candida glabrata* as a pathogen

Candida glabrata is a haploid fungus, which only exists in the unicellular yeast form. It has been renamed several times and, despite its role as potent human fungal pathogen, is evolutionary more related to *Saccharomyces cerevisiae* than to *Candida albicans* (Miceli, Díaz and Lee, 2011; Gerwien *et al.*, 2017; Kumar *et al.*, 2019).

The rise of immunocompromised patients in the late 1990s brought the previously almost non-pathogenic yeast into focus (Fidel, Vazquez and Sobel, 1999). However, infection studies are difficult due to the lack of proper animal models. The fungus is not a murine commensal and stable colonisation is difficult, since it is not a primary pathogen for mice. Additionally, systemic invasive infections display low virulence and inflammatory potential, leading to a long-lasting persistence within the murine host (Fidel *et al.*, 1996; Jacobsen *et al.*, 2010).

C. glabrata, which is categorized under "non-*albicans*" Candida spp. during infections, however, displays a more significant role than that. It is inherently low susceptible to azoles, a major class of antifungal drugs (Sanguinetti *et al.*, 2005; Pfaller *et al.*, 2010). Additionally, it displays a lowered susceptibility to cationic peptides with antimicrobial activities (Helmerhorst *et al.*, 2005). Reliance on slow, culture-based and biochemical assays for diagnosis and a lack of fast detection methods with high specificity and sensitivity are other major reasons for poor infection outcomes. Assays relying on the detection of fungal antigens, like the cell wall component (1,3)-ß-D-glucan, still have problems with sensitivity and interpretation difficulties, due to *C. glabrata´*s human commensal state (Ostrosky-Zeichner *et al.*, 2005; Miceli, Díaz and Lee, 2011; Silva *et al.*, 2012). In conclusion, despite recent advances, clinical detection and treatment of *C. glabrata* remains challenging, making it a potent clinical pathogen.

3.2.1 Interaction between host immune system and *C. glabrata*

Candida glabrata has developed unique virulence traits allowing it to replicate intracellularly. Macrophages, immune cells that phagocytose and kill invading pathogens, are used by the fungus as Trojan horse to establish a long-lasting infection (Kasper, Seider and Hube, 2015; Carreté *et al.*, 2018; Kumar *et al.*, 2019). Usually, these phagocytic cells, which are present in almost all tissues, engulf invaders and eradicate them by acidification and secretion of reactive oxygen species (ROS) and nitrogen species (NO) into dedicated compartments, called phagosomes (Vieira, Botelho and Grinstein, 2002; Haas, 2007; Pollard, 2009; Plüddemann *et al.*, 2011). In contrast, *C. glabrata* subverts the maturation and subsequent acidification of phagosomes, suppresses ROS production and is highly resistant to oxidative and metabolic stress (Cuéllar-Cruz *et al.*, 2014; Kasper *et al.*, 2014). Further, it is able to dampen the release of pro-inflammatory cytokines (Seider *et al.*, 2011). While lacking an active process to exit phagosomes, macrophages eventually lyse under high fungal loads, possibly leading to dissemination within organs (Dementhon, El-Kirat-Chatel and Noël, 2012).

In summary, *C. glabrata* establishes a biological niche for replication within macrophages, undetected from further immune cell clearing, thereby persisting and disseminating in a low-level inflammatory infection.

3.3 Innate immune surveillance

Throughout life, mammals encounter countless microbes, colonizing our skin, intestinal tract, oral and vulvovaginal cavities, which influence us more than we previously thought (Schroeder and Bäckhed, 2016; Gilbert *et al.*, 2018). To keep pathogenic microbes in check, multicellular life has developed a sophisticated defence machinery, the immune system. The mammalian immune system consists of the innate and the adaptive immune response. The first one provides an unspecific and broad protection against all invaders. The latter one, is highly specific and responsible for memory formation of previously encountered pathogens (Chaplin, 2010). For effective host protection against fungal pathogens, both are needed (Netea *et al.*, 2015). However, this work focuses only on the innate immune response and will therefore only introduce such.

3.3.1 Innate immune response during fungal infections

The first layer of defence against fungal pathogens is the limitation of entry sites. Thereby, the skin exhibits important tissue barrier functions. Fungi entering the lungs, the gastrointestinal tract or other vulnerable sites encounter dedicated phagocytes and innate immune cells (Lionakis, Iliev and Hohl, 2017), like dendritic cells (DCs), monocytes, macrophages (Mϕ), neutrophils, natural killer (NK) cells and possibly ILCs, which protect the tissue from fungal infections (Netea *et al.*, 2015). Innate immune cells recognize body-foreign structures via pattern recognition receptors (PRRs), present on the cell surface, within phagosomes and the cytoplasm. Non-self-structures are termed pathogen-associated molecular patterns (PAMPs), which are conserved molecular structures throughout different species (Chaplin, 2010), for example, ß-glucans, part of most fungal cell walls, are recognized to elicit a fungal specific immune response (Lionakis, Iliev and Hohl, 2017). PRRs are a very diverse class of receptors with defined spatial expression patterns on innate immune cells (Figure 1). Thereby, certain receptors (like Dectin-2, TLR7 or TLR9) are more important in activating a fungal-specific response, as seen by lowered survival in *Clec4n*$^{-/-}$ and *Tlr7/9*$^{-/-}$ knock-out mice during *C. albicans* infections (Saijo *et al.*, 2010; Biondo *et al.*, 2012). Subsequently, PRRs activate

downstream signaling pathways, leading to the release of cytokines, effector functions and further immune cell recruitment (Bourgeois *et al.*, 2010; Netea *et al.*, 2015).

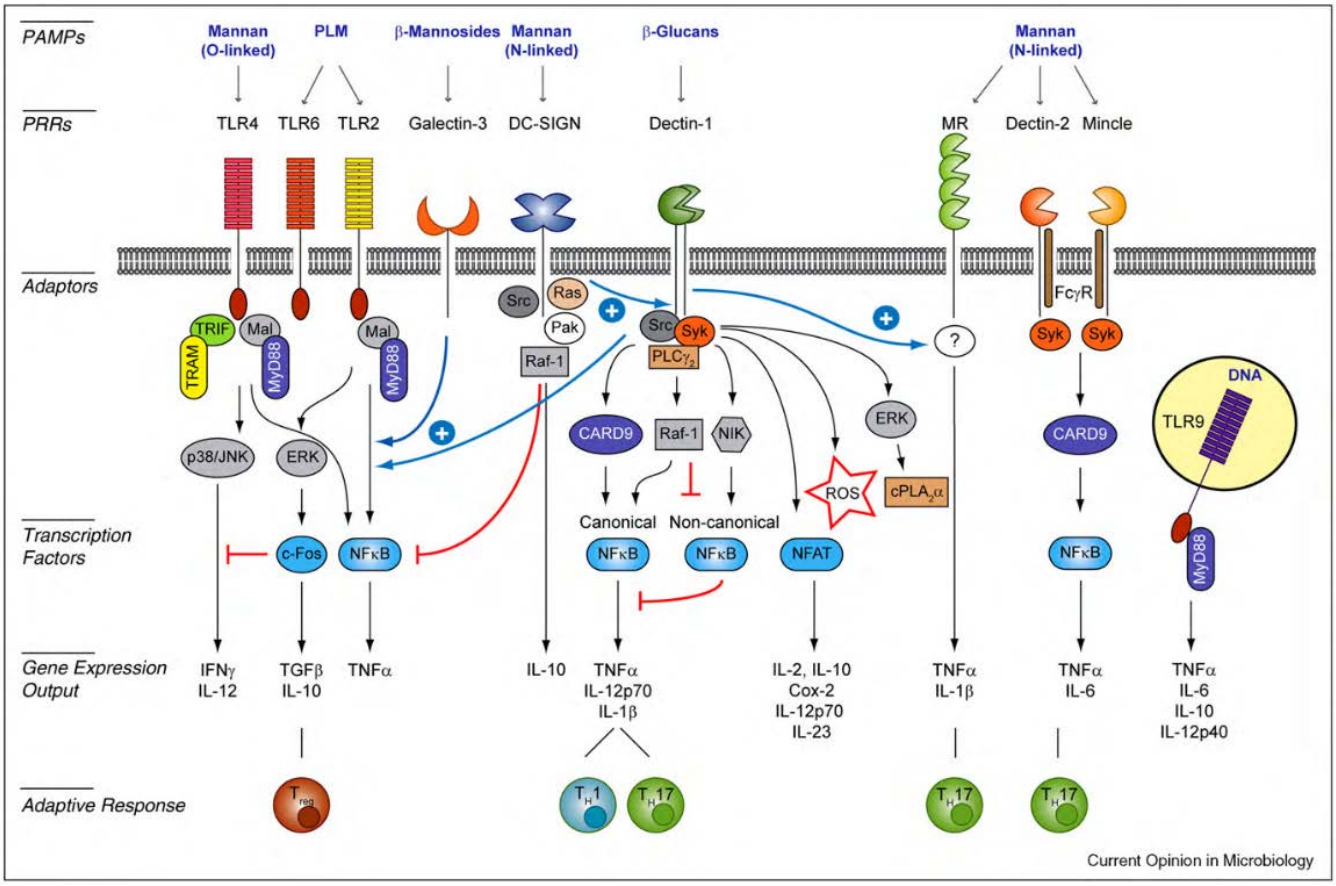

Figure 1. Detection of fungal PAMPs by PRRs and downstream effector activation (Bourgeois *et al.*, 2010).

In response to human *Candida* spp. infections, neutrophils are important to mediate resistance by exposing invaders to oxidative effectors like ROS and to neutrophil extracellular traps (NETs). NETs consist of antimicrobial peptides like ß-defensins, lysozyme, lactoferrin and calprotectin for pathogen killing (Aratani *et al.*, 2002; Urban *et al.*, 2009; Amulic *et al.*, 2012).

Tissue-resident macrophages combat fungal infections by phagocytosis, release of ROS and recruitment of additional immune cells (Erwig and Gow, 2016). Repeated exposure to *Candida* spp. leads to enhanced inflammatory cytokine production via epigenetic reprogramming of macrophages (Bistoni *et al.*, 1988; Netea, Quintin and van der Meer, 2011).

Further, DCs activate a Th_1 and Th_{17} type response, which is finally necessary to mount a proper antifungal immune response during *Candida* spp. infections (Netea *et al.*, 2015).

3.4 Type I interferons

Interferons were initially identified as peptides with the ability to protect cells in chorio-allantoic membranes from viral infections (Isaacs and Lindenmann, 1957). Until now, three types of the cytokine family, with antiviral, antiproliferative and antitumor activities have been identified (type I, type II and type III interferons). Whereas type II and III IFNs consist of only one member, IFN-γ and IFN-λ respectively, type I interferons (type I IFNs or IFNs-I) encompass several members, classified by sequence homology, peptide mapping and interaction with IFN receptor subunits (López de Padilla and Niewold, 2016). Thereby, IFNs-I bind to the heterodimeric transmembrane receptor IFNAR, which is composed of two subunits, IFNAR1 and IRNAR2 (Figure 2) (Uzé *et al.*, 2007).

PRR activation and subsequent interferon-regulatory factors (IRFs) signaling drives cells (mainly plasmacytoid DCs (pDCs)), to initial transcriptional activation of *IFNB* and *IFNA4*. Then, an autocrine positive feedback loop drives the release of several other IFN-α members (Honda, Takaoka and Taniguchi, 2006). Additionally, type I IFNs activate surrounding cells in a paracrine manner via the classical JAK-STAT signaling pathway (Figure 2). Consequently, hundreds of downstream target genes are modulated (Ivashkiv and Donlin, 2014).

The human genome encodes at least 13 IFN-α subtype genes and one gene for IFN-ß, IFN-κ, IFN-ω and IFN-ε belonging to type I IFNs. Because IFN-κ, IFN-ω and IFN-ε are exerting specialized roles in local tissues, these members were excluded from this study (Pestka, Krause and Walter, 2004).

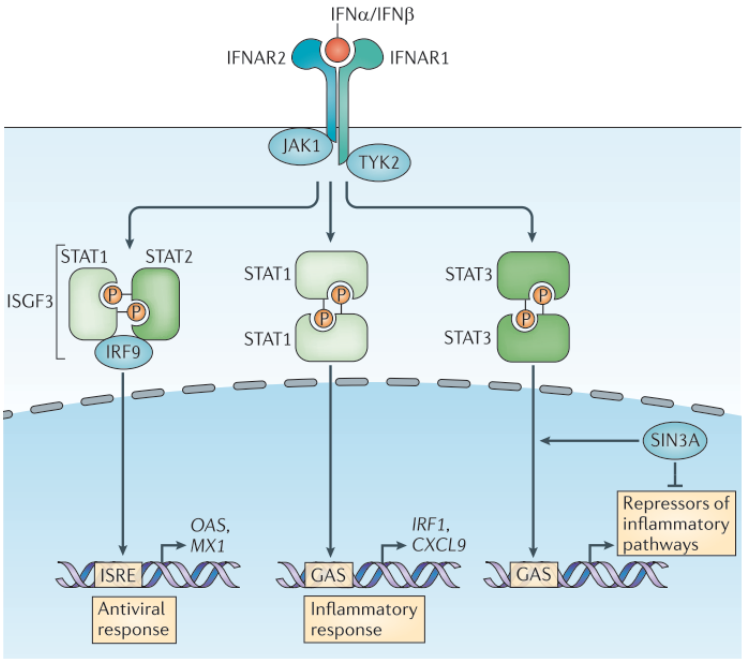

Figure 2. JAK-STAT signaling upon IFNAR activation (Ivashkiv and Donlin, 2014).

3.4.1 The role of type I IFNs during fungal infections

Surprisingly, IFNs display both positive and negative effects for the host after encountering bacterial and fungal pathogens (Decker, Müller and Stockinger, 2005; McNab *et al.*, 2015). Gain-of-function mutations in the IFNAR signaling cascade have been associated with disseminated fungal diseases suggesting a detrimental role during infections, possibly by modulating $CD4^+$ T helper cell populations (Liu *et al.*, 2011; Casanova, Holland and Notarangelo, 2012). After encountering Candida spp., conventional DCs are the main producers of IFNß, which depends on proper phagocytosis and recognition via TLR 7 and 9. Thereafter, IFN signaling drives a secondary IFN response in an autocrine manner (Biondo *et al.*, 2011; Bourgeois *et al.*, 2011). In mouse infection models with *Candida albicans* controversial results have been published describing beneficial roles by enhancing immune cell migration (Biondo *et al.*, 2011; del Fresno *et al.*, 2013), and detrimental effects of type I IFNs (Majer *et al.*, 2012). The latter publication could show that IFNs-I facilitate increased recruitment into infected kidneys and activation of inflammatory monocytes and neutrophils leading to immunopathology. Further, Bourgeois *et al.* (2011b) revealed the promotion of *C. glabrata* persistence in mouse organs by type I IFN signaling, depicting another deleterious effect.

3.4.2 Type I IFNs and trace metal homeostasis

During bacterial and fungal infections, iron and zinc homeostasis of the host is influenced by IFNs (Guevara-Ortiz *et al.*, 2005; Ganz and Nemeth, 2015; Read *et al.*, 2017). For example, IFNγ decreases iron levels of human monocytes and macrophage-like cells by upregulation of storage proteins and transporters in steady-state conditions (Byrd and Horwitz, 1993), as well as during infections with Salmonella (Nairz *et al.*, 2008). Further, IFNγ interferes with iron homeostasis via nitric oxide-mediated degradation of iron regulatory protein 2 (IRP2) (Kim and Ponka, 2000). Additionally, IFNγ intermingles with zinc homeostasis during infection with bacterial pathogens (Brechting *et al.*, 2019). Yet, not much is known about the regulation of trace metals during *C. glabrata* infections by type I IFNs.

3.5 Transition metals in immunity

Inorganic metals including iron and zinc are frequently positioned at the catalytic centre of enzymes responsible for transcription, respiration, biosynthetic and metabolic processes in pro- and eukaryotes (Finkelstein, 2009; Hood and Skaar, 2012). Thereby, their function varies strongly. Redox-inert metal ions, like zinc (Zn), are used to stabilize negative enzyme charges, whereas redox-active metal ions, like iron (Fe), can also be used as redox centres (Andreini *et al.*, 2008).

The heightened reactivity makes both ion groups toxic at high concentrations (Imlay, 2014). Therefore, cells associate ions with organic cofactors, to keep the concentration of transition metals in a range beneficial for biological processes and avoid toxic side effects (King, Shames and Woodhouse, 2000; Soares and Hamza, 2016; Gerwien *et al.*, 2018). Whereas, Fe is the predominant redox metal in biological systems taking over a variety of sites and cofactors, including haem groups, Zn is the second-most abundant metal ion in enzymes (Andreini *et al.*, 2008).

3.5.1 Nutritional immunity

The term “nutritional immunity” was first coined in 1975 and described the withholding of iron from microbial invaders (Weinberg, 1975). Today, the term is used for withholding or redirecting essential transition metals among others, from pathogens by the host immune system (Hood and Skaar, 2012; Crawford and Wilson, 2015).

Patients with dysregulated trace metal homeostasis, like chronic anaemias, manifesting in excess iron serum levels, are associated with elevated pathogen susceptibility (Wang *et al.*, 2003). Additionally, the importance of nutritional immunity can be exemplified by the need of trace metals for the pathogen during infections. Immune cells produce ROS, an antimicrobial effector, which induces apoptosis in the invader due to oxidation of DNA, proteins and lipids (Yang, Zhu and Xi, 2018). To detoxify ROS bacterial and fungal superoxide dismutases and catalases, Zn- and Fe-dependent enzymes respectively, are needed. By sequestering these essential metals during ROS generation, the host restricts the pathogenic detoxification mechanisms to boost the clearance of pathogens and help the host resolve infections (Crawford and Wilson, 2015). The following section emphasises on macrophages and their mechanisms to enforce nutritional immunity during infections in respect to iron and zinc.

3.5.2 Iron homeostasis in the host

Iron is a potent redox-sensitive metal required for electron transfer reactions and indispensable for almost all living organisms (Frey and Reed, 2012). Thereby, iron is a component of iron-sulfur cluster containing proteins (electron transport complexes), heme-containing proteins (haemoglobin) or iron-containing enzymes with nucleic acid-binding functions (e.g. polymerases, helicases, and nucleases) (Gunsalus *et al.*, 1977; White and Dillingham, 2012; Roche *et al.*, 2013). In mammalian cells, iron is most common in the ferrous (Fe^{2+}) or the insoluble ferric (Fe^{3+}) form (Pantopoulos *et al.*, 2012). Ferrous iron can form superoxide radicals upon O_2 reduction, which damages DNA, proteins and lipids (Lane *et al.*, 2015; Silva and Faustino, 2015).

Macrophages exert a special role in iron homeostasis, since specialized erythrophagocytic macrophages recycle senescent erythrocytes (Soares and Hamza, 2016). After uptake by erythrophagocytosis, blood cells are catabolized to release the prosthetic iron-containing heme group and transported into the cytoplasm via heme-responsive gene 1 (HRG1), divalent metal transporter 1 (DMT1) or natural resistance associated macrophage protein 1 (NRAMP1) (Soe-Lin *et al.*, 2009). Inside the cell iron enters the labile iron pool (LIP), containing ferrous iron in the low micromolar range (0.3-1.6 µM) (Anderson *et al.*, 2012; Philpott and Ryu, 2014). Macrophages can store iron bound to ferritin, which binds up to 4500 Fe^{3+} ions (Liu and Theil, 2005; Almeida, Wilson and Hube, 2009), or export Fe via ferroportin 1 (FPN1), which is particularly highly expressed in splenic and hepatic macrophages (Pollard, 2009). Cellular iron transport in mammalian cells is tightly regulated to avoid toxic effects and minimize pathogenic exploitation (Shi *et al.*, 2008; Leidgens *et al.*, 2013).

3.5.3 Iron homeostasis during infections

In general, elevated iron levels tend to increase the pathogenicity of microbes, which is counteracted by host Fe sequestration strategies. For example, exogenous iron leads to higher fungal burden in Aspergillus infections (Leal *et al.*, 2013; Malavia, Crawford and Wilson, 2017). However, the host differentiates between intracellular and extracellular replicating microbes (Soares and Weiss, 2015). Extracellular pathogens trigger iron retention within macrophages by downregulation of the iron exporter FPN1, via hepcidin-mediated endocytosis (Nemeth, Tuttle, *et al.*, 2004). As a result, during acute phase infections, the type I IFN upregulated liver hormone hepcidin, leads to hypoferraemia, stirs macrophage polarization and alters the ability to release NO and cytokines (Mencacci *et al.*,

1997; Nicolas *et al.*, 2002; Nemeth, Rivera, *et al.*, 2004; Wrighting and Andrews, 2006; Recalcati *et al.*, 2010; Ichiki *et al.*, 2014).

By contrast, upon intracellular infections, pathogens decrease the iron content of macrophages by upregulation of FPN1 and minimizing uptake by transferrin receptor 1 (TfR1) and Dmt1. At the same time depleting the phagocytosed intruder via iron exporters NRAMP1 and FPN1 (Figure 3) (Canonne-Hergaux *et al.*, 1999; Nairz *et al.*, 2009, 2014; Ganz and Nemeth, 2015; Soares and Weiss, 2015; Soares and Hamza, 2016). NRAMP1, which is induced by type II IFNs or lipopolysaccharide (LPS) during infections, is located in the late endosome, lysosome and phagosome membranes and depletes invaders of iron. Humans with an inherent mutation in NRAMP1 suffer from recurring microbial infections (Fortier *et al.*, 2005).

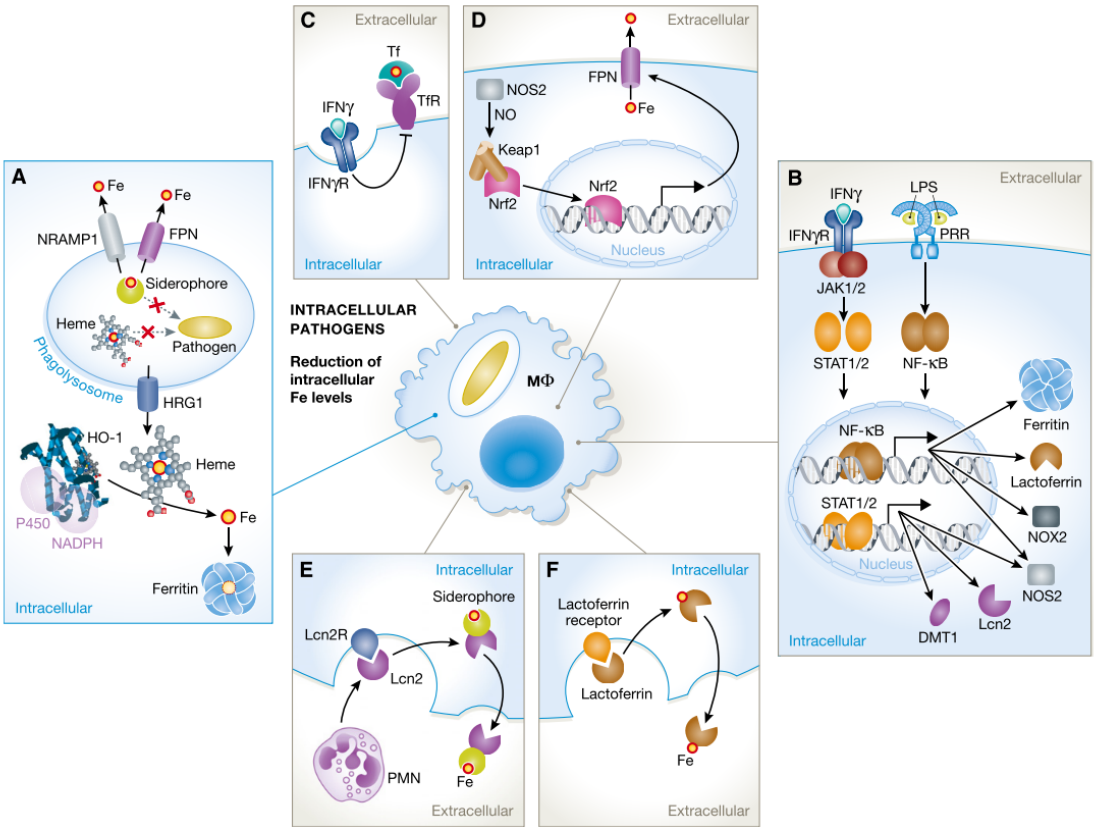

Figure 3. Regulation of iron homeostasis in MPH during infection with intracellular pathogens.

Macrophages manipulate intracellular iron levels after encountering an intracellular pathogen (A-F)(Soares and Weiss, 2015).

The modulation of the intracellular iron pools in macrophages in turn also regulates antimicrobial effector functions and inflammatory signaling (Fritsche *et al.*, 2003). For example, FPN1 is activated in macrophages by NO species, which are influenced by the intracellular Fe content (Van Zandt *et al.*, 2008; Botella *et al.*, 2011; Nairz *et al.*, 2013). Additionally, iron depletion in macrophages triggers pro-inflammatory effects by stabilising HIF-1α and promoting the transcription and synthesis of the pro-inflammatory cytokine IL-1ß. In turn, iron accumulation represses IFN-γ signaling and induction of TNF, IL-6 or IL-12 expression (Philpott and Ryu, 2014; Ganz and Nemeth, 2015). In summary, iron is needed by both the host and the pathogen and it exerts a multitude of functions, which require tight regulation during infections.

3.5.4 Iron uptake in *Candida glabrata*

Evolutionary, microbial invaders have adapted to acquire iron despite the harsh host environmental conditions. In systemic *Candida glabrata* infections, a substantial part of the fungal pathogens are eliminated by the host immune system, whereas a small fraction can establish environmental niches within myeloid cells (Duggan *et al.*, 2015; Praußе *et al.*, 2018).

Surprisingly, *C. glabrata*, in comparison to its *genus* relative *C. albicans*, cannot take up iron bound by haeme/haemoglobine or transferrin (Gerwien *et al.*, 2017). The fungus utilizes host iron sources via the high-affinity (HA) reductive iron acquisition system (Ftr1), for unbound Fe^{3+}/Fe^{2+} and ferritin-bound iron (Srivastava, Suneetha and Kaur, 2014) and the siderophore-mediated uptake of Fe^{3+} by Sit1 (Figure 4) (Kornitzer, 2009). Interestingly, *C. glabrata* has never been shown to produce its own siderophores, instead utilizing only fungal xenosiderophores. Of note, a survival defect of *C. glabrata* without the siderophore transporter Sit1 during macrophage infections could only be shown with siderophore-primed cells (Nevitt and Thiele, 2011). The purpose may lay in the ability to scavenge siderophore-derived iron in their natural environmental niche, the gastrointestinal tract. Fe uptake primes fungal cells with iron, which is stored and utilized during subsequent infections (Crawford and Wilson, 2015). The fungus also has a low affinity (LA) iron uptake system consisting of the divalent metal transporter Fet4, which plays only a minor role (Gerwien *et al.*, 2016). During iron deplete conditions, as are present in phagocytes, an upregulation of the iron permease Ftr1, part of the HA iron acquiring systems, can be observed (Sharma, Purushotham and Kaur, 2016).

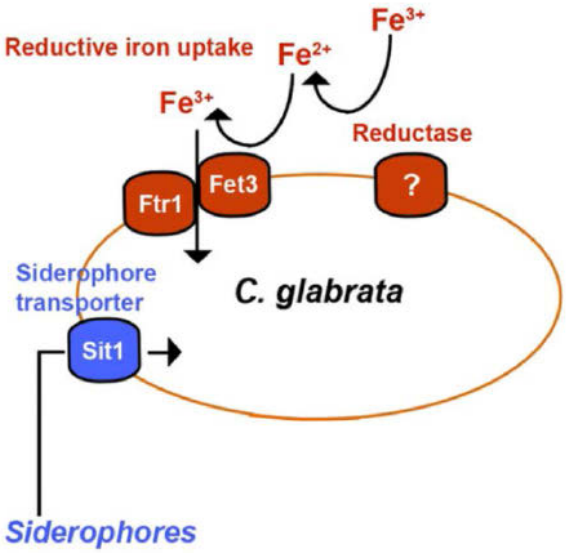

Figure 4. Iron uptake mechanisms by *C. glabrata* (adapted from Bairwa, Hee Jung and Kronstad, 2017).

Ftr1/Fet3 are part of the HA iron uptake system, Sit1 imports Fe bound to siderophores.

3.5.5 Zinc homeostasis in the host

The second most abundant trace metal in mammalian cells is zinc (Zn^{2+}). Divalent Zn^{2+} transduces redox signals and takes part in mitochondrial functions, gene expression and metabolic energy generation (Maret, 2006). More than 300 zinc-dependent enzymes have been identified so far in humans and around 10 % of the human genes encode zinc-binding proteins (Claudia Andreini *et al.*, 2005; Claudia Andreini *et al.*, 2006). Most of the zinc is bound to metalloenzymes, while the labile fraction comprises of concentrations between 10^{-9}-10^{-12} M, over which tight control is necessary, since increased or decreased levels trigger oxidative stress for cells (Maret, 2006).

Transport of zinc in eukaryotic cells requires two families of transporters, ZIPs and ZnTs. The ZIP (Zrt-, Irt- like Protein), also Solute carrier 39 (SLC39) metal transport family transports Zn^{2+} into the cytoplasm from the extracellular space and the lumen of organelles (mitochondria, endoplasmatic reticulum or endosomes) to increase the intracellular zinc levels. Conversely, the family of ZnT (zinc transporter), also SLC30, transports zinc into the opposite direction (Eide, 2006; Lichten and Cousins, 2009). The numerous ubiquitously and tissue-specifically expressed zinc transports and zinc binding proteins like metallothioneins (MTs) are regulated by transcription factor metal response element-binding TF1 (MTF1) and nuclear factor erythroid 2-related factor 2 (Nrf2/NFE2L2). Together, they provide mammalian cells with the ability to manipulate the available zinc pool in specific subcellular compartments (Eide, 2006).

Additionally, zinc also affects innate and adaptive immune cell functions including differentiation, activation and phagocytic activity in macrophages (Gao *et al.*, 2018). Zn^{2+} also alters maturation and expression of MHC II in DCs (Kitamura *et al.*, 2006) and surprisingly, exhibits characteristics of a second messenger molecule in mast cells after activation by the Fcε receptor I (Yamasaki *et al.*, 2007). Thus, a tight zinc regulation is required for proper activation and function of the immune system (Rink and Haase, 2007).

3.5.6 Zinc homeostasis during infections

Contrary to iron, macrophages can either deplete Zn^{2+} from the pathogen by shuttling it outside of the phagosome or redirect high amounts towards the invaders as part of a Zn intoxication process (Figure 5) (Subramanian Vignesh and Deepe, 2016). For example, during *Mycobacterium tuberculosis* infections, macrophages increase the zinc levels in late phagolysosomes, which contain the bacterial pathogen (Botella *et al.*, 2011). Prior activation of the immune cells with pro-inflammatory cytokines (TNF-α or IFN-γ) could elevate zinc levels even further (Wagner *et al.*, 2005). While initially independent of exogenous Zn^{2+} uptake, prolonged Zn requirement leads to upregulation of zinc importers as in *Mycobacterium bovis*-infected monocytes (Begum *et al.*, 2002; Subramanian Vignesh and Deepe, 2016).

Contrary, the fungal pathogen *Histoplasma capsulatum* leads macrophages to sequester zinc via the upregulation of MT1/2 and Zn relocalization into different subcellular compartments (Subramanian Vignesh *et al.*, 2013). The sequestration and reintroduction of zinc was directly associated with intracellular growth of pathogens showing its importance during infections (Winters *et al.*, 2010). Although both processes are well investigated, the zinc transporters and their exact interplay with MTs remains unclear, as well as when macrophages choose to sequester or intoxicate microbes.

Figure 5. Zn defenses of macrophages encountering intracellular microbes (Subramanian Vignesh and Deepe, 2016).

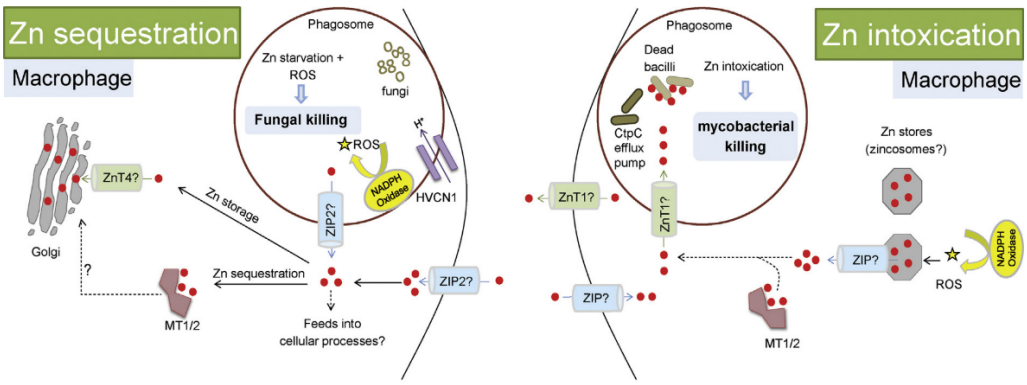

Hypothesis and Aims

During systemic mouse infections with *C. glabrata*, type I IFNs exert deleterious effects on the host with heightened fungal organ loads (Bourgeois *et al.*, 2011). Although the pleiotropic functions of IFNs-I are broadly established, little is known about the exact molecular mechanism which promotes detrimental effect for the host and their influence on nutritional immunity.

Additionally, mechanisms of the nutritional immune response during *C. glabrata* infections have been described merely, despite the clinical importance. Further, fungal adaption for host metal acquisition in host tissue environments and its link to *C. glabrata´*s virulence is still ill defined and needs further investigation. We speculated that type I IFNs can alter the outcome of fungal infection through the modulation of trace metal homeostasis. To investigate our hypothesis, we divided it into smaller sub-questions, which we tried to answer in this study.

The main questions in this study were:

- Which nutritional counter measurements are employed by macrophages during *C. glabrata* infections?
- Do type I IFNs modulate iron or zinc homeostasis during fungal infections?
- Which molecular players of the IFNAR signaling pathway are involved in the regulation of trace metal homeostasis and which molecular mechanisms are altered?
- Are iron acquisition systems part of *C. glabrata´*s virulence mechanisms during infections?

4. Results

4.1 Type I IFNs modulate Fe homeostasis in primary macrophages

Type I IFNs are a diverse class of cytokines with IFN-α and IFN-ß as best described members. Generally, results from one of the two cytokines are displayed as representative. Iron exists in several oxidative states whereby Fe^{2+} and Fe^{3+} are the most common in biological systems. If not stated otherwise, the term iron (Fe) refers to all states that are relevant during detection.

4.1.1 IFN-I signaling promotes survival of *C. glabrata* in BMDMs

Previous data of our group established a detrimental role of type I IFNs in *C. albicans* and *C. glabrata* infections (Bourgeois *et al.*, 2011; Majer *et al.*, 2012). Therefore, we investigated the influence of IFNs-I during *C. glabrata* infections of macrophages. After pre-treatment with IFN-ß, bone marrow-derived macrophages (BMDMs) showed impaired killing efficiency of fungal cells, yielding elevated fungal loads (Figure 6a). *Ifnar1*$^{-/-}$ BMDMs, deficient of type I IFN signaling by knock-out of the IFNAR 1 receptor chain, displayed enhanced abilities to clear fungal cells. In accordance, *Candida* isolated from IFNs-I primed macrophages had a significantly reduced ratio of killed cells compared to fungal cells isolated from untreated immune cells (Figure 6b). Indeed, pro-inflammatory activation of macrophages with type I IFNs prior to *C. glabrata* infections enhances the pathogens survival.

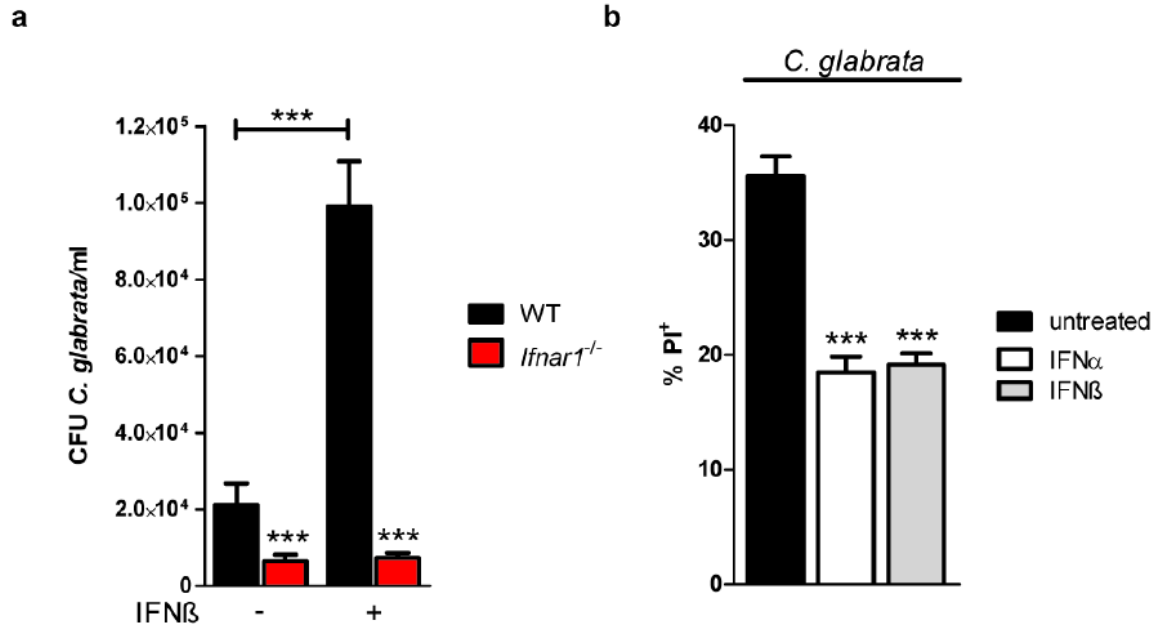

Figure 6. Type I IFNs response promotes fungal survival in BMDMs.
(a) *In vitro* survival of wild-type *C. glabrata* after infection of wild-type (WT) or *Ifnar1*$^{-/-}$ deficient BMDM for 24h. Viable cells were counted by plating on solid YPD. Data is representative for 3 independent experiments. Experiment and analysis was performed by Michael Riedelberger.
(b) Fungal cells isolated 8 hours after infection of WT bone marrow-derived macrophages (BMDMs). Cells were stained with propidium iodide (PI), a marker for cell death and analyzed via flow cytometry. Before infection WT macrophages were untreated or pre-treated with IFNα or IFNß with 500 U/ml for 17h. Mean and SD are shown. * p-value < 0.05; ** p-value < 0.01; *** p-value < 0.001.

4.1.2 Type I IFNs affect intracellular iron levels

Around 20% of the human iron content is distributed between hepatocytes and macrophages, making them key players in iron turnover (Lane *et al.*, 2015). Especially during *C. glabrata* infections, in which the pathogen resides primarily in macrophages, a tight regulation is important (Gilbert, Wheeler and May, 2015). Preliminary data obtained before suggested a dysregulation of trace metal homeostasis by type I IFN signaling. Therefore, we investigated the role IFN-I have on the iron homeostasis during *C. glabrata* infections of macrophages.

A small, ferritin-unbound Fe fraction, the labile iron pool (LIP), is maintained within cells, in order to be manipulated swiftly to cover quick demands. Therefore, the LIP displays a high significance in physiological and pathophysiological processes (Cabantchik, 2014). Calcein-AM is a fluorescence dye specific for Fe, which measures the LIP in a non-disruptive manner. In short, iron is chelated by the dye and quenches its fluorescence (Figure 7a). Addition of Fe via a FeCl2/8-hydroxyquinoline (FeHQ) complex further quenches the signal. The difference of initial quenching and after iron addition, results in the quenchable iron pool (QIP) (Figure 7b) (Singh, Ahmad and Rao, 1994; Espósito et al., 2002; Petrat et al., 2002). Because Fe-starved cells can take up higher amounts of Fe via FeHQ, cells with high cellular iron pools cause a low QIP. Thereby, the QIP scale is non-linear and lysosomal and endosomal LIP is not measured by Calcein-AM (Tenopoulou et al., 2007).

We observed that IFNAR1-dependent activation of macrophages lowered the cytoplasmatic iron pool both in uninfected and *C. glabrata*-infection conditions (Figure 7d). *C. glabrata* infected WT and *Ifnar1*$^{-/-}$ macrophages displayed a rise in the cytoplasmatic iron pools. The rise of Fe seems counterintuitive for the immune cell when encountering intracellular pathogens however, the fungus resides within immature phagosomes (Gilbert, Wheeler and May, 2015). Riedelberger et al. (unpublished data) could show a lower Fe amount in *C. glabrata*- containing phagosomal compartments during infection, which is counteracted by type I IFN signaling.

Further, a rise in the intracellular Fe pool was observed both in mCherry^{+} and mCherry^{-} WT and knock-out macrophages. Thereby, mCherry^{-} macrophages either didn´t phagocytose *C. glabrata* or already cleared ingested fungal cells, hence degraded the mCherry fluorophore. Although we didn´t distinguish for either possibility, macrophages are able to release small amounts of hepcidin, triggering iron retention, suggesting the possibility of extrinsic cellular signaling (Sow et al., 2007).

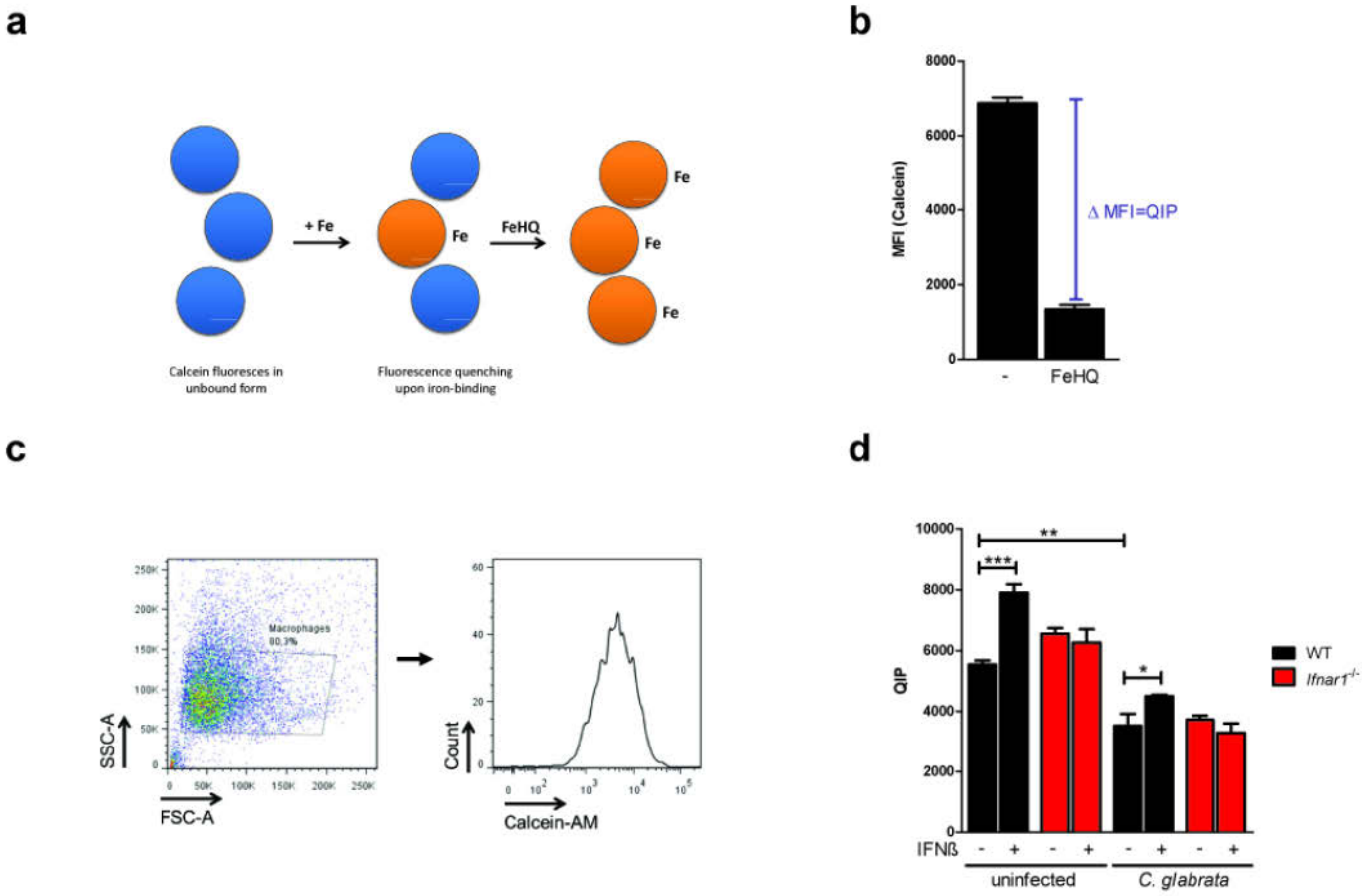

Figure 7. Intracellular iron amounts are altered by type I IFNs.
(a) Schematic depiction of Calcein-AM fluorescence quenching by iron and the addition of iron-hydroquinone (FeHQ).
(b) The QIP is calculated by different fluorescence intensity (MFI) of Calcein-AM before and after FeHQ addition.
(c) Gating strategy by FACS for BMDMs. After selection by size (FSC-A/SSC-A), the mean fluorescence signal of Calcein-AM (FITC) was analyzed and the QIP was calculated as shown in a and b.
(d) Wild-type and *Ifnar1*$^{-/-}$ BMDMs were pre-treated with 500 U/ml IFNß for 17 hours before infection with mCherry expressing *C. glabrata* at MOI=2. After 8 hours, cells were harvested and analyzed according to point a-c. Note, the higher the QIP, the smaller the labile iron pool.
Mean and SD are shown. * p-value < 0.05; ** p-value < 0.01; *** p-value < 0.001. Data represents at least 2 independent biological experiments.

4.1.3 *C. glabrata* can acquire more iron in IFNß-activated macrophages

The increase of the Fe levels within macrophages during infections with *C. glabrata* prompted us to determine the cytoplasmatic iron levels in fungal cells phagocytosed by immune cells. Previous results found, that the Fe-deprived niche for pathogens within phagocytes leads to decreased iron levels (Nairz *et al.*, 2014; Soares and Weiss, 2015; Soares and Hamza, 2016).

Indeed, *C. glabrata* isolated from macrophages after 6 hours infection displayed a decreased amount of cytoplasmatic iron compared to fungal cells in medium alone (Figure 8c). In comparison, fungal cells isolated from macrophages pre-treated with IFNß could acquire more Fe from the immune cell, which was even further elevated by pre-loading of macrophages with high amounts of exogenous iron.

The initial iron status of the immune cell seems to play a fundamental role for the ability to acquire iron during infection. As reported, high iron diet renders mouse models more susceptible to bacterial and fungal infections (Hor *et al.*, 2000). Here, despite lower cytoplasmatic iron levels after type I IFN activation of macrophages (4.1.2), a dysregulated host iron homeostasis promotes Fe acquisition of the fungal pathogen.

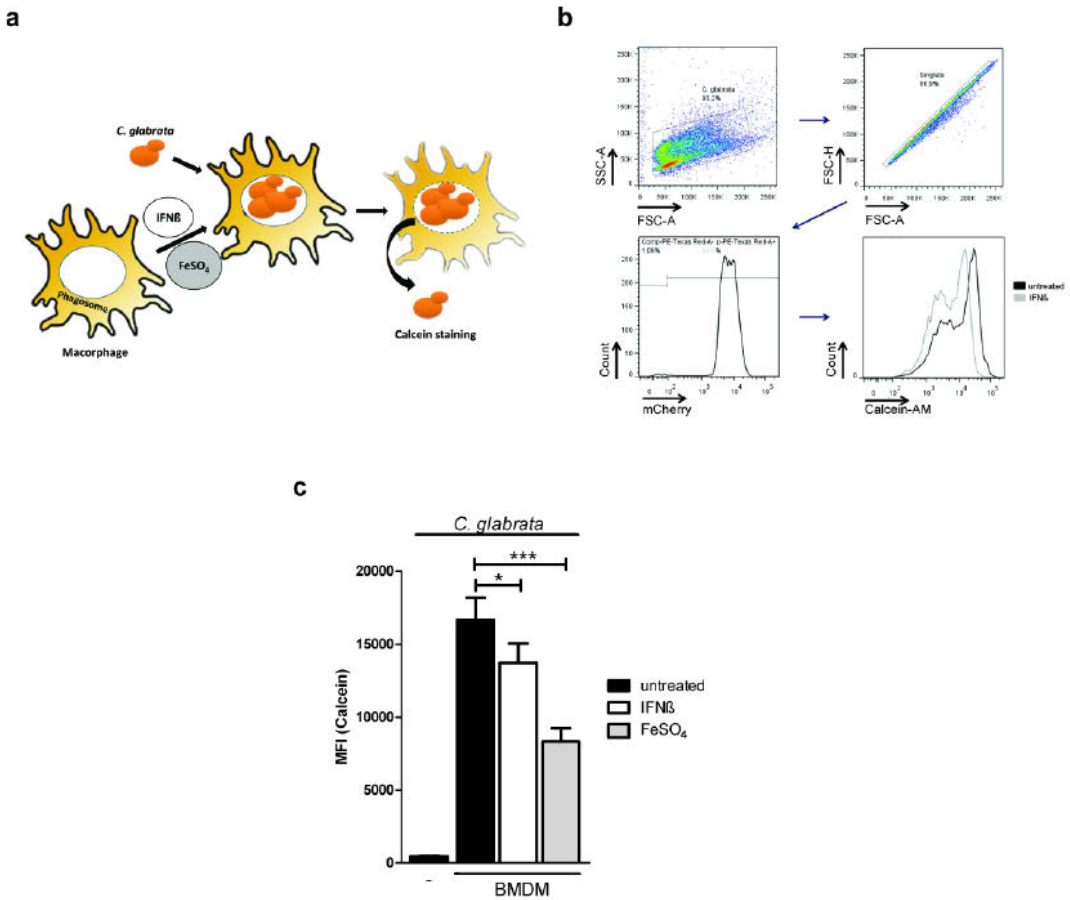

Figure 8. Type I IFN promote fungal iron acquisition within BMDMs.
(a) Schematic work flow. Macrophages were pretreated with 500 U/ml IFNß or 50 µM $FeSO_4$ for 17 hours before infection with mCherry labelled *C. glabrata* at MOI=2. After 6 h interaction, extracellular *C. glabrata* were washed away and phagocytosed cells were harvested by lysing macrophages.
(b) Flow cytometric gating strategy for *C. glabrata* isolated as in (a). Fungal cells were gated for their size (FSC-A/SSC-A), single cells were selected (FSC-A/FSC-H) and mCherry$^+$ *Candida* cells were analyzed for their MFI (Calcein-AM).
(c) *Candida* grown in YPD medium and isolated after 6 h from wild-type BMDM treated as in (a) were measured for their intracellular iron pool. Note, the higher the QIP, the lower the amount of intracellular iron.
Mean and SD are displayed. * p-value < 0.05; ** p-value < 0.01; *** p-value < 0.001. Data represents 2 independent experiments.

4.1.4 Key transcription factors of iron homeostasis are influenced by type I IFNs

The transcription factors BTB and CNC homology 1 (BACH1) and nuclear factor (erythroid-derived 2)-like-2 (Nrf2) are two competing factors for the regulation of oxidative stress responses and iron homeostasis. Nrf2 activates Fe homeostatic gene expression, which is counteracted by BACH1 (Zhang *et al.*, 2018). Further, this axis is also modulated by inflammatory stimuli during infections (Soares and Weiss, 2015).

Our data indicated a transcriptional and translational dysregulation of both transcription factors during pro-inflammatory activation of macrophages with type I IFNs. *Bach1* mRNA levels were significantly upregulated within the first 2 hours of IFNß treatment leading to slightly delayed elevated protein levels (Figure 9a and c). A return to basal levels is partially mediated by Nrf2 (Zhang *et al.*, 2018). The counter player *Nfe2l2* was significantly downregulated in BMDMs within the first hour of IFNß treatment. Return to basal levels could take up to more than 24 hours in activated macrophages indicating a long-lasting effect. The INTERFEROME database (Rusinova *et al.*, 2012) indicates several predicted binding sites in the upstream region of BACH1 for transcription factors activated by the type I IFN signaling pathway (Figure 9d), but would need further validation. No binding sites in the regulatory regions of *Nfe2l2* have been found in *Mus musculus*.

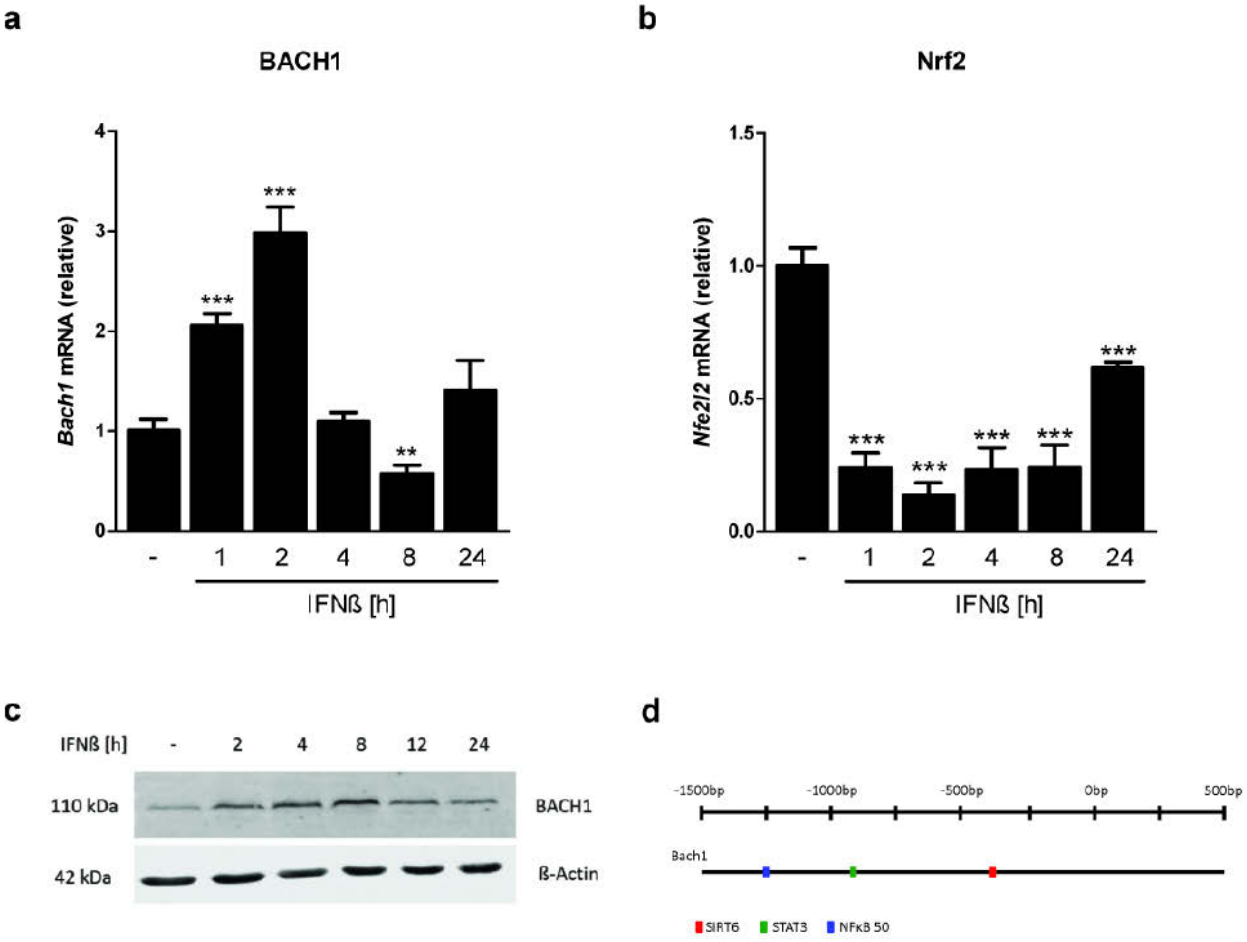

Figure 9. Key transcription factors in iron homeostasis are dysregulated by IFN-I.

(a,b) RT-qPCR analysis of BACH1 and Nrf2 in BMDMs treated with IFNß (500 U/ml) for indicated time points. Values are standardized to ß-Actin expression and normalized to untreated condition. Mean and SD are displayed. * p-value < 0.05; ** p-value < 0.01; *** p-value < 0.001.

(c) Western blot analysis of BACH1 protein expression in whole cell lysates. BMDMs were treated with IFNß 500 U/ml for indicated time points. Data represents at least 2 independent experiments.

(d) Computational annotation of type I IFN-activated transcription factors binding to BACH1 5`upstream flanking region according to (Rusinova *et al.*, 2012).

4.1.5 Regulation of transcription factors is Jak1 dependent

The classical signaling pathway of type I IFN involves Janus kinases (JAKs), which activate the transcription factors signal transducer and activator of transcription (STATs), thereby inducing interferon regulated genes (IRGs) (Kalliolias and Ivashkiv, 2010).

To elucidate the players involved in the modulation of the BACH1-Nrf2 axis, several single STAT knock-out macrophages were tested in their ability to alter the transcriptional levels of the two TFs, with no apparent contribution (Riedelberger *et al.*, unpublished). Possibly, this is due to the redundant nature of the different STATs and the ability to form both homo- and heterodimers. Nevertheless, inhibition of the upstream signal transducer JAK1 by Filgotinib (Van Rompaey *et al.*, 2011) could ameliorate the transcriptional activation and repression of *Bach1* and *Nfe2l2*, respectively, after IFN-I stimulation of macrophages (Figure 10). In contrast, restoration to transcriptional baseline levels could not be achieved by the inhibition of Tyk2 (data not shown), not necessarily needed for IFN-I signal transduction in murine cells (Majoros *et al.*, 2017).

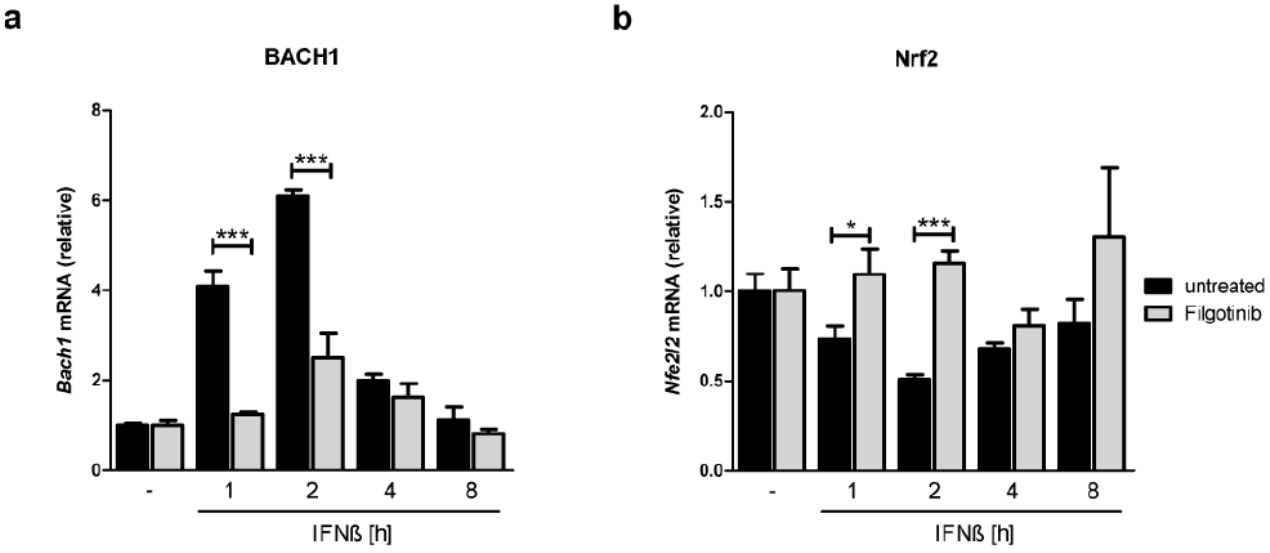

Figure 10. IFN-I regulation of iron homeostatic TFs is Jak1-dependent.
(a,b) RT-qPCR analysis of transcription factors BACH1 and Nrf2. BMDMs were treated with 10 µM Filgotinib for 1h prior to stimulation with 500 U/ml IFNß. Mean and SD are displayed. * p-value < 0.05; ** p-value < 0.01; *** p-value < 0.001. Data represent 2 independent experiments.

4.1.6 IFN-I signaling counteracts the upregulation of FPN1 during *C. glabrata* infection

During infections, Nrf2 is activated by inflammation signals and oxidative stress, which releases the co-factor KEAP1 and promotes Nrf2 translocation into the nucleus. Further, Nrf2 has been shown to activate transcription of *SLC40A1*, encoding the iron exporter FPN1, which decreases the cytoplasmatic iron levels in macrophages (Marro et al., 2010; Nairz et al., 2013).

Similarly, after macrophages encountered *C. glabrata*, elevated Nrf2 expression could be observed. However, priming of immune cells with type I IFNs led to a significant reduction of the transcriptional and the whole cell translational level, blocking the infection stimuli (Figure 11a-b). Subsequently, IFN-I impeded the upregulation of *SLC40A1* throughout the infection course (Figure 11c).

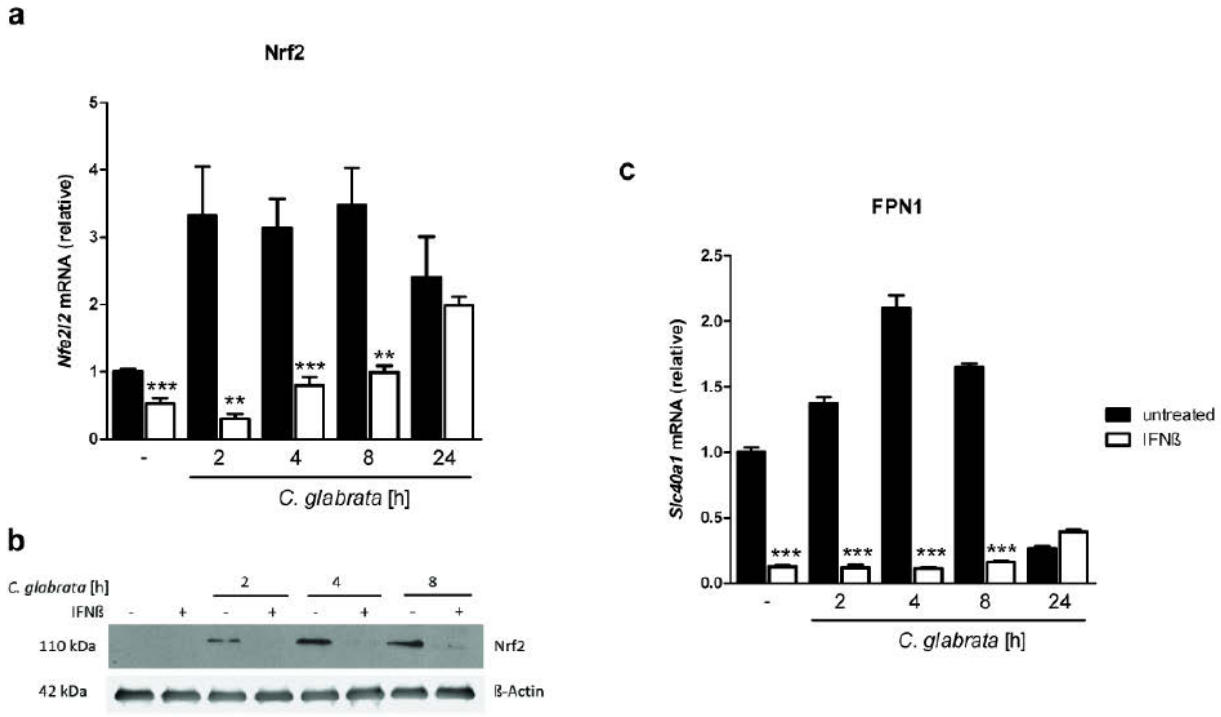

Figure 11. Type I IFNs counteract the upregulation of FPN1 in macrophages during *C. glabrata* infections.
(a,c) RT-qPCR analysis of Nrf2 and FPN1 in BMDMs, untreated or pre-treated with IFNß (500 U/ml) for 17h before infection with *C. glabrata*. Values are standardized to ß-Actin expression and normalized to uninfected condition. Mean and SD are shown. * p-value < 0.05; ** p-value < 0.01; *** p-value < 0.001.
(b) Western blot analysis of Nrf2 protein expression in whole cell lysates. BMDMs were treated with IFNß 500 U/ml for 17h before infection with wild-type *C. glabrata*. Data represents at least 2 independent experiments.

4.1.7 FPN1 limits Fe availability for *C. glabrata* and restricts fungal replication

Due to the proposed role of FPN1 as exporter in microbe-containing phagosomes (Van Zandt *et al.*, 2008) we tested the role during *C. glabrata* infections in FPN1 knock-out macrophages. Due to the availability of FPN1 deletion macrophage-like RAW 264.7 cells we use these cells instead of primary immune cells.

Fungal cells had a significantly higher Fe amount when isolated from *Fpn1*$^{-/-}$ macrophages compared to WT in the initial phase of the infection (12h), indicating the creation of iron-restricted conditions by FPN1. After 24 hours, no difference could be seen (Figure 12a). Fungal cells ended up with higher intracellular iron levels after 24 hours compared to 12 hours after infection. RAW cells, in contrast to wild-type macrophages, seem to be unable to restrict iron for a prolonged period, despite the presence of additional exporters in phagosomal membranes (DMT1 or HRG1) (Soares and Hamza, 2016). However, possibly due to the functional absence of the iron exporter NRAMP1 in the phagosome, higher iron levels are present within phagosomes at later time points (Vidal *et al.*, 1996).

However, these temporal changes in iron homeostasis led to altered fungal burden within macrophages. After 24 hours, *C. glabrata* infected *Fpn1*$^{-/-}$ RAW cells showed a 3-fold higher survival compared to WT RAW 264.7 cells (Figure 12b).

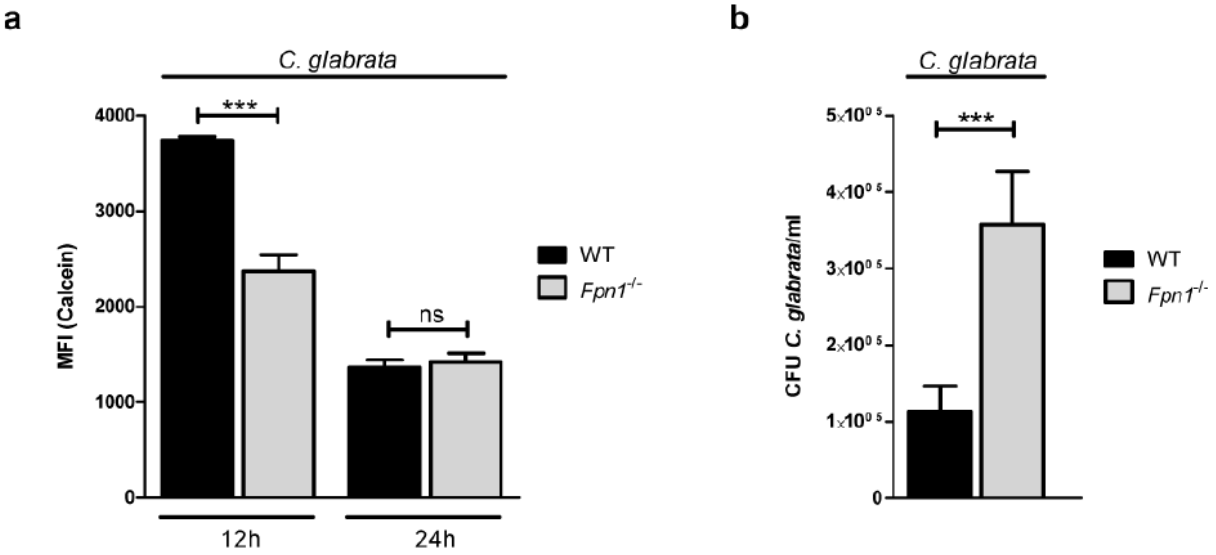

Figure 12. FPN1 depletes fungal pathogens of iron inside macrophages.
(a) Intracellular iron content of fungal cells was analyzed by mean fluorescence intensity (MFI) of Calcein-AM. After indicated interaction time of *C. glabrata* with WT or *Fpn1*$^{-/-}$ knock-out RAW cells, fungal cells were isolated and analyzed as indicated in Figure 8. Note, the higher the fluorescence, the lower the amount of intracellular iron.
(b) Cell lysates were plated after 24 hours of interaction with WT or *Fpn1*$^{-/-}$ RAW 264.7.
Mean and SD are displayed. * p-value < 0.05; ** p-value < 0.01; *** p-value < 0.001. Data represents at least 2 independent experiments.

4.2 Iron uptake is vital for fungal fitness during infections

To determine the impact of iron uptake in *Candida glabrata* on fungal fitness and virulence during infections, we used single knock-outs of the iron permease Ftr1 and the siderophore transporter Sit1. A complete knock-out of both transport systems could not be created, showing the importance of proper iron acquisition. Therefore, an inducible conditional knock-out of Ftr1 in the *sit1*Δ background was used (*sit1*Δ ftr1cΔ), which was created by Sabrina Jenull.

4.2.1 Fungal iron uptake systems are differently expressed in macrophages

Under low iron conditions, an Aft1/2-dependent upregulation of *SIT1* and *FTR1* can observed as soon as 2 hours after iron depletion (Sharma, Purushotham and Kaur, 2016). Similarly, we observed the upregulation of both iron transport systems of *C. glabrata* isolated from macrophages, compared to *C. glabrata* growing in iron-rich medium such as YPD. Although harsh medium changes can impact activation of iron acquisition genes, most macrophages (75%) phagocytosed *Candida* cells already after 45 minutes. Extracellular replicating *C. glabrata* were sorted out by flow cytometry (Figure 13a). Interestingly, *SIT1* and *FTR1* were significantly higher expressed in macrophages pretreated with IFNß (Figure 13b).

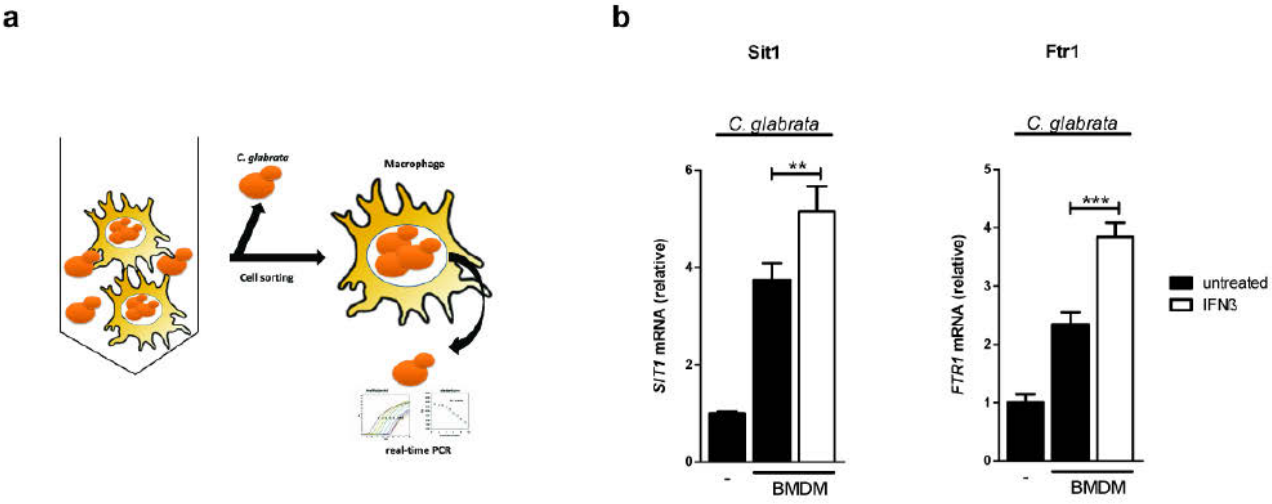

Figure 13. *C. glabrata* iron acquisition systems are upregulated in IFN-I activated macrophages.
(a) Macrophages were sorted by size (FSC-A/SSC-A) after 8 hours infection with WT *C. glabrata*. Transcriptional expression levels of phagocytosed fungal cells were analyzed by RT-qPCR.
(b) Expression levels of iron acquisition genes in *C. glabrata* isolated from BMDMs untreated or treated with 500 U/ml IFNß for 17h or directly after growth in YPD (-).Values are standardized to ß-Actin expression and normalized to untreated condition. Mean and SD are shown. * p-value < 0.05; ** p-value < 0.01; *** p-value < 0.001. Data represents 2 independent experiments.

4.2.2 Iron uptake promotes fungal growth

To address the importance of fungal iron acquisition systems, *C. glabrata* wild-type and knock-out strains were grown in iron-rich YPD medium and in iron-depleted YPD-BPS medium (bathophenanthroline dislufonate). BPS chelates all ferrous iron (Fe^{2+}) making it inaccessible for the fungus (Cowart, Singleton and Hind, 1993). As Sit1 is important for the siderophore-mediated iron uptake, lack of Sit1 did not have any effect on the growth ability compared to wild-type cells. However, the uptake of Fe^{2+} by the iron permease Ftr1 was important for the fungus, as deleting the system slightly reduced growth in YPD (Figure 14a) and apparently reduced it in YPD-BPS (Figure 14b).

Growth retardation in Fe-depleted medium to around 10% (OD_{600}=2.5) when compared to YPD after 24 hours (OD_{600}=25-30) indicates the absolute importance of ferrous iron for fungal growth. Surprisingly, loss of both iron transporters Sit1 and Ftr1 abrogated growth under deplete conditions (Figure 14b), opening speculations for a compensatory role of Sit1 in the *ftr1*Δ mutant.

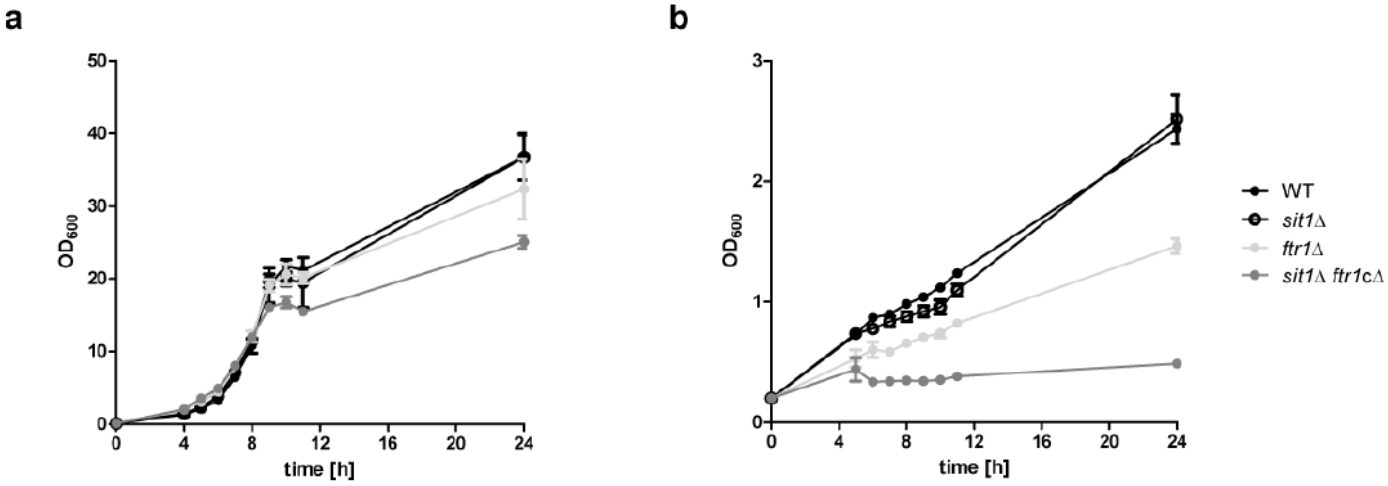

Figure 14. The HA reductive iron uptake system is crucial for growth.
(a) Growth of *C. glabrata* WT, *sit1*Δ, *ftr1*Δ and *sit1*Δ *ftr1*cΔ strains in YPD medium.
(b) Growth of *C. glabrata* WT, *sit1*Δ, *ftr1*Δ and *sit1*Δ *ftr1*cΔ strains in YPD medium supplemented with 100 µM bathophenanthroline disulfonate (BPS). In (a) and (b) fungal growth was measured by optical density at 600nm (OD_{600}). Mean and SD are shown. Data represents 2 independent experiments.

4.2.3 Reduced iron uptake suppresses fungal fitness during infections

To investigate the correlation of iron uptake with fitness during macrophage infections, we stained isolated fungal cells with Calcein-AM and plated them on solid YPD. *C. glabrata* sit1Δ isolated from BMDMs displayed almost unaltered iron levels compared to WT cells. In contrast, *ftr1*Δ seemed indispensable for iron acquisition during infections (Figure 15a). However, iron levels in the double knock-out strain were significantly lowered compared to WT and *ftr1*Δ *C. glabrata* (Figure 15a).

Despite the absence of iron acquisition defects, *sit1*Δ had significantly lower survival rates in macrophages compared to the WT fungal cells. The survival decreased further in the *sit1*Δ *ftr1*cΔ strain, which also showed a clear decrease in the cytoplasmatic iron pool (Figure 15b).

Although, neutrophils being the primary responders in Candida i.p infections within the first few hours, macrophages are the predominant cell population after 24 hours (Jan Kullberg Franck Amiot et al., 2019). Therefore, we infected mice with *C. glabrata*, WT and the double knock-out, via intraperitoneal administration to investigate the importance of iron acquisition during murine infections (Figure 15c). *C. glabrata sit1*Δ *ftr1*cΔ displayed reduced survival compared to the WT, suggesting that iron uptake is a major part of the fungal fitness both *in vitro* and *in vivo*.

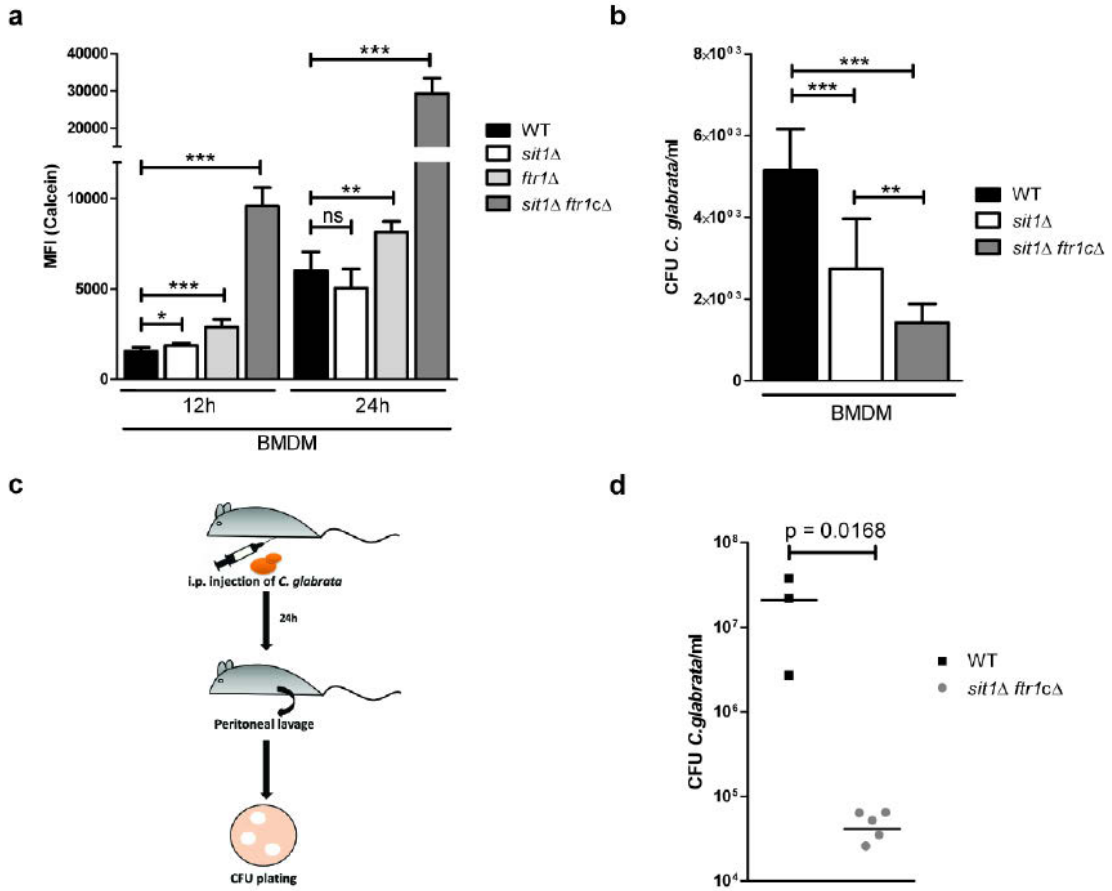

Figure 15. The ability to acquire iron is essential for *in vivo* fitness.
(a) Intracellular iron staining of wild-type (WT), *sit1*Δ, *ftr1*Δ and *sit1*Δ *ftr1*cΔ *C. glabrata*. Fungal cells were isolated after infection of BMDMs for indicated time points. Mean fluorescence intensity of Calcein- AM was measured by flow cytometry. Note, the higher the fluorescence, the lower the amount of intracellular iron. Data is representative for 2 independent experiments.
(b) *In vitro* survival of *C. glabrata* strains from (a) after infection of BMDM for 24h. Viable cells were counted by plating cells on solid YPD. Data is representative for 3 independent experiments.
(c) Scheme of *in vivo* infection of *C. glabrata* by administration into the peritoneum (i.p.) of wild-type mice. After 24h the peritoneum was flushed with PBS and viable cells were plated on YPD.
(d) *In vivo* survival of wild-type (WT) and *sit1*Δ *ftr1*cΔ *C. glabrata* after i.p. infection as in (c). Experiment and analysis was performed by Micheal Riedelberger. Mean and SD are shown. * p-value < 0.05; ** p-value < 0.01; *** p-value < 0.001.

4.3 Type I IFNs dysregulate Zn homeostasis

Zinc has a multitude of functions within macrophages ranging from differentiation to cell fate decisions (Gao *et al.*, 2018). As iron, cellular Zn distribution is partly controlled by cytokines (Subramanian Vignesh *et al.*, 2013; Subramanian Vignesh *et al.*, 2016). Therefore, we investigated the influence of type I IFNs on zinc homeostasis within macrophages.

4.3.1 Type I IFNs modulate the intracellular Zn pool

Pro-inflammatory stimuli (IFN-γ or GM-CSF) constrict intracellular Zn^{2+} pools in macrophages, whereas anti-inflammatory signals (IL-4 and IL-13) mediate alternatively activated M2 macrophages, thereby increasing the intracellular zinc pool and promoting pathogenic survival (Subramanian Vignesh *et al.*, 2013; Subramanian Vignesh *et al.*, 2016).

To investigate the zinc response in macrophages after type I IFN treatment and during infection with *C. glabrata*, BMDMs were harvested and stained with the zinc dye Zinpyr-1. To differentiate between macrophages, which did take up fungal cells, mCherry expressing *C. glabrata* was used. After 8 hours, most immune cells (more than 80%) had phagocytosed fungal cells. After infection $mCherry^{+}$ macrophages displayed elevate labile zinc levels (Figure 16b), while $mCherry^{-}$ BMDMs did not elicit a rise (data not shown), suggesting a cell intrinsic signaling upon encountering fungal PAMPs. In contrast to iron modulation, bystander cells are not influenced in their zinc homeostasis during infections.

Further, IFN-ß-treated macrophages displayed significantly less free Zn^{2+} than naïve immune cells during infections (Figure 16b). In summary, type I IFNs hampered the accumulation of free zinc during fungal infections.

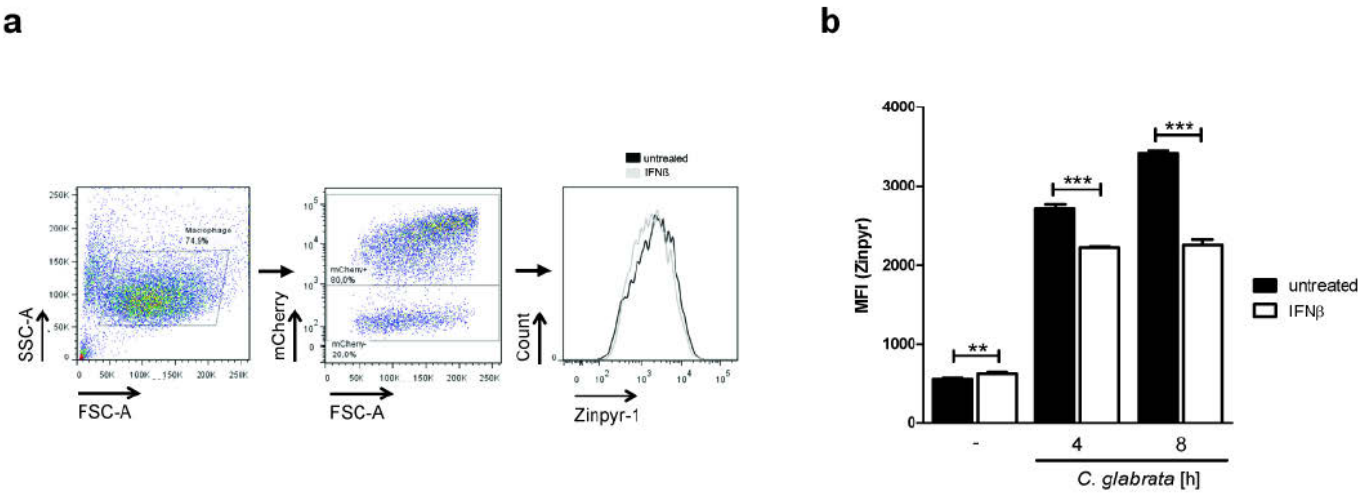

Figure 16. Type I IFNs reduce Zn^{2+} accumulation in infected macrophages.
(a) Gating strategy for Zinpyr-1 staining of macrophages. After infection with mCherry expressing *C. glabrata*, macrophages were harvested and selected for size (FSC-A/SSC-A). Macrophages positive for mCherry (PE Texas Red) were selected and MFI of Zinpyr-1 was measured.
(b) Bone marrow-derived macrophages, untreated or IFNß-treated (500 U/ml) for 17 h, were infected with mCherry expressing *C. glabrata* at MOI=2 for indicated time points. Gating was performed according to (a) and mean and SD are shown. * p-value < 0.05; ** p-value < 0.01; *** p-value < 0.001. Data represents 2 independent experiments.

4.3.2 IFN-I signaling interferes with regulation of Zinc transporters

Every pathogen stimulates a defined combinatorial set of zinc transporters during infections (Gao *et al.*, 2018). How macrophages trigger a specific combination of transporters is still enigmatic, although one hint might be the pathogen-specific activation of different PRRs (Lahiri and Abraham, 2014).

Stimulation of macrophages with IFN-ß led to downregulation of metal-response element-binding transcription factor 1 (*Mtf1*), the main transcriptional regulator of zinc responsive genes (Figure 17a). Surprisingly, even after 24 hours, the transcriptional expression was suppressed, indicating a long-lasting effect on macrophages by type I IFNs.

Subsequently, type I IFNs significantly inhibit the fungal-mediated transcriptional upregulation of zinc exporter *Slc30a1* and zinc importers *Slc39a4* and *Slc39a14* (Figure 17b-d). Interestingly, ZIP4 was upregulated, whereas ZIP14 was downregulated in *Ifnar1*$^{-/-}$ BMDMs compared to WT macrophages during infections, arguing for opposing roles in regulation of these transporters. Surprisingly, type I IFN priming and the lack of type I IFN signaling both led to downregulation of *Slc39a14* during fungal infection (Figure 17d).

Despite significant changes of the master transcriptional regulator MTF1 during IFN-I treatment, only *Slc39a4* showed altered basal expression levels. Taken together, the upregulation of pathogen-specific zinc transporters seemed to be regulated by a complex network, combining parts of the type I IFN signaling pathway, which were inhibited by IFNs-I.

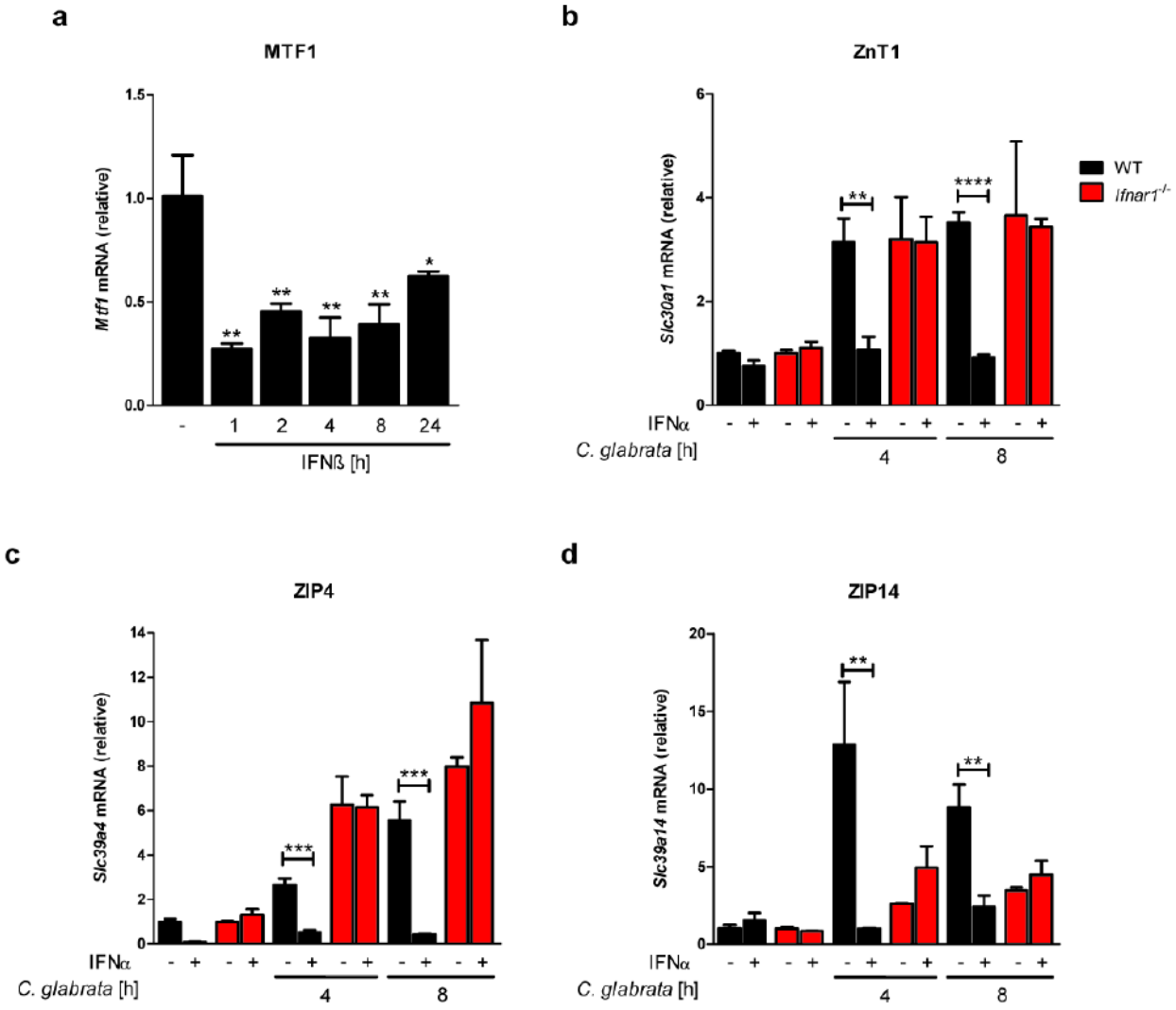

Figure 17. Type I IFNs dysregulate zinc importer and exporter expression.
(a) RT-qPCR analysis of BMDMs stimulated with 500 U/ml IFNß for indicated time points. Values are standardized to ß-Actin expression and normalized to untreated condition.
(b-d) RT-qPCR analysis of WT and *Ifnar1*$^{-/-}$ BMDMS infected with *C. glabrata* at MOI=2 for 4 and 8 hours. BMDMs were pretreated with 500 U/ml IFNα for 17 hours (+). Values are standardized to ß-Actin expression and normalized to uninfected condition. Mean and SD are shown. * p-value < 0.05; ** p-value < 0.01; *** p-value < 0.001. Data represents 2 independent experiments.

4.3.3 Type I IFNs impair Zn intoxication of *C. glabrata*

Elevated levels of the total exchangeable Zn^{2+} pool during *C. glabrata* infections led us to test fungal zinc levels after phagocytosis, to determine, whether *C. glabrata* faces a limited zinc environment or encounters high zinc stress (Subramanian Vignesh and Deepe, 2016).

Growth curves of *C. glabrata* showed that supplementation with 4-6mM $ZnSO_4$ already displayed fungistatic properties by impairing fungal growth and 8mM $ZnSO_4$ reduced fungal growth by 50 % after 24 hours (Figure 18a).

Fungal cells isolated from IFN-ß-activated BMDMs (Figure 18b), exhibited a significantly decreased number of zinc positive, dead cells compared to untreated ones (Figure 18c). In depth-analysis revealed significantly lower intracellular Zn levels in phagocytosed live *C. glabrata* cells, isolated from type I IFN-activated macrophages compared to naïve ones (Figure 18d). In accordance, the fungal methallothionen MT-1 was higher expressed in yeast cells isolated from naïve macrophages compared to primed ones after 8 hours (Figure 18e). Despite a further rise of intracellular "free" zinc in dead fungal cells, a difference between untreated and IFNß-treated condition couldn´t be observed. The rise of zinc levels in dead fungal cells indicates an intoxication mechanism that seems to be deployed by the host cell. These results are strengthened by microscopy analysis revealing a massive rise in zinc in *Candida*-containing phagosomes (Riedelberger *et at.,* unpublished).

Lower zinc levels in alive *Candida* cells could be due to detoxification mechanisms (extrusion or sequestration of zinc) (Crawford *et al.*, 2018). Subsequently, killing of the fungus would lead to elevated intracellular zinc concentration.

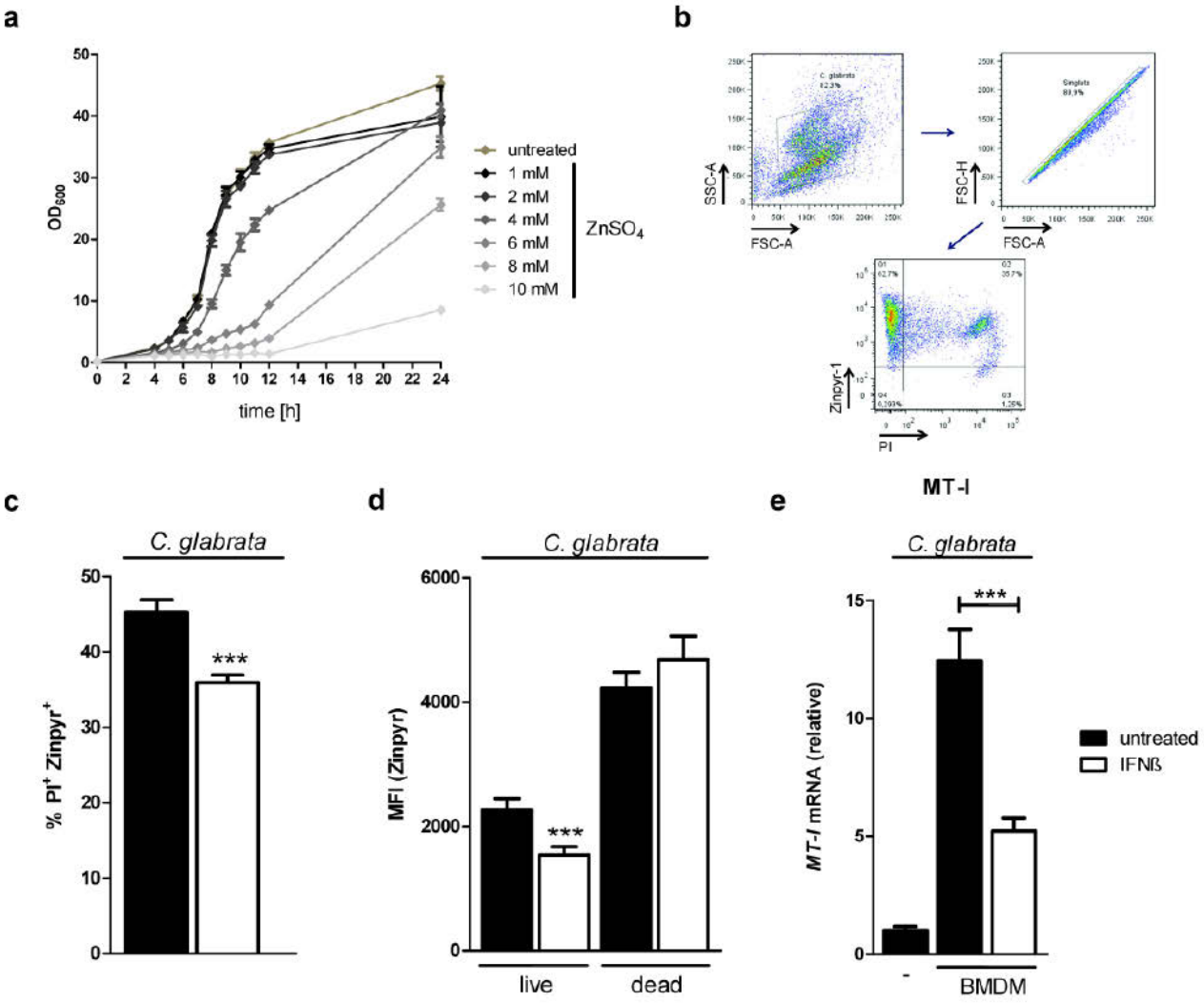

Figure 18. Type I IFNs impair Zn intoxication of *C. glabrata* by macrophages.

(a) Growth curve of wild-type *Candida glabrata* in YPD medium supplemented with increasing concentrations of zinc ranging from 1-10mM. Mean and SD are shown. Data represents 3 independent experiments.

(b) Gating strategy for *C. glabrata* after isolation from co-culture with BMDMs. Wild-type fungal cells were select for size (FSC-A/SSC-A) and single cells (FSC-A/FSC-H). Lower panel shows live/dead cells (PI^-/PI^+) blotted against Zinpyr-1 signal.

(c) Quantification of dead (PI^+), $Zinpyr^+$ *C. glabrata* cells. Fungal cells were isolated from untreated or IFNß treated (500 U/ml 17h) WT BMDMs after 8 hours and gated as in (b).

(d) MFI of intracellular Zn^{2+} (Zinpyr) staining from live (PI^-) or dead (PI^+) *C. glarata*. Fungal cells were isolated from untreated or IFNß treated (500 U/ml 17h) wild-type BMDMs and gated as in (b).

(e) RT-qPCR analysis of *C. glabrata* isolated from BMDMs, untreated or treated with 500 U/ml IFNß for 17h, or directly after growth in YPD (-).Values are standardized to ß-Actin expression and normalized to untreated condition.

Mean and SD are shown. * p-value < 0.05; ** p-value < 0.01; *** p-value < 0.001. Data represents 2 independent experiments.

4.3.4 Host MT-1 and MT-2 are required for Zn redistribution in BMDMs

Metallothionein 1 and 2 exert a multitude of functions, sequestering labile Zn^{2+} to keep a homeostatic balance, as well as trafficking zinc within intracellular compartments during infections (Subramanian Vignesh and Deepe, 2016). During *C. glabrata* infections, macrophages upregulated both *Mt1* and *Mt2* expression, which was dampened by prior activation with type I IFNs (Figure 19a-b). Reduced expression happened both on the basal level and after infection indicating a pathogen-independent modulation of the zinc binding proteins by type I IFNs. Consequently, fungal cells isolated from *Mt1*$^{-/-}$ *Mt2*$^{-/-}$ RAW 264.7 cells displayed a significant reduction in zinc levels, compared to cells infecting WT RAW 264.7 cells (Figure 19c). Seemingly, MT-1 and MT-2 are indispensable for intracellular relocalization of zinc, therefore, assisting in the intoxication process of *C. glabrata* during infections of macrophages.

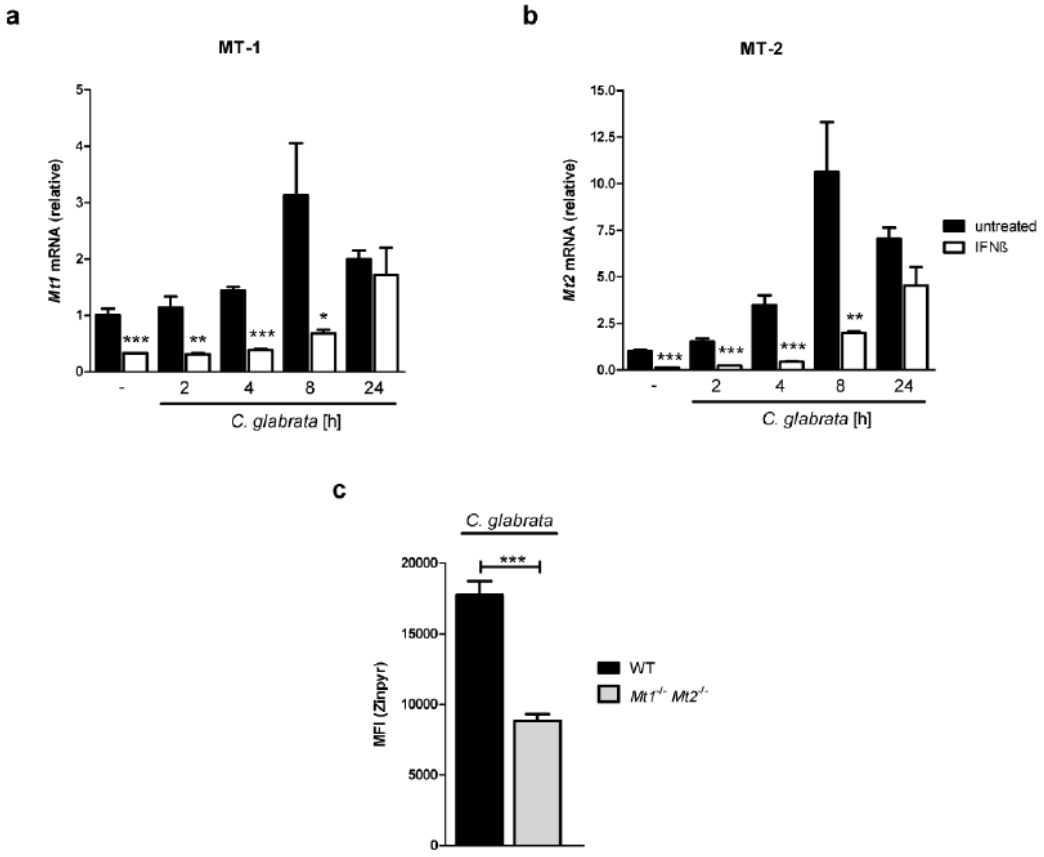

Figure 19. Host MT1/2 play key roles in zinc distribution within macrophages.
(a/b) RT-qPCR analysis of WT BMDMs infected with *C. glabrata* at MOI=2 for indicated time points. BMDMs were untreated or pretreated with 500 U/ml IFNß for 17 hours prior to infection. Values are standardized to ß-Actin expression and normalized to uninfected condition.
(c) mCherry expressing *C. glabrata* was isolated after infection of wild-type or *Mt1*$^{-/-}$ *Mt2*$^{-/-}$ macrophage-like cell line RAW 264.7 for 12 hours. Isolation was performed as described in Figure 8b and MFI of Zinpyr-1 is displayed.
Mean and SD are shown. * p-value < 0.05; ** p-value < 0.01; *** p-value < 0.001. Data represents at least 2 independent experiments.

5. Discussion

5.1 Macrophage responses

Macrophages are a heterogeneous immune cell population of high plasticity, displaying metabolic, transcriptional and epigenetic differences depending on their resident tissue (skin, spleen, intestine or peritoneum). They are derived from embryonic progenitors and often functionally unique. Further, circulating monocytes, which differentiate during stimulation, represent only a minor fraction of the total macrophage pool (Epelman, Lavine and Randolph, 2014; Ginhoux and Guilliams, 2016). Therefore, to generalize a macrophage response, several tissue phagocytes should be investigated.

Here, we show the impact of type I IFNs on Fe and Zn homeostasis in BMDMs and macrophage cell line RAW 264.7. Although, Winters, Chan, Caruso, & Deepe, Jr, (2010) could show similar responses to the cytokine GM-CSF on the trace metal homeostasis in several different macrophage populations, a detailed study of unpolarized, pro-inflammatory (M1-type) and anti-inflammatory (M2-type) polarized human macrophages, revealed differences in iron homeostatic regulation (Recalcati *et al.*, 2010). Differently polarized macrophages are distinguished in parts by their different metabolic activity that promotes either the M1 type, which kills the pathogen and causes tissue damage, or the M2 type, which exerts tissue healing functions. Both types are necessary for a successful host response, as both the clearing of the invader and resolving of inflammation and return to homeostasis are necessary (Ley, 2017).

Therefore, we tested several populations, including peritoneal and splenic macrophages and observed similar effects in all macrophage populations, indicating a universally dysregulated nutritional defense mechanism by type I IFNs against *C. glabrata*. A further limitation of isolated macrophage cultures is, that sometimes they don`t reflect the global host response, due to absence of systemic factors like the liver-derived hormone hepcidin, causing iron retention within cells (Andrews, 2008), or the release of zinc-scavenging protein calprotectin (Amulic *et al.*, 2012). Therefore, responses might differ significantly in primary cell cultures and *in vivo*. Nevertheless, it is a useful tool to investigate local responses of cell populations and adds valuable insight of cellular processes. For example, macrophages, which did not phagocytose *C. glabrata*, displayed a similar iron homeostatic response as infected immune cells *ex vivo* (4.1.2).

5.2 Type I IFNs and Fe homeostasis

5.2.1 Fe homeostasis dysregulation drives *C. glabrata* survival

Pro-inflammatory cytokines of type I IFNs can display detrimental roles for the host during infections with different pathogens (McNab *et al.*, 2015), often due to immunopathology (Davidson, Maini and Wack, 2015). Here, we show that IFN-α and IFN-ß exert a deleterious effect on macrophages by impairing pathogen clearance and promoting *C. glabrata* survival and persistence.

Macrophages themselves do not release notable amounts of type I IFNs during *C. glabrata* infections, probably due to the characteristics of the fungus-immune cell interaction. TLR7 and 9 recognize fungal nucleic acids in endosomal compartments of DCs, triggering the release of type I IFNs during *Candida* spp. encounter (Bourgeois *et al.*, 2011). Conversely, the persistent nature of *C. glabrata* in macrophages might limit the release of intracellular structures (nucleic acids), and therefore block type I IFN release. Priming with type I IFN leads to a lowered cytoplasmatic iron pool in macrophages but conversely, to elevated fungal survival. Riedelberger *et al* (unpublished) showed that the subcompartmental distribution favors the growth of *C. glabrata*. Especially phagososmes, in which the fungus resides, display elevated iron levels in type I IFN-treated macrophages. Surprisingly, subtle changes in the iron pool within macrophages manifest in solid changed fungal burdens during infections. Indeed, resistance to invading pathogens is established by nutritional immunity and antimicrobial effector mechanisms, like the generation of ROS and NO (Netea *et al.*, 2015). Both processes are tightly intertwined (Soares and Hamza, 2016), hence minor changes in the Fe homeostasis possibly exacerbates changed antimicrobial activity. Here, the focus was primarily on the contribution of type I IFNs on trace metal homeostasis, however further investigations into subsequent metabolic and effector changes in macrophages would be necessary to complete the picture.

5.2.2 The BACH1- Nrf2 axis

Central in the regulation of iron homeostasis are the two transcription factors BACH1 and Nrf2. The transcriptional activator Nrf2 can be activated by the accumulation of ROS and other reactive species, stimulation with growth factors or in response to PRR signaling, by sensing of the co-protein Kelch-like ECH-associated protein (KEAP1). Thereby, the proteolytic degradation of Nrf2 by KEAP1 is inhibited, allowing for the translocation into the nucleus and the activation of target genes involved

in iron homeostasis (Ashino et al., 2008; Hayes and Dinkova-Kostova, 2014; Soares and Hamza, 2016). In turn, BACH1 constitutively represses iron homeostasis genes by binding to the transcriptional co-factor MAF and recognition of the antioxidant response element (ARE) or MARE DNA binding motifs (Sun et al., 2004). BACH1 could be shown to sense labile heme as part of the alert system for tissue damage or stress (Ogawa et al., 2001). In addition, BACH1 also might play a role in the transcriptional regulation of Nrf2 due to a functional MARE element in the *Nfe2l2* promotor region (Chapple et al., 2016).

Whether type I IFNs modulate transcriptional levels directly by canonical signaling or alternatives was not elucidated. However the dependence on JAK1 was established (4.1.5). Computational methods annotate the expression of *Bach1* under the influence of type I IFNs, which could in turn be responsible for the transcriptional repression of *Nfe2l2*. Conversely, the transcriptional downregulation of *Nfe2l2* is long-lasting, while Bach1 returns to baseline levels after a short time, promoting the involvement of other factors (4.1.4). The target of Nrf2, the sole mammalian iron exporter FPN1, was similarly regulated on the transcriptional level. Interestingly, reduced *SLC40A1* expression levels were detected with decreased levels of cytoplasmatic iron after IFN-I treatment during infections. FPN1, which has been shown to reside within the membranes of phagosomes and deplete internalized pathogens of iron (Van Zandt *et al.*, 2008; Nairz *et al.*, 2013), could be responsible for the depletion of Fe during infection with *C. glabrata*. The rise of the labile iron pool within macrophages during *C. glabrata* infection may point to a localization of FPN1 towards phagosomes rather than the outer membrane. Further, *C. glabrata* after infection of macrophages, with IFN-I mediated downregulation of FPN1 (4.1.1), and *Fpn1*$^{-/-}$ RAW cells (4.1.7) displays similar elevated survival rates compared to untreated and WT controls respectively, indicating the importance of FPN1 during fungal infections.

5.2.3 Therapeutic possibilities during *C. glabrata* infections

The high resistance of *C. glabrata* against antimycotic agents like azoles, cationic peptides and echinocandins (Helmerhorst *et al.*, 2005; Pfaller *et al.*, 2010; Vale-Silva and Sanglard, 2015) makes the development of new therapeutics highly necessary. The massively lowered fungal loads in cells unresponsive to type I IFNs and, and in turn, heightened fungal loads in type I IFN treated-macrophages (4.1.1) opens speculation about targeting those cytokines. However, most humans suffering from fungal infections are already immunocompromised and further reduction could prone them susceptible to viral infections. Further, while gain-of-function mutations in the type I IFNs

signaling pathway are associated with high susceptibility to *Candida* spp. infections (Liu *et al.*, 2011), activation of the type I IFN pathway is central for the human host defense (Smeekens *et al.*, 2013). This might be attributed to a regulation towards a Th17 immune response, making a targeted regulation of IFN-I difficult.

Moreover, another approach is to target the iron homeostasis of the host. Proof of principle was already provided for both intracellular and extracellular replicating pathogens by promoting Fe efflux from macrophages or reducing the circulating Fe levels by pharmacological agents (Van Zandt *et al.*, 2008; Ganz, 2009; Arezes *et al.*, 2015). Unfortunately, clinical data from patients is rather contradictory with examples of worsened outcome after treatment with the iron chelator desferasirox (Spellberg *et al.*, 2012). Blocking the fungal iron acquisition might be a feasible alternative in limiting the microbial proliferation as shown in the example of the fungus *Aspergillus* spp. (Schrettl *et al.*, 2004).

5.3 Iron acquisition by *C. glabrata* during infections

To establish a successful infection, fungal pathogens like *C. glabrata* have to acquire a sufficient amount of nutrients, particularly iron among other trace metals, because of their functional importance in replication, transcription, metabolism and other cellular processes (Hood and Skaar, 2012). Therefore, iron-uptake systems of pathogens are of central importance for successful host infections and have been linked to virulence (Gerwien *et al.*, 2018). Here, we link *C. glabrata*`s iron acquisition during macrophage infections and intraperitoneal infections of mice to fungal fitness. Hence, by deleting Sit1 and Ftr1 we observed decreased fungal loads both *in vitro* and *in vivo* (4.2.3). Nevertheless, the persistent nature of the fungus during infection in murine models makes it hard to draw conclusions about the importance of iron transporters for virulence. We can only speculate that elevated fungal loads exert negative effects on the host, limiting its survival. Besides the siderophore and high affinity Fe-uptake system *C. glabrata* uses the low affinity divalent metal transporter Fet4 (Gerwien *et al.*, 2016), which is insufficient to take up iron in ferrous iron-deplete conditions as seen by complete growth retardation in the s*it1*Δ ftr1cΔ mutant (4.2.2). Consequently, fungal cells struggle to take up iron during macrophage infections (4.2.3), as phagosomes are highly iron-restrictive niches (Kasper, Seider and Hube, 2015).

Surprisingly, Sit1 displays additional functions to the role as siderophore transporter. Sit1 was thought to contribute to fungal xenosiderophore uptake (e.g. in intestinal tract) before subsequent infections, which was confirmed with siderophore priming (Nevitt and Thiele, 2011; Kumar *et al.*,

2019). Here, despite a lack of iron uptake function during macrophage infections, Sit1 seems to be important for survival within macrophages. Accordingly, *SIT1* is upregulated in fungal cells isolated from immune cells (4.2.1). Interestingly, in *C. glabrata* cells defective of the high-affinity iron acquisition pathway (*ftr1*Δ), Sit1 points to iron acquisition functions, independent of hydroxamate-type xenosiderophore uptake, both in iron rich and deplete medium and during macrophage infections. These novel results would attribute Sit1 a new role during infections with *C. glabrata*.

5.4 Host zinc homeostasis during fungal infections

5.4.1 Zn intoxication of *C. glabrata* by macrophages

To combat infections, macrophages can either perform Zn intoxication or sequestration. Here, immune cells restrict the fungal growth by intoxication of *C. glabrata* with high zinc levels. This process is mediated by the upregulation of a specific subset of zinc transporters, namely ZnT1, ZIP4 and ZIP14 and is accompanied by the upregulation of MT-1 and MT-2. Interestingly, reports of zinc intoxication are more common in bacterial microbes (Subramanian Vignesh and Deepe, 2016). Not surprisingly, because bacteria like *Escherichia coli* need 10^5 Zn atoms, whereas the fungus *Saccharomyces cerevisiae* needs 10^7 Zn atoms for optimal growth. Despite the comparable physiological bacterial and fungal zinc concentrations (0.1-0.5 millimolar), a microbe, which has a bigger volume, needs more Zn ions to reach the same concentration. Therefore, the number of total Zn ions in microbes with different volumes might shift over several orders of magnitude (Eide, 2006).

To intoxicate a fungal cell with Zn^{2+}, despite differences in the detoxification mechanisms, is a consuming task for macrophages. The exchangeable fraction of zinc within mammalian cells resides in the nanomolar to pikomolar range (Maret, 2006). However, import from extracellular space or released from intracellular compartments can elevate those levels (Subramanian Vignesh *et al.*, 2013). Nevertheless, the binding of catalytic enzymes to non-activating metals, termed “mismetallation”, which renders them inactive, poses a high threat to cells. Indeed, binding sites generally exhibit higher metal affinities to zinc than iron or manganese (Imlay, 2014). A relative small pool of excess Zn^{2+} might therefore be enough to tilt the balance of metallation.

Thereby, the upregulation of metallothionein 1/2 has an important role in the redistribution of labile Zn^{2+} within the host during infections. The roles of MT-1 and MT-2 range from sequestering and storing zinc in compartments during zinc depletion (Subramanian Vignesh *et al.*, 2013) to shuttling Zn^{2+} to the phagosome, where oxidative conditions favor the Zn release, as part of the

intoxication process (Botella *et al.*, 2011). The latter is the case during *C. glabrata* infections in macrophages. MT-1 and MT-2 are upregulated during infection and responsible for loading fungal invaders with zinc (4.3.4). In contrast, type I IFNs dampen the upregulation and lower the labile zinc pool during infections.

5.4.2 Pathogen-specific zinc transporter regulation

The encounter with different pathogens triggers pathogen-distinct expression patterns of zinc importers (SLC39- family) and exporter (SLC30- family transports) within macrophages (Botella *et al.*, 2011; Vignesh *et al.*, 2013; Subramanian Vignesh and Deepe, 2016; Gao *et al.*, 2018). The mechanism was proposed, by which transporters passively associate with newly formed endosomal or phagosomal membranes (Subramanian Vignesh *et al.*, 2013). Thereby, the combination of upregulated transporters might determine the zinc flow towards different compartments in the cell, leading to different zinc resistance mechanisms. How the cell decides, which transporters are upregulated, is still not fully understood However this process might depend on the activation of pathogen-specific PRRs (Lahiri and Abraham, 2014).

Further, cytokines influence regulation of zinc transporters. For example, ZIP14 and ZIP4 are affected by IL-6 and GM-CSF respectively during bacterial infection (Taylor *et al.*, 2005; Subramanian Vignesh and Deepe, 2016). Here, type I IFNs impede the transcriptional upregulation of ZnT1, ZIP4 and ZIP14 during *C. glabrata* infections. Interestingly, ZnT1 upregulation could be observed in macrophages intoxicating phagocytosed pathogens (Subramanian Vignesh and Deepe, 2016). ZIP4 is important for the dietary zinc uptake in intestinal enterocytes (Küry *et al.*, 2002; Dufner-Beattie *et al.*, 2003), and ZIP14 is responsible for transport of extracellular zinc into the cytosol, also in response to acute phase stimuli via IL-6, to reduce serum zinc levels (Liuzzi *et al.*, 2005; Taylor *et al.*, 2005; Lichten and Cousins, 2009).

Taken together our data shows that, *C. glabrata* is intoxicated with high amounts of Zn^{2+} after uptake into the phagolysosomes of macrophages. Thereby, the immune cells use a MT1 and MT2-dependent metal shuttling mechanism to relocate zinc into the different subcompartments, possibly using the transporter ZnT1 for Zn^{2+} transport into the phagosome. Further, ZIP4 and ZIP14 are upregulated to possibly import Zn^{2+} from the extracellular space, to ensure prolonged zinc availability. Type I IFNs interrupt this process in every step by transcriptional downregulation of zinc transporters and methallothioneins.

5.4.3 Zinc acquisition by *C. glabrata* during infections

While defense strategies deployed by the fungus *C. glabrata* to survive within phagocytes are well investigated, little attention was given to *C. glabrata* zinc homeostasis during infection. While most other human pathogenic yeasts like *C. albicans* or *H. capsulatum* face tight Zn^{2+} restrictions, they display an upregulation of zinc transporters (Crawford and Wilson, 2015). The fungal response to high amounts of Zn^{2+} is to sequester, store and detoxify these ions within the vacuole (Gerwien *et al.*, 2018). Recently the vacuolar proton-translocating ATPase (V-ATPase) was found to be important in coping with ion stress such as Zn^{2+} in *C. glabrata* (Minematsu *et al.*, 2019). However, Butler *et al.* (2009) showed that the fungus has lost the zincophore gene *PRA1* and encodes the *C. albicans* orthologue for Zrt2, a low affinity zinc importer. A complete understanding of how the pathogen deals with ion stress during infections is still missing and could be the focus of future studies.

5.5 Final summary and outlook

During this study we could establish that type I IFNs display another detrimental role for the host by promoting survival and persistence of *C. glabrata* during macrophage infection. These deleterious effects are mainly due to the dysregulation of both iron and zinc homeostasis during infection.

We could answer the main questions:

- Macrophages, when encountering *C. glabrata*, shuttle iron away from the phagolysosome but load high amounts of Zn into the *C. glabrata*-containing phagolysosomes.
- Type I IFN signaling influences major transcription factors of both the iron (BACH1-Nrf2) and zinc (MTF1) homeostasis during infection in a Jak1-dependent manner.
- Thereby type I IFNs dysregulate transporters for iron (FPN1) and zinc (ZnT1, ZIP4 and ZIP14) and zinc shuttling proteins (MT1/2).
- Iron acquisition systems are essential for fungal fitness *in vivo* and *in vitro.*

Additionally, we opened several new questions to be addressed in future studies:

- How does *C. glabrata* tolerate high zinc stress during infections?
- Which downstream proteins are involved in IFNs-I trace metal homeostasis dysregulation?
- Does Sit1 have a compensatory/ iron uptake independent role in *C. glabrata*?

6. Material and Methods

6.1 Fungal methods

Wilde-type, mCherry expressing and f*tr1*Δ *Candida glabrata* background strain ATCC 2001 and *sit1*Δ and *sit1*Δ *ftr1*cΔ strain *tR(ACG)4* was used for experiments (Dujon *et al.*, 2004).

6.1.1 Media and plates for *C. glabrata*

Liquid media

Bacto Yeast extract (Difco)	10 g/l
Bacto pepton (BD)	20 g/l
Glucose	2 %(*w/v*)

All ingredients are mixed for 1x YPD full medium

- Yeast extract (Difco) and Bacto peptone (BD) was dissolved in ddH_2O and autoclaved immediately (for 1x YP).
- Glucose (20 %) solution was prepared separately.
- Solutions were stored at room temperature separately until needed.
- 1x YPD media was prepared by adding 10 % of the total volume of glucose solution to 1x YP for 2 % final concentration (f.c.) of glucose in a sterile environment and stored at room temperature.

Solid media

Bacto Yeast extract (Difco)	10 g/l
Bacto pepton (BD)	20 g/l
Glucose	2 %(*w/v*)
Agar	5 g/l

- Yeast extract (Difco) and Bacto peptone (BD) was dissolved in ddH_2O and autoclaved immediately (for 2x YP).
- Separate solutions for glucose (20 %) and agar were prepared and autoclaved.
- All solutions were stored at room temperature until usage.

- Agar was molten in a microwave and mixed with 2x YP and glucose. Mixture was then poured into petri dishes (92x 16 mm; Sarstedt). All steps were performed in sterile environments.
- YPD plates were then stored at room temperature until usage.

6.1.2 *C. glabrata* growth and culture preparation

- *Candida glabrata* was streaked onto YPD plates directly from frozen (-80 °C) glycerol stocks (20%) and grown at room temperature.
- Material from a single colony was picked under sterile conditions and inoculated in 5ml liquid YPD in the morning. Cells were then grown in Snapcap™ tubes (STARLAB) under constant agitation (200 rpm at 30 °C).
- After growth throughout the day, OD_{600nm} was measured and *C. glabrata* was further diluted to reach OD_{600nm}= 1,0 the next day at the time of harvesting.
  The following formula was used calculate the dilution:

$$V = \frac{Innoculation\ volume\ [ml]}{2^{time\ to\ harvesting\ [h]}} \Big/ Current\ OD_{600nm}$$

- *C. glabrata* was harvested at the calculated time point by transferring the medium into a 15 ml centrifuge tube (STARLAB). A small aliquot (~ 200- 500 µl) was taken and kept to measure OD_{600nm} and check for contaminations under the light microscope.
- If several tubes were used over night, total volume was pooled in 50ml centrifuge tubes.
- Cells were centrifuged at 3000 g for 2 min at room temperature and supernatant was discarded.
- Pellet was resuspended in the same volume PBS as grown in the overnight culture and centrifuged again as before.
- Cells were then resuspended in 1ml PBS and counted on the CASY™ (Schärfe System GmbH) cell counter.
    - Counting range between 2,5 and 7,5 µm.
    - Dilutions were made according to the assays performed.

- Viable *C. glabrata* was detected as colony forming units (CFUs) by plating on YPD plates

6.1.3 Growth curves

- *C. glabrata* strains were inoculated into liquid YPD from a single colony in the morning.
- After several hours of growth, OD_{600} was measured and diluted to reach OD_{600}=1 on the next day according to 6.1.2. If the double knock-out strain was used, cells were grown over night with doxycycline (f.c. 50 µg/ml).
- Fungal cells were then diluted to OD_{600}=0,2 and OD_{600} was then measured continuously as time points indicate. Double knock-out was grown in 50 µg/ml doxycycline.

6.1.4 Background of *sit1*Δ *ftr1cΔ* double knock-out

It was not possible to create the *sit1*Δ *ftr1*Δ knock-out, because at least one of the systems need to be present in *C. glabrata*. Sabrina Jenull created the conditional knock-out for *FTR1* in a *sit1*Δ background strain according to (Nakayama *et al.*, 1998).

In short, to control the Ftr1 expression, *FTR1* was inserted downstream of a tetracycline operator chimeric promotor (*tetO::ScHOP1*). The strain used carried a tetracycline repressor-transactivator fusion *tetR::GAL4* construct that is inducible by antibiotics like doxycycline, as used in this study. The addition of doxycycline induces the repression of the target gene resulting in transcriptional silencing.

50 µg/ml doxycycline treatment for 8 hours completely abolished transcription of *FTR1* in *sit1*Δ *ftr1*cΔ, not in *sit1*Δ *C. glabrata* strains.

6.2 Culture conditions of primary cells and RAW 264.7 cells

All cell culture incubations were done at 37 °C, with 5 % CO_2 and 95 % humidity environment.

6.2.1 Media

DMEM	Dulbecco´s modified Eagle´s medium, high glucose (4,5 g/l), L-Glutamine, without pyruvate (Gibco)
hiFCS	Fetal calve serum (Sigma-Aldrich) that was heat inactivated according to 6.2.2.

Full DMEM

DMEM

hiFCS 10 % (*v/v*)

Penicillin 100 U/ml

Streptomycin 100 µg/ml

Macrophage medium (Mϕ medium)

Full DMEM

L- conditioned medium 15 % (*v/v*) (see 6.2.3)

Phosphate-buffered saline (PBS)

NaCl 140 mM

KCl 27 mM

Na_2HPO_4 90 mM

KH_2PO_4 15 mM

FACS buffer

PBS

BSA 1 % (*w/v*)

Freezing medium

hiFCS

DMSO 10 % (*v/v*)

Red blood cell lysis buffer (RBC)

Tris/HCl pH 7,0 0,01 M

NH_4Cl 8,3 g/l

6.2.2 Heat inactivation of FCS (hiFCS)

In this procedure, fetal calve serum (FCS) was heated to 56 ^{o}C in a water bath to destroy heat-labile complement proteins prior to use in cell growth medium. This procedure was adopted from Richard Davis/ Robert Hsueh and is recommended by HyClone (HyClone handling serum procedure; 1-800 HYCLONE)

- FCS (Sigma-Aldrich) was thawed at 4 ^{o}C over night.
- Serum was then placed in a 37 ^{o}C water bath to thaw completely and mixed, to allow for complete equilibration with the surrounding temperature.
- To inactivate the serum, temperature was elevated to 56 ^{o}C under constant equilibration and incubated for 30 min with periodically inversion of the bottle.
- Serum was then cooled down at room temperature and 50 ml aliquots were prepared and stored at -20 ^{o}C until usage.

6.2.3 L(929)- conditioned medium preparation

L-929 cells (ATCC® CCL-1™), derived from mouse adipose tissue, were transformed to produce the cytokine macrophage- colony stimulating factor M-CSF (CSF-1) (Boltz-Nitulescu *et al.*, 1987).

- L-929 cells were thawed from a frozen stock and incubated in 100 mm round tissue culture dished (TC treated from Thermo Fisher Scientific) with Full DMEM medium and split when reaching 95 % confluency.
- After 8 days incubation, cells were transferred into 175 cm^2 cell culture flasks with 80ml Full DMEM and grown for another 4 days.
- Medium was exchanged to 100 ml DMEM (without FCS or antibiotics) per flask and incubated for 10 additional days.
- Supernatant (L- conditioned medium) was then collected and filtered with 0.22 µm Steritop GP Express PLUS membranes (Millipore, Billerica, MA, USA). Aliquots were stored at -20 ^{o}C and 4 ^{o}C for subsequent testing.

L- conditioned media testing

- Mϕ medium was prepared with different concentrations of the new L- conditioned medium batch. Thereby concentrations of 10 %, 15 % and 20 % of L- conditioned media were compared to previous batches.
- Standard differentiation protocol for Mϕ was follow (6.2.5) with the new L- cond. medium concentrations, cells were harvested and tested for their differentiation potential and effective cell number generation:
    - Cells were counted on the CASY cell counter
    - Cells were analysed on the FACS for surface marker expression

      CD11b: A general marker for myeloid cell lineages

      F4/80: Specific marker for murine macrophages

CD11b	FITC	eBioscience	11-0112-85	
F4/80	PE	BioLegend	123110	clone BM8

- Cells were harvested as in 6.4.1 and transferred into a tube, washed once with 1 ml FACS buffer and resuspended in 50 µl FACS buffer.
- Anti-CD16/32 (anti-Fcγ) antibody was used to block unspecific antibody binding (f.c. 1 µg) and incubated on ice for 10 min.
- Antibody mastermix (50 µl/sample) was prepared with 1 µl antibody/sample and incubated on ice in the dark for 30 min.
- After 2 washing steps with 1 ml FACS buffer, cells were resuspended in 300 µl FACS buffer, transferred into 12x75 tubes and measured on a BD LSR Fortessa™.

    - Cellular response was tested after infection with *Candida* spp.

      RT-qPCR analysis of cytokines TNF-α, IL-1ß and IL-10 were tested under uninfected/ (heat killed) *C. glabrata*- / (heat killed) *C. albicans*- infected and IFN-ß treated conditions in macrophages.

6.2.4 Isolation of mouse bone marrow

- 8-12-week-old mice were sacrificed by cervical dislocation and femur and tibia were isolated immediately, rinsed with 70 % ethanol and kept on 4 ^{o}C in PBS until processing.
- Bones were then rinsed in 70 % ethanol and placed in ice cold DMEM under sterile conditions.
- Up to 10 animal legs were then pooled in an ice-cold pistil with 10 ml DMEM and bones were grinded with a mortar until all cells were released from the marrow.
- Cell suspension was filtered through a 40µm Nylon Corning® Cell Strainer and cells were pelleted at 300 g for 6.5 min at 4 ^{o}C.
- Medium was aspired and red blood cells were lysed with lysis buffer (0.5 ml per leg) exactly for 2 minutes at RT. To neutralize the buffer 40 ml DMEM was added and cells were pelleted at 300 g for 6.5 min at 4 ^{o}C.
- Pellet was resuspended in 0.5 ml Freezing medium per leg, aliquoted into cryogenic vials (Starlab) and frozen at -80 ^{o}C.
- After several days, vials were transferred to -150 ^{o}C and stored until use.

6.2.5 Differentiation of bone marrow derived macrophages (BMDM)

Adopted from Boltz-Nitulescu et al., 1987.

- An aliquot of frozen bone marrow was thawed in a 37 ^{o}C water bath and quickly transferred into 10 ml 37 ^{o}C-prewarmed DMEM. Cells were centrifuged at 300 g for 6.5 min at RT.
- The resulting pellet was resuspended in 1ml Mϕ medium and placed into 100 mm square tissue culture dish (not TC treated) with 8 ml prewarmed Mϕ media (9 ml in total) and incubated.
- At day 3, 5 ml of fresh Mϕ media was added.
- At day 7, confluency was checked under light microscope and cells were split 1:2 into new 100 mm square petri dishes with 12 ml total Mϕ media. Old media was exchanged by new Mϕ media and cells were detached with mechanical force applied by a soft rubber spatula.
- On day 10, macrophages were collected by scraping, pooled and centrifuged at 300 g for 6.5 min at RT. Pellet was resuspended in 1 ml and 10 µl were taken for CASY measurement.
    - Counting range between 7.5 and 22.5 µm (45 µm capillary).
    - Dilutions were made according to the assays performed.

6.2.6 RAW 264.7 cell culture conditions

- An aliquot of frozen RAW 264.7 cells were thawed in a 37 ^{o}C water bath and quickly transferred into 10 ml 37 ^{o}C prewarmed DMEM. Cells were centrifuged at 300 g for 6.5 min at RT.
- The resulting pellet was resuspended in 1 ml full DMEM medium and placed into 100 mm round tissue culture dish (TC treated) with 11 ml prewarmed full DMEM (12 ml in total) and incubated.
- Cells were split when 90-100% confluent. 1:2 for the next day, 1:4 for the use in 2 days or 1:6 over the weekend. Before every splitting, old medium was aspired and cells were washed once with pre-warmed PBS. RAW cells were scraped for harvesting.
- For assays, cells were prepared as Mϕ.

6.3 Interaction of innate immune cells with *C. glabrata*

For all assays if type I IFNs were added, recombinant IFNα and IFNß were used of 500 U/ml for 17 hours prior to assays after initial seeding.

6.3.1 *In vitro* survival assay

- Mϕ /RAW 264.7 cells were prepared according to 6.2.5 and 6.2.6.
- Mϕ /RAW 264.7 cells were seeded at 1x 10^5 cells /96-well in 100 µl of the respective medium.
- *C. glabrata* cells were prepared as in 6.1.2 and added for MOI 2 (2x 10^5 cells) in 50 µl of the respective medium for BMDMs or RAW cells.
- After 24 h incubation, plate was put on ice to stop interaction.
- 50 µl of a 4 % Triton-X 100 (Sigma Aldrich)/PBS solution was added and mixed in.
- Wells were scratch with a yellow tip for 10 sec, supernatant collected into a tube containing 400 µl PBS. All steps performed on ice.
- Wells were washed 2x with 200 µl ice-cold PBS again scratched and supernatants pooled with previous supernatants adding up to a final 1 ml.
- Dilutions were made accordingly and 100 µl were plated out onto YPD plates.
- Plates were incubated for 24 h at 37 ^{o}C and counted.

6.3.2 RNA isolation of mammalian cells

- Mϕ were prepared according to 6.2.5.
- Mϕ were seeded at 1x 10^6 cells /35 mm dish.
- *C. glabrata* cells were prepared as in 6.1.2 and added for MOI 2 (2x 10^6 cells).
- At the end of stimulation, medium was discarded and 1 ml Trizol (TRI Reagent® - LabConsulting) was added and cells were scraped off the dish.
- Samples were frozen at -80 ^{0}C.

Trizol extraction of RNA

- Samples were thawed on ice and vortexed shortly, then incubate for 5 min at room temperature.
- 200 µl chloroform were added, tube was inverted by hand 15 times and incubate at RT for 3 min.
- To separate liquid phase from protein extracts, the tube was centrifuge at 15000 g, 15 min at 4 ^{o}C.
- The nucleic acids containing upper phase was transfer into a new tube.
- 500 µl isopropanol (-20 ^{o}C) was added and incubate at RT for 10 min, then centrifuged at 15000 g for 10 min at 4 ^{o}C.
- Supernatant was removed and 1 ml of 75 % ethanol (-20 ^{o}C) added.
- After centrifugation at 15000 g, 5 min at 4 ^{o}C supernatant was removed, tube centrifuged shortly and remaining ethanol was removed.
- Pellet was air dried for 5-10 min at RT and dissolved in 40 µl H_2O (DNAse, RNAse free) on an Eppendorf™ Thermomixer *comfort* at 56 ^{o}C for 10 min with agitation (800 rpm)

6.3.3 RNA isolation of *C. glabrata*

- Mϕ were prepared according to 6.3.2 and *C. glabrata* cells were prepared as in 6.1.2 and added for MOI 2 (2x 10^6 cells).
    - At the end of stimulation, medium was discarded and 1 ml Trizol (TRI Reagent® - LabConsulting) was added, cells were scraped off the dish and stored at -80 ^{o}C.

- Or after interaction time, cells were washed with PBS and macrophages were harvested with 1x Trypsin (dissolved in PBS from Sigma without calcium and magnesium chloride with 50 mM EDTA) incubation at 37 °C for 5 min.
- Trypsinization was stopped by adding 2x volume of DMEM+ 10 % hiFCS before pipetting cells off the dish.
- Cells were centrifuged at 400 g for 5 min at 4 °C and resuspended in FACS buffer.
- Macrophages were then sorted for their size (FSC-A and SSC-A) on the BD FACSCalibur™ and pelleted again.
- Pellet was suspended in 1 ml Trizol and stored at -80 °C.

- After thawing, cells were mixed with glass beads and fungal cells were lysed with a FastPrep-24™ 5G (MP Biomedicals™). With speed 6 m/s for 40 sec with 2 cycles. In between cycles, samples were incubated on ice for 1 min.
- Further Trizol extraction was performed as mentioned in 6.3.2.

6.3.4 RNA processing and reverse transcription

Genomic DNA digestion

- After measuring nucleic acid amount on Nanodrop™, 5 µg were used for genomic DNA digestion.
- Protocol from DNAse I treatment Thermo™.

	Final concentration
RNA	5 µg
10x DNAse I buffer	1x
DNAse I	10 U
Ribolock RNAse inhibitor	50 U
RNAse free water	Up to 100 µl

- Reaction was incubated at 37 °C for 30 min.
- 100 µl phenol chloroform isoamyl (PCI) was mixed with the reaction volume by pipetting up and down until solution was homogenous and centrifuge 15000 g, 5 min at 4 °C.
- Upper phase was transferred in a new tube and 100 µl chloroform added as in the previous step.

- After centrifugation at 15000 g for 5 min at 4 °C, upper phase was transferred and mixed with 1/10 volume 3M NaAc (pH 5.3) and 3 volumes 100% (-20 °C) ethanol and incubated o/n at -20 °C.
- Next day RNA was precipitated at 15000 g for 20 min at 4 °C.
- Supernatant was removed and 1 ml of 75 % ethanol (-20 °C) added.
- After centrifugation at 15000 g, 5 min at 4 °C supernatant was removed, tube centrifuged shortly and remaining ethanol was removed.
- Pellet was air-dried for 5-10 min at RT and dissolved in 20 µl H_2O (DNAse, RNAse free) on an Eppendorf™ Thermomixer *comfort* at 56 °C for 10 min with agitation (800 rpm).
- Nucleic acid concentration was measured by Nanodrop™.
- Quality of RNA was assessed by loading 1 µl on a 1 % agarose gel and checked for degradation of rRNA bands and 1µl for a Phusion PCR reaction with genomic primers (GAPDH for mammalian cells, MR1i for *C. glabrata*), to check for genomic DNA contaminations
- Phusion PCR cycle conditions:

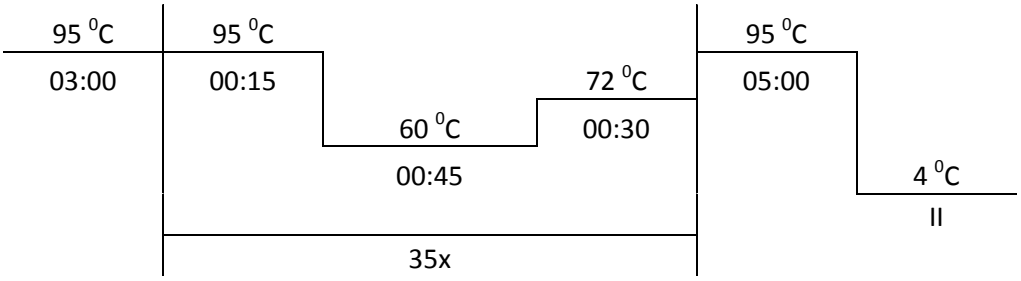

Reverse transcription

- 1 µg was used for the reverse transcription performed as stated in the Original Promega protocol

	Final concentration
MgCl2	5 mM
Reverse transcription buffer	1x
dNTPs (10 mM each)	1 mM
Ribonuclease inhibitor	20 U
Oligo (dT) primer	0,5 µg
Random primers	0,5 µg
AMV-RT	15 U/µg
RNA	1000 ng
H_2O	up to 20µl

- Reverse transcription cycle conditions:

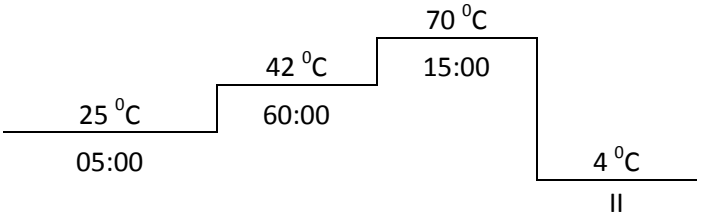

- After reverse transcription, cDNA was diluted to 3,125 ng/µl with RNAse free water

6.3.5 Quantitative real time PCR (RT-qPCR)

- Each sample was measured with technical triplicates.
- qPCR mix:

	Final concentration
Primer mix fwd/rev	10 µM each
Luna® Universal (NEB)	10µl
H_2O	Up to 15 µl

- To each well 5 µl of the cDNA (15ng) was added.
- PCR plate (twin tec. White) was sealed with Icycler iQ sheet.
- Plate was mixed for 1 minute with 500 rpm in the dark and spinned down (all steps in the dark).
- Reaction was started with the Eppendorf Mastercycler® ep realplex[4].
- RT-qPCR cycle conditions (fast cycle conditions):

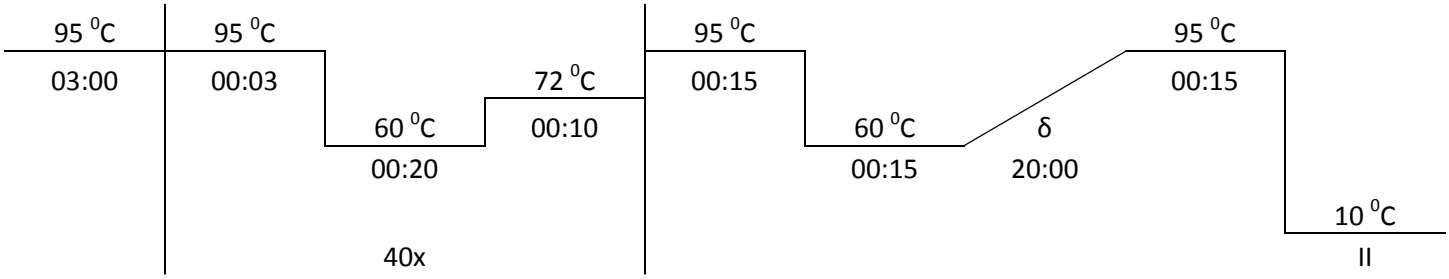

- Melting curve was analysed for eventual primer duplex formation or DNA contaminations.
- Raw Ct values were taken after QualQPlex analysis.
- Genes were analysed for the fold induction relative to untreated/uninfected control and normalized to the reference gene (ß-Actin for mammalian, Actin for *C. glabrata*).
- Double delta Ct analysis:

$$\Delta Ct_{GOI} = Ct_{exp} - \Delta Ct_{ref}$$

$$\Delta\Delta Ct_{GOI} = \Delta Ct_{untreated} - \Delta Ct_{treated}$$

$$R = 2^{-\Delta\Delta CtGOI}$$

- With GOI (Gene of interest), exp (experimental value), ref (reference gene)

Primers used

Primer	Sequence (5´-> 3´)	Purpose
mGAPDH fw	CACAGTCCATGCCATCACTG	Phusion PCR
mGAPDH rev	GAGTTGGGATAGGGCCTCTC	Phusion PCR
***CgMR1i* fw**	TGTGAAGCTTGCTCGTTCAC	Phusion PCR (binds in *CgFTR1*)
***CgMR1i* rev**	ACCCGTTGCCTTGTTGAATC	Phusion PCR (binds in *CgFTR1*)
***mßActin* fw**	CCTTCCTTCTTGGGTATGGA	RT-pPCR
***mßActin* rev**	ACGGATGTCAACGTCACACT	RT-pPCR
***mNfe2l2* fw**	TGAAGCTCAGCTCGCATTGA	RT-pPCR
***mNfe2l2* rev**	TGGGCGGCGACTTTATTCTT	RT-pPCR
***mFpn1* fw**	GTCATCCTCTGCGGAATCAT	RT-pPCR
***mFpn1* rev**	AAGGACCCATCCATGGTACA	RT-pPCR
***mBach1* fw**	TGAGTGAGAGTGCGGTATTTGC	RT-pPCR
***mBach1* rev**	GTCAGTCTGGCCTACGATTCT	RT-pPCR
***mMtf1* fw**	TTCTCACAATTGGGCTGAGCA	RT-pPCR
***mMtf1* rev**	ACCAGTCCGTTGTCATCCAC	RT-pPCR
***mSlc30a1* fw**	GCTCTCGAGTTGGTCCTGTC	RT-pPCR
***mSlc30a1* rev**	GCCTCATGGTGAGGTAGGAA	RT-pPCR
***mSlc39a4* fw**	CTTGGCTCTAGGCAAACCTG	RT-pPCR
***mSlc39a4* rev**	AGTGTGGCCAGGTAATCGTC	RT-pPCR
***mSlc39a14* fw**	CGTGGGAGCCAACTGATAAT	RT-pPCR
***mSlc39a14* rev**	AACGGCCACATTTTCAACTC	RT-pPCR
***mMT1* fw**	CACCAGATCTCGGAATGGAC	RT-pPCR
***mMT1* rev**	GTTCGTCACATCAGGCACAG	RT-pPCR
***mMT2* fw**	CCGATCTCTCGTCGATCTTC	RT-pPCR
***mMT2* rev**	ACTTGTCGGAAGCCTCTTTG	RT-pPCR
***CgSIT1* fw**	AATTGCAGCCGGTTTGTTCT	RT-pPCR
***CgSIT1* rev**	ACCCGTTGCCTTGTTGAATC	RT-pPCR
***CgFTR1* fw**	TGTCTGGGCCTCATTTGCTA	RT-pPCR
***CgFTR1* rev**	GTACAGGTAGTCAGCAGCCA	RT-pPCR

6.3.6 Protein isolation from mammalian cells

- Mϕ were prepared according to 6.2.5.
- Mϕ were seeded at 1x 10^6 cells /35 mm dish.
- *C. glabrata* cells were prepared as in 6.1.2 and added for MOI 2 (2x 10^6 cells).
- After indicated time points medium was discarded, 60 µl cell lysis buffer (RIPA buffer) was added and cells were scraped off the dish at 4 ^oC and frozen at -80 ^oC.
- Cells were sonicated 3x 15 sec ON/ 15 sec OFF at high Intensity on Bioruptor©.
- Afterwards 30 µl 4x SDS buffer was added and sample was heated to 95 ^oC for 5 min and stored again at -20 ^oC.
- Samples were thawed, heated to 95 ^oC for 1 min and centrifuged at 21000 g for 5 min at 4 ^oC.

- 10 µl were loaded on a 10 % SDS gel and run at 120 V for 1.5 h.
- Proteins were transferred via semi-dry method onto a PVDF membrane.
- 6 Whatman® papers were put in anode buffer 1 and place on the transfer machine.
- On top were 3 Whatman® with anode buffer 2.
- The PVDF membrane (15 sec activated in methanol and equilibrated in dH_2O) was placed on the stack and then the gel stuck to a Whatman® paper with cathode buffer.
- 8 more Whatman® papers sought in cathode buffer were added and transfer ran 1 h with 25 V.
- Afterwards membrane was cut around the bands and put into TBS-T.
- Membrane was blocked according to antibody data sheet, usually with 5 % skim milk/ TBS-T for 1 h with stirring at RT and washed 3x 5 min with TBS-T.
- Primary antibody was added, diluted in 5 % BSA/ TBS-T (as recommended on data sheet) o/n at 4 ^{o}C and washed 3x 5 min with TBS-T.
- Secondary antibody was either linked to HRP enzyme or Odyssey® fluorophore and developed.
- Reprobing was performed after stripping of membrane for 10 min at room temperature under constant agitation and washing 4x 5 min with TBS-T.
- Membrane was either stored in TBS at 4 ^{o}C or dried and frozen at -20 ^{o}C.

Reagents

4x SDS buffer

Tris/HCl pH 6.8	200 mM
Glycerol	40 %
SDS	8 %
Bromphenol blue	0.4 %
ß-Mercaptoethanol	freshly added to 4 %

RIPA (Radioimmunoprecipitation assay buffer)

Tris/HCl pH 8.0	50 mM
NaCl	150 mM
Triton X-100	0.1 %
Sodium deoxycholate	0.5 %
SDS	0.1 %

Sodium orthovanadate	1 mM
NaF	1 mM
Protease inhibitors tablet (Roche)	

Running buffer for SDS PAGE

Tris	25 mM
Glycin	325 mM
SDS	0.1 %

Anode buffer 1

Tris	300 mM
Methanol (added after autoclaving)	20 %

Anode buffer 2

Tris	250 mM
Methanol (added after autoclaving)	20 %

Cathode buffer

Tris	250 mM
6-Amino-n-hexanoic acid	40 mM
Methanol (added after autoclaving)	20 %

TBS (Tris-buffered saline)-T

Tris	20 mM
NaCl	150 mM
Adjusted to pH 7.6	
Tween 20	0.1 %

Stripping buffer

Tris/HCl pH 6.7	62.5 mM
SDS	2 %
β-mercaptoethanol	103 mM added immediately before usage

Antibodies used

Antibody	Company	Reference n^{0}.	Dilution
ß-Actin (8H10D10) Mouse mAb	Cell Signaling Technologies	3700	1:5000
Mouse BACH1 Antibody	R&D Systems	AF5777	1 µg/mL
NRF2 (D1Z9C) XP® Rabbit mAb	Cell Signaling Technologies	12721	1:1000

6.4 Flow cytometry analysis

6.4.1 Quenchable iron pool of macrophages

- Mϕ were prepared according to 6.2.5.
- Mϕ were seeded at 2x 10^5 cells /24-well in triplicates per condition. For each experimental condition one untreated and one FeHQ treated is set up.
- *C. glabrata* cells were prepared as in 6.1.2 and added for MOI 2 (4x 10^5 cells).
- After 8 h, medium was discarded and wells washed 3x with PBS.
- 300 µl 1 µM Calcein-AM was added to the cells and incubated at 37 ^{o}C for 15 min.
- The plate was then washed again 3x with PBS and per experimental condition either 300 µl PBS or FeHQ solution was added and incubated for 30 min at 37 ^{o}C.
- After interaction time cells were washed with PBS and macrophages were harvested with 1x Trypsin 250 µl per well (dissolved in PBS from Sigma without calcium and magnesium chloride with 50 µM EDTA) incubation at 37 ^{o}C for 5 min.
- Trypsinization was stopped by putting plate on ice and adding 2x volume ice cold DMEM+ hiFCS before pipetting cells off the dish.
- Cells were transferred and centrifuged at 400 g for 5 min at 4 ^{o}C and resuspended in 200 µl FACS buffer.
- Macrophages were then analysed for Calcein fluorescence (FITC channel) on a BD LSR Fortessa^{TM}.

Reagents

FeHQ

$FeCl_2$	5 µM in ICP-MS H_2O
8-hydroxychinoline	10 µM in DMSO

Prepared freshly 30 min before usage

FACS buffer

PBS+ 1% bovine serum albumin (BSA) and 0.02%NaN_3

6.4.2 Zinpyr-1 staining of macrophages

- Mϕ were prepared according to 6.2.5.
- Mϕ were seeded at 2x 10^5 cells /24-well in 4 technical replicates per condition.
- mCherry labelled *C. glabrata* cells were prepared as in 6.1.2 and added for MOI 2 (4x 10^5 cells).
- After indicated time points, medium was discarded and wells washed 3x with PBS.
- 300 µl 10 µM Zinpyr-1 was added to the cells and incubated at 37 ^oC for 30 min.
- The plate was washed and harvested with Trypsin as in 6.4.1.
- Cells were transferred and centrifuged at 400 g for 5 min at 4 ^oC and resuspended in 200 µl FACS buffer.
- *Candida*-positive macrophages were then gated (4.1.1) and analysed for their Zinpyr-1 fluorescence (FITC channel).

6.4.3 Fe and Zn staining of *C. glabrata*

- Mϕ were prepared according to 6.2.5.
- Mϕ were seeded at 1x 10^6 cells /6-well in 4 technical replicates per condition.
- Before infection the medium was changed to DMEM.
- mCherry labelled *C. glabrata* cells were prepared as in 6.1.2 and added for MOI 1 (1x 10^6 cells).
- After indicated time points, medium was discarded and wells washed 3x with 2 ml PBS.

- 1 ml 0.005 % SDS/H_2O (ICP-MS grade) was added and incubated for 15 min on ice.
- Cells were then harvested by pipetting cells off the dish and vortexed 3x 10 sec with ice incubation in between. Cells were then split for either Calcein-AM or Zinpyr-1 (ZP-1) staining.
- Cells were centrifuged for 10 min with 21000 g at 4 ^{o}C, supernatant discarded and again centrifuged for 2 min to get rid of every supernatant.
- *Candida* cells were placed at RT and either
    - 5 µl of Calcein-AM (1 mM) was added
    - 20 µl of ZP-1 (500 µM) was added
- Tubes were then put on 30 ^{o}C at 850 rpm in the dark for 2 hours.
- Few µl were transferred into 300 µl FACS buffer and signal was analysed with FITC channel

6.4.4 Live-dead assay

- Mϕ were prepared according to 6.2.5.
- Mϕ were seeded at 2,5x 10^5 cells /24-well in triplicates in 300 µl Mϕ media.
- *C. glabrata* cells were prepared as in 6.1.2 and added for MOI 2 (5x 10^5 cells) in 50 µl.
- After respective time points, medium was discarded and cells stained with 300 µl/well 10 µM ZP-1 in PBS for 30 min at 37 ^{o}C.
- Wells were washed 3x with PBS and put on ice.
- 300 µl 0.2% Triton-X were added and incubated for 15 min at 4 ^{o}C.
- Then 700 µl PBS were added and *Candida* cells harvested by pipetting them off.
- Cells were centrifuged for 2 min with 21000 g at 4 ^{o}C, supernatant discarded cells resuspended in 200 µl propidium iodide (PI) 2 µg/ml in PBS for 5 min in the dark at RT.
- Cells were centrifuged for 2 min with 21000 g at 4 ^{o}C.
- Washed once with 900 µl PBS and resuspended in 400 µl PBS to analyse by flow cytometry (4.3.3)

6.5 Intraperitoneal infection

- *C. glabrata* wild-type and *sit1*Δ *ftr1*cΔ cells were prepared as in 6.1.2 and resuspended in PBS from Sigma without calcium and magnesium chloride.
- 5* 10^7 cells/ 25 g mouse weight was administered into the peritoneum of wild-type C57BL/6J mice.

- After 24 hours, mice were sacrificed by cervical dislocation, the peritoneum was flushed with 10 ml PBS and lavage was then diluted accordingly and plated on YPD plates to count viable CFUs.

6.6 Statistics

Flow cytometry data was analysed with FlowJo Version 7.6.5 and all subsequent statistical analysis and graphics preparation was performed with GraphPad Prism 5 (Release 5.04) both for windows. Figures were then further prepared with Adobe Illustrator CS5 (Product improvement program 5.0.0.2021; Version 15.0.0). Nonparametric unpaired, two-tailed, students t-test from GraphPad Prism 5 software was used for all statistical analysis. In all figures: Data points and bars indicate mean ± SD; * p-value < 0.05; ** p-value < 0.01; *** p-value < 0.001.

6.7 Abbreviations

In order of appearance

COPD	Chronic obstructive pulmonary disease
PAMP	Pathogen-associated molecular pattern
PRR	Pattern recognition receptor
IRF	Interferon-regulatory factors
pDCs	Plasmacytoid dendritic cells
ROS	Reactive oxygen species
LIP	Labile iron pool
MT	Methallothioneins
BMDMs	Bone marrow-derived macrophages
LIP	Labile iron pool
QIP	Quenchable iron pool
JAK	Janus kinases
STAT	Signal transducer and activator of transcription
TF	Transcription factor
NO	Reactive nitrogen species
MARE	MAF-associated responsive elements

7. References

Almeida, R. S., Wilson, D. and Hube, B. (2009) '*Candida albicans* iron acquisition within the host', *FEMS Yeast Research*. doi: 10.1111/j.1567-1364.2009.00570.x.

Amulic, B. *et al.* (2012) 'Neutrophil Function: From Mechanisms to Disease', *Annual Review of Immunology*. Annual Reviews , 30(1), pp. 459–489. doi: 10.1146/annurev-immunol-020711-074942.

Anderson, C. P. *et al.* (2012) 'Mammalian iron metabolism and its control by iron regulatory proteins', *Biochimica et Biophysica Acta (BBA) - Molecular Cell Research*. Elsevier, 1823(9), pp. 1468–1483. doi: 10.1016/J.BBAMCR.2012.05.010.

Andreini, C. *et al.* (2008) 'Metal ions in biological catalysis: from enzyme databases to general principles', *JBIC Journal of Biological Inorganic Chemistry*. Springer-Verlag, 13(8), pp. 1205–1218. doi: 10.1007/s00775-008-0404-5.

Andrews, N. C. (2008) 'Forging a field: the golden age of iron biology.', *Blood*. American Society of Hematology, 112(2), pp. 219–30. doi: 10.1182/blood-2007-12-077388.

Aratani, Y. *et al.* (2002) 'Critical Role of Myeloperoxidase and Nicotinamide Adenine Dinucleotide Phosphate–Oxidase in High-Burden Systemic Infection of Mice with *Candida albicans*', *The Journal of Infectious Diseases*. Narnia, 185(12), pp. 1833–1837. doi: 10.1086/340635.

Arezes, J. *et al.* (2015) 'Hepcidin-Induced Hypoferremia Is a Critical Host Defense Mechanism against the Siderophilic Bacterium Vibrio vulnificus', *Cell Host & Microbe*, 17(1), pp. 47–57. doi: 10.1016/j.chom.2014.12.001.

Ashino, T. *et al.* (2008) 'Negative feedback regulation of lipopolysaccharide-induced inducible nitric oxide synthase gene expression by heme oxygenase-1 induction in macrophages', *Molecular Immunology*. Pergamon, 45(7), pp. 2106–2115. doi: 10.1016/J.MOLIMM.2007.10.011.

Bairwa, G., Hee Jung, W. and Kronstad, J. W. (2017) 'Iron acquisition in fungal pathogens of humans', *Metallomics : integrated biometal science*. The Royal Society of Chemistry, pp. 215–227. doi: 10.1039/c6mt00301j.

Begum, N. A. *et al.* (2002) 'Mycobacterium bovis BCG Cell Wall and Lipopolysaccharide Induce a Novel Gene, BIGM103, Encoding a 7-TM Protein: Identification of a New Protein Family Having Zn-Transporter and Zn-Metalloprotease Signatures'. doi: 10.1006/geno.2002.7000.

Biondo, C. *et al.* (2011) 'Recognition of yeast nucleic acids triggers a host-protective type I interferon response', *European Journal of Immunology*. John Wiley & Sons, Ltd, 41(7), pp. 1969–1979. doi: 10.1002/eji.201141490.

Biondo, C. *et al.* (2012) 'Recognition of fungal RNA by TLR7 has a nonredundant role in host defense against experimental candidiasis', *European Journal of Immunology*. John Wiley & Sons, Ltd, 42(10), pp. 2632–2643. doi: 10.1002/eji.201242532.

Bistoni, F. *et al.* (1988) 'Immunomodulation by a low-virulence, agerminative variant of Candida albicans. Further evidence for macrophage activation as one of the effector mechanisms of nonspecific anti-infectious

protection.', *Journal of medical and veterinary mycology : bi-monthly publication of the International Society for Human and Animal Mycology*, 26(5), pp. 285–99. Available at: http://www.ncbi.nlm.nih.gov/pubmed/2853217 (Accessed: 4 July 2019).

Boltz-Nitulescu, G. *et al.* (1987) 'Differentiation of Rat Bone Marrow Cells Into Macrophages Under the Influence of Mouse L929 Cell Supernatant', *Journal of Leukocyte Biology*, 41(1), pp. 83–91. doi: 10.1002/jlb.41.1.83.

Bongomin, F. *et al.* (2017) 'Global and Multi-National Prevalence of Fungal Diseases-Estimate Precision.', *Journal of fungi (Basel, Switzerland)*. Multidisciplinary Digital Publishing Institute (MDPI), 3(4). doi: 10.3390/jof3040057.

Botella, H. *et al.* (2011) 'Mycobacterial P1-Type ATPases Mediate Resistance to Zinc Poisoning in Human Macrophages', *Cell Host & Microbe*. Cell Press, 10(3), pp. 248–259. doi: 10.1016/J.CHOM.2011.08.006.

Bourgeois, C. *et al.* (2010) 'Fungal attacks on mammalian hosts: pathogen elimination requires sensing and tasting', *Current Opinion in Microbiology*. Elsevier Current Trends, 13(4), pp. 401–408. doi: 10.1016/J.MIB.2010.05.004.

Bourgeois, C. *et al.* (2011) 'Conventional dendritic cells mount a type I IFN response against Candida spp. requiring novel phagosomal TLR7-mediated IFN-β signaling.', *Journal of immunology (Baltimore, Md. : 1950)*. American Association of Immunologists, 186(5), pp. 3104–12. doi: 10.4049/jimmunol.1002599.

Bradford, L. L. and Ravel, J. (2017) 'The vaginal mycobiome: A contemporary perspective on fungi in women's health and diseases', *Virulence*. Taylor & Francis, 8(3), pp. 342–351. doi: 10.1080/21505594.2016.1237332.

Brechting, P. J. *et al.* (2019) 'Histoplasma Responses to Nutritional Immunity Imposed by Macrophage Activation', *Journal of Fungi*. Multidisciplinary Digital Publishing Institute, 5(2), p. 45. doi: 10.3390/jof5020045.

Brown, G. D. *et al.* (2012) 'Hidden killers: human fungal infections.', *Science translational medicine*. American Association for the Advancement of Science, 4(165), p. 165rv13. doi: 10.1126/scitranslmed.3004404.

Butler, G. *et al.* (2009) 'Evolution of pathogenicity and sexual reproduction in eight Candida genomes', *Nature*. doi: 10.1038/nature08064.

Byrd, T. F. and Horwitz, M. A. (1993) 'Regulation of transferrin receptor expression and ferritin content in human mononuclear phagocytes. Coordinate upregulation by iron transferrin and downregulation by interferon gamma.', *The Journal of clinical investigation*. American Society for Clinical Investigation, 91(3), pp. 969–76. doi: 10.1172/JCI116318.

Cabantchik, Z. I. (2014) 'Labile iron in cells and body fluids: Physiology, pathology, and pharmacology', *Frontiers in Pharmacology*. doi: 10.3389/fphar.2014.00045.

Canonne-Hergaux, F. *et al.* (1999) 'The Nramp1 Protein and Its Role in Resistance to Infection and Macrophage Function', *Proceedings of the Association of American Physicians*. John Wiley & Sons, Ltd (10.1111), 111(4), pp. 283–289. doi: 10.1046/j.1525-1381.1999.99236.x.

Carreté, L. *et al.* (2018) 'Patterns of Genomic Variation in the Opportunistic Pathogen Candida glabrata Suggest the Existence of Mating and a Secondary Association with Humans', *Current Biology*, 28(1), pp. 15-27.e7. doi:

10.1016/j.cub.2017.11.027.

Casanova, J.-L., Holland, S. M. and Notarangelo, L. D. (2012) 'Inborn errors of human JAKs and STATs.', *Immunity*. NIH Public Access, 36(4), pp. 515–28. doi: 10.1016/j.immuni.2012.03.016.

Chaplin, D. D. (2010) 'Overview of the immune response.', *The Journal of allergy and clinical immunology*. NIH Public Access, 125(2 Suppl 2), pp. S3-23. doi: 10.1016/j.jaci.2009.12.980.

Chapple, S. J. *et al.* (2016) 'Bach1 differentially regulates distinct Nrf2-dependent genes in human venous and coronary artery endothelial cells adapted to physiological oxygen levels', *Free Radical Biology and Medicine*, 92, pp. 152–162. doi: 10.1016/j.freeradbiomed.2015.12.013.

Claudia Andreini *et al.* (2006) 'Zinc through the Three Domains of Life'. American Chemical Society . doi: 10.1021/PR0603699.

Claudia Andreini *et al.* (2005) 'Counting the Zinc-Proteins Encoded in the Human Genome'. American Chemical Society. doi: 10.1021/PR050361J.

Cowart, R. E., Singleton, F. L. and Hind, J. S. (1993) 'A Comparison of Bathophenanthrolinedisulfonic Acid and Ferrozine as Chelators of Iron(II) in Reduction Reactions', *Analytical Biochemistry*. Academic Press, 211(1), pp. 151–155. doi: 10.1006/ABIO.1993.1246.

Crawford, A. C. *et al.* (2018) 'Biphasic zinc compartmentalisation in a human fungal pathogen.', *PLoS pathogens*. Public Library of Science, 14(5), p. e1007013. doi: 10.1371/journal.ppat.1007013.

Crawford, A. and Wilson, D. (2015) 'Essential metals at the host-pathogen interface: Nutritional immunity and micronutrient assimilation by human fungal pathogens', *FEMS Yeast Research*. doi: 10.1093/femsyr/fov071.

Cuéllar-Cruz, M. *et al.* (2014) 'Differential Response of Candida albicans and Candida glabrata to Oxidative and Nitrosative Stresses', *Current Microbiology*. Springer US, 69(5), pp. 733–739. doi: 10.1007/s00284-014-0651-3.

Davidson, S., Maini, M. K. and Wack, A. (2015) 'Disease-promoting effects of type I interferons in viral, bacterial, and coinfections.', *Journal of interferon & cytokine research : the official journal of the International Society for Interferon and Cytokine Research*. Mary Ann Liebert, Inc., 35(4), pp. 252–64. doi: 10.1089/jir.2014.0227.

Decker, T., Müller, M. and Stockinger, S. (2005) 'The Yin and Yang of type I interferon activity in bacterial infection', *Nature Reviews Immunology*. Nature Publishing Group, 5(9), pp. 675–687. doi: 10.1038/nri1684.

del Fresno, C. *et al.* (2013) 'Interferon-β Production via Dectin-1-Syk-IRF5 Signaling in Dendritic Cells Is Crucial for Immunity to C. albicans', *Immunity*. Cell Press, 38(6), pp. 1176–1186. doi: 10.1016/J.IMMUNI.2013.05.010.

Dementhon, K., El-Kirat-Chatel, S. and Noël, T. (2012) 'Development of an in vitro model for the multi-parametric quantification of the cellular interactions between Candida yeasts and phagocytes.', *PloS one*. Public Library of Science, 7(3), p. e32621. doi: 10.1371/journal.pone.0032621.

Dufner-Beattie, J. *et al.* (2003) 'The acrodermatitis enteropathica gene ZIP4 encodes a tissue-specific, zinc-regulated zinc transporter in mice.', *The Journal of biological chemistry*. American Society for Biochemistry and Molecular Biology, 278(35), pp. 33474–81. doi: 10.1074/jbc.M305000200.

Duggan, S. *et al.* (2015) 'Host response to Candida albicans bloodstream infection and sepsis.', *Virulence*. Taylor & Francis, 6(4), pp. 316–26. doi: 10.4161/21505594.2014.988096.

Dujon, B. *et al.* (2004) 'Genome evolution in yeasts', *Nature*. Nature Publishing Group, 430(6995), pp. 35–44. doi: 10.1038/nature02579.

Eide, D. J. (2006) 'Zinc transporters and the cellular trafficking of zinc', *Biochimica et Biophysica Acta (BBA) - Molecular Cell Research*. Elsevier, 1763(7), pp. 711–722. doi: 10.1016/J.BBAMCR.2006.03.005.

Epelman, S., Lavine, K. J. and Randolph, G. J. (2014) 'Origin and functions of tissue macrophages.', *Immunity*. NIH Public Access, 41(1), pp. 21–35. doi: 10.1016/j.immuni.2014.06.013.

Erwig, L. P. and Gow, N. A. R. (2016) 'Interactions of fungal pathogens with phagocytes', *Nature Reviews Microbiology*. Nature Publishing Group, 14(3), pp. 163–176. doi: 10.1038/nrmicro.2015.21.

Espósito, B. P. *et al.* (2002) 'A Review of Fluorescence Methods for Assessing Labile Iron in Cells and Biological Fluids', *Analytical Biochemistry*. Academic Press, 304(1), pp. 1–18. doi: 10.1006/ABIO.2002.5611.

Fidel, P. L. *et al.* (1996) 'A Murine Model of Candida glabrata Vaginitis', *Journal of Infectious Diseases*, 173(2), pp. 425–431. doi: 10.1093/infdis/173.2.425.

Fidel, P. L., Vazquez, J. A. and Sobel, J. D. (1999) 'Candida glabrata: review of epidemiology, pathogenesis, and clinical disease with comparison to C. albicans.', *Clinical microbiology reviews*. American Society for Microbiology Journals, 12(1), pp. 80–96. doi: 10.1128/CMR.12.1.80.

Finkelstein, J. (2009) 'Metalloproteins', *Nature*, 460(7257), pp. 813–813. doi: 10.1038/460813a.

Fortier, A. *et al.* (2005) 'Single gene effects in mouse models of host: pathogen interactions', *Journal of Leukocyte Biology*. John Wiley & Sons, Ltd, 77(6), pp. 868–877. doi: 10.1189/jlb.1004616.

Frey, P. A. and Reed, G. H. (2012) 'The Ubiquity of Iron', *ACS Chemical Biology*. American Chemical Society, 7(9), pp. 1477–1481. doi: 10.1021/cb300323q.

Fritsche, G. *et al.* (2003) 'Nramp1 functionality increases inducible nitric oxide synthase transcription via stimulation of IFN regulatory factor 1 expression.', *Journal of immunology (Baltimore, Md. : 1950)*. American Association of Immunologists, 171(4), pp. 1994–8. doi: 10.4049/jimmunol.171.4.1994.

Ganz, T. (2009) 'Iron in innate immunity: starve the invaders.', *Current opinion in immunology*. NIH Public Access, 21(1), pp. 63–7. doi: 10.1016/j.coi.2009.01.011.

Ganz, T. and Nemeth, E. (2015) 'Iron homeostasis in host defence and inflammation', *Nature Reviews Immunology*. Nature Publishing Group, 15(8), pp. 500–510. doi: 10.1038/nri3863.

Gao, H. *et al.* (2018) 'The Role of Zinc and Zinc Homeostasis in Macrophage Function', *Journal of Immunology Research*. Hindawi, 2018, pp. 1–11. doi: 10.1155/2018/6872621.

Gerwien, F. *et al.* (2016) 'A Novel Hybrid Iron Regulation Network Combines Features from Pathogenic and Nonpathogenic Yeasts', *mBio*. American Society for Microbiology, 7(5), pp. e01782-16. doi: 10.1128/mbio.01782-16.

Gerwien, F. *et al.* (2017) 'The fungal pathogen Candida glabrata does not depend on surface ferric reductases for iron acquisition', *Frontiers in Microbiology*. Frontiers Media SA, 8(JUN), p. 1055. doi: 10.3389/fmicb.2017.01055.

Gerwien, F. *et al.* (2018) 'Metals in fungal virulence', *FEMS Microbiology Reviews*. Oxford University Press, 42(1). doi: 10.1093/FEMSRE/FUX050.

Gilbert, A. S., Wheeler, R. T. and May, R. C. (2015) 'Fungal Pathogens: Survival and Replication within Macrophages'. doi: 10.1101/cshperspect.a019661.

Gilbert, J. A. *et al.* (2018) 'Current understanding of the human microbiome', *Nature Medicine*. Nature Publishing Group, 24(4), pp. 392–400. doi: 10.1038/nm.4517.

Ginhoux, F. and Guilliams, M. (2016) 'Review Tissue-Resident Macrophage Ontogeny and Homeostasis', *Immunity*, 44, pp. 439–449. doi: 10.1016/j.immuni.2016.02.024.

Guevara-Ortiz, J. M. *et al.* (2005) 'Interferon alpha induction of metallothionein in rat liver is not linked to interleukin-1, interleukin-6, or tumor necrosis factor alpha', *Experimental and Molecular Pathology*. Academic Press, 79(1), pp. 33–38. doi: 10.1016/J.YEXMP.2005.02.005.

Gunsalus, I. C. *et al.* (1977) 'Oxygen Sensing Heme Proteins: Monoxygenases, Myoglobin and Hemoglobin', in. Springer, Boston, MA, pp. 37–50. doi: 10.1007/978-1-4615-9035-4_3.

Haas, A. (2007) 'The Phagosome: Compartment with a License to Kill', *Traffic*. John Wiley & Sons, Ltd (10.1111), 8(4), pp. 311–330. doi: 10.1111/j.1600-0854.2006.00531.x.

Hallen-Adams, H. E. and Suhr, M. J. (2017) 'Fungi in the healthy human gastrointestinal tract.', *Virulence*. Taylor & Francis, 8(3), pp. 352–358. doi: 10.1080/21505594.2016.1247140.

Havlickova, B., Czaika, V. A. and Friedrich, M. (2008) 'Epidemiological trends in skin mycoses worldwide', *Mycoses*, 51, pp. 2–15. doi: 10.1111/j.1439-0507.2008.01606.x.

Hayes, J. D. and Dinkova-Kostova, A. T. (2014) 'The Nrf2 regulatory network provides an interface between redox and intermediary metabolism', *Trends in Biochemical Sciences*. Elsevier Current Trends, 39(4), pp. 199–218. doi: 10.1016/J.TIBS.2014.02.002.

Helmerhorst, E. J. *et al.* (2005) 'Candida glabrata is unusual with respect to its resistance to cationic antifungal proteins', *Yeast*. John Wiley & Sons, Ltd, 22(9), pp. 705–714. doi: 10.1002/yea.1241.

Honda, K., Takaoka, A. and Taniguchi, T. (2006) 'Type I Inteferon Gene Induction by the Interferon Regulatory Factor Family of Transcription Factors', *Immunity*. Cell Press, 25(3), pp. 349–360. doi: 10.1016/J.IMMUNI.2006.08.009.

Hood, M. I. and Skaar, E. P. (2012) 'Nutritional immunity: Transition metals at the pathogen-host interface', *Nature Reviews Microbiology*. NIH Public Access, pp. 525–537. doi: 10.1038/nrmicro2836.

Hope, W. W., Walsh, T. J. and Denning, D. W. (2005) 'The invasive and saprophytic syndromes due to *Aspergillus* spp.', *Medical Mycology*, 43(s1), pp. 207–238. doi: 10.1080/13693780400025179.

Hor, L.-I. *et al.* (2000) 'Mechanism of High Susceptibility of Iron-Overloaded Mouse to *Vibrio vulnificus* Infection', *Microbiology and Immunology*. John Wiley & Sons, Ltd (10.1111), 44(11), pp. 871–878. doi: 10.1111/j.1348-0421.2000.tb02577.x.

Ichiki, K. *et al.* (2014) 'Upregulation of iron regulatory hormone hepcidin by interferon α', *Journal of Gastroenterology and Hepatology*. John Wiley & Sons, Ltd (10.1111), 29(2), pp. 387–394. doi: 10.1111/jgh.12348.

Imlay, J. A. (2014) 'The mismetallation of enzymes during oxidative stress.', *The Journal of biological chemistry*. American Society for Biochemistry and Molecular Biology, 289(41), pp. 28121–8. doi: 10.1074/jbc.R114.588814.

Isaacs, A. and Lindenmann, J. (1957) 'Virus interference. I. The interferon', *Proceedings of the Royal Society of London. Series B - Biological Sciences*, 147(927), pp. 258–267. doi: 10.1098/rspb.1957.0048.

Ivashkiv, L. B. and Donlin, L. T. (2014) 'Regulation of type I interferon responses', *Nature Reviews Immunology*. Nature Publishing Group, 14(1), pp. 36–49. doi: 10.1038/nri3581.

Jacobsen, I. D. *et al.* (2010) 'Candida glabrata persistence in mice does not depend on host immunosuppression and is unaffected by fungal amino acid auxotrophy.', *Infection and immunity*. American Society for Microbiology Journals, 78(3), pp. 1066–77. doi: 10.1128/IAI.01244-09.

Jan Kullberg Franck Amiot, B. *et al.* (2019) *Candida albicans of Recruitment of Neutrophils and Phagocytosis Systemic Candidiasis Through Impaired Double Knockout Mice to α Lymphotoxin-α Increased Susceptibility of TNF*, *J Immunol References*. Available at: http://www.jimmunol.org/content/163/3/http://www.jimmunol.org/content/163/3/1498.full#ref-list-1 (Accessed: 7 July 2019).

Kalliolias, G. D. and Ivashkiv, L. B. (2010) 'Overview of the biology of type I interferons.', *Arthritis research & therapy*. BioMed Central, 12 Suppl 1(Suppl 1), p. S1. doi: 10.1186/ar2881.

Kasper, L. *et al.* (2014) 'Identification of Candida glabrata genes involved in pH modulation and modification of the phagosomal environment in macrophages.', *PloS one*. Public Library of Science, 9(5), p. e96015. doi: 10.1371/journal.pone.0096015.

Kasper, L., Seider, K. and Hube, B. (2015) 'Intracellular survival of *Candida glabrata* in macrophages: immune evasion and persistence', *FEMS Yeast Research*. Edited by M. Bolotin-Fukuhara. Narnia, 15(5), p. fov042. doi: 10.1093/femsyr/fov042.

Kernien, J. F. *et al.* (2017) 'The Interface between Fungal Biofilms and Innate Immunity', *Frontiers in Immunology*. Frontiers Media SA, 8. doi: 10.3389/FIMMU.2017.01968.

Kim, S. and Ponka, P. (2000) 'Effects of interferon-gamma and lipopolysaccharide on macrophage iron metabolism are mediated by nitric oxide-induced degradation of iron regulatory protein 2.', *The Journal of biological chemistry*. American Society for Biochemistry and Molecular Biology, 275(9), pp. 6220–6. doi: 10.1074/jbc.275.9.6220.

King, J. C., Shames, D. M. and Woodhouse, L. R. (2000) 'Zinc Homeostasis in Humans', *The Journal of Nutrition*. Narnia, 130(5), pp. 1360S-1366S. doi: 10.1093/jn/130.5.1360S.

Kitamura, H. *et al.* (2006) 'Toll-like receptor–mediated regulation of zinc homeostasis influences dendritic cell function', *Nature Immunology*. Nature Publishing Group, 7(9), pp. 971–977. doi: 10.1038/ni1373.

Kornitzer, D. (2009) 'Fungal mechanisms for host iron acquisition', *Current Opinion in Microbiology*. Elsevier Current Trends, 12(4), pp. 377–383. doi: 10.1016/J.MIB.2009.05.005.

Kumar, K. *et al.* (2019) 'Candida glabrata: A Lot More Than Meets the Eye', *Microorganisms*. Multidisciplinary Digital Publishing Institute, 7(2), p. 39. doi: 10.3390/microorganisms7020039.

Küry, S. *et al.* (2002) 'Identification of SLC39A4, a gene involved in acrodermatitis enteropathica', *Nature Genetics*. Nature Publishing Group, 31(3), pp. 239–240. doi: 10.1038/ng913.

Lahiri, A. and Abraham, C. (2014) 'Activation of pattern recognition receptors up-regulates metallothioneins, thereby increasing intracellular accumulation of zinc, autophagy, and bacterial clearance by macrophages.', *Gastroenterology*. NIH Public Access, 147(4), pp. 835–46. doi: 10.1053/j.gastro.2014.06.024.

Lane, D. J. R. *et al.* (2015) 'Cellular iron uptake, trafficking and metabolism: Key molecules and mechanisms and their roles in disease', *Biochimica et Biophysica Acta (BBA) - Molecular Cell Research*. Elsevier, 1853(5), pp. 1130–1144. doi: 10.1016/J.BBAMCR.2015.01.021.

Leal, S. M. *et al.* (2013) 'Targeting Iron Acquisition Blocks Infection with the Fungal Pathogens Aspergillus fumigatus and Fusarium oxysporum', *PLoS Pathogens*. Edited by M. Feldmesser. Public Library of Science, 9(7), p. e1003436. doi: 10.1371/journal.ppat.1003436.

Leidgens, S. *et al.* (2013) 'Each member of the poly-r(C)-binding protein 1 (PCBP) family exhibits iron chaperone activity toward ferritin.', *The Journal of biological chemistry*. American Society for Biochemistry and Molecular Biology, 288(24), pp. 17791–802. doi: 10.1074/jbc.M113.460253.

Ley, K. (2017) 'M1 Means Kill; M2 Means Heal', *The Journal of Immunology*. The American Association of Immunologists, 199(7), pp. 2191–2193. doi: 10.4049/jimmunol.1701135.

Lichten, L. A. and Cousins, R. J. (2009) 'Mammalian Zinc Transporters: Nutritional and Physiologic Regulation', *Annual Review of Nutrition*, 29(1), pp. 153–176. doi: 10.1146/annurev-nutr-033009-083312.

Lionakis, M. S., Iliev, I. D. and Hohl, T. M. (2017) 'Immunity against fungi.', *JCI insight*. American Society for Clinical Investigation, 2(11). doi: 10.1172/jci.insight.93156.

Liu, L. *et al.* (2011) 'Gain-of-function human STAT1 mutations impair IL-17 immunity and underlie chronic mucocutaneous candidiasis.', *The Journal of experimental medicine*. The Rockefeller University Press, 208(8), pp. 1635–48. doi: 10.1084/jem.20110958.

Liu, X. and Theil, E. C. (2005) 'Ferritin as an Iron Concentrator and Chelator Target', *Ann. N.Y. Acad. Sci*, 1054, pp. 136–140. doi: 10.1196/annals.1345.016.

Liuzzi, J. P. *et al.* (2005) 'Interleukin-6 regulates the zinc transporter Zip14 in liver and contributes to the hypozincemia of the acute-phase response.', *Proceedings of the National Academy of Sciences of the United States of America*. National Academy of Sciences, 102(19), pp. 6843–8. doi: 10.1073/pnas.0502257102.

López de Padilla, C. M. and Niewold, T. B. (2016) 'The type I interferons: Basic concepts and clinical relevance in

immune-mediated inflammatory diseases.', *Gene*. NIH Public Access, 576(1 Pt 1), pp. 14–21. doi: 10.1016/j.gene.2015.09.058.

Majer, O. *et al.* (2012) 'Type I interferons promote fatal immunopathology by regulating inflammatory monocytes and neutrophils during Candida infections.', *PLoS pathogens*. Public Library of Science, 8(7), p. e1002811. doi: 10.1371/journal.ppat.1002811.

Majoros, A. *et al.* (2017) 'Canonical and Non-Canonical Aspects of JAK–STAT Signaling: Lessons from Interferons for Cytokine Responses', *Frontiers in Immunology*. Frontiers, 8, p. 29. doi: 10.3389/fimmu.2017.00029.

Malavia, D., Crawford, A. and Wilson, D. (2017) 'Nutritional Immunity and Fungal Pathogenesis: The Struggle for Micronutrients at the Host–Pathogen Interface', in *Advances in Microbial Physiology*. doi: 10.1016/bs.ampbs.2017.01.006.

Maret, W. (2006) 'Zinc Coordination Environments in Proteins as Redox Sensors and Signal Transducers', *Antioxidants & Redox Signaling*, 8(9–10), pp. 1419–1441. doi: 10.1089/ars.2006.8.1419.

Marro, S. *et al.* (2010) 'Heme controls ferroportin1 (FPN1) transcription involving Bach1, Nrf2 and a MARE/ARE sequence motif at position -7007 of the FPN1 promoter.', *Haematologica*. Haematologica, 95(8), pp. 1261–8. doi: 10.3324/haematol.2009.020123.

McNab, F. *et al.* (2015) 'Type I interferons in infectious disease', *Nature Reviews Immunology*. Nature Publishing Group, 15(2), pp. 87–103. doi: 10.1038/nri3787.

Mencacci, A. *et al.* (1997) 'Iron Overload Alters Innate and T Helper Cell Responses to *Candida albicans* in Mice', *The Journal of Infectious Diseases*. Narnia, 175(6), pp. 1467–1476. doi: 10.1086/516481.

Miceli, M. H., Díaz, J. A. and Lee, S. A. (2011) 'Emerging opportunistic yeast infections', *The Lancet Infectious Diseases*. Elsevier, 11(2), pp. 142–151. doi: 10.1016/S1473-3099(10)70218-8.

Minematsu, A. *et al.* (2019) 'Vacuolar proton-translocating ATPase is required for antifungal resistance and virulence of Candida glabrata.', *PloS one*. Public Library of Science, 14(1), p. e0210883. doi: 10.1371/journal.pone.0210883.

Nairz, M. *et al.* (2008) 'Interferon-γ limits the availability of iron for intramacrophage *Salmonella typhimurium*', *European Journal of Immunology*. John Wiley & Sons, Ltd, 38(7), pp. 1923–1936. doi: 10.1002/eji.200738056.

Nairz, M. *et al.* (2009) 'Slc11a1 limits intracellular growth of Salmonella enterica sv. Typhimurium by promoting macrophage immune effector functions and impairing bacterial iron acquisition.', *Cellular microbiology*. NIH Public Access, 11(9), pp. 1365–81. doi: 10.1111/j.1462-5822.2009.01337.x.

Nairz, M. *et al.* (2013) 'Nitric oxide-mediated regulation of ferroportin-1 controls macrophage iron homeostasis and immune function in Salmonella infection.', *The Journal of experimental medicine*. The Rockefeller University Press, 210(5), pp. 855–73. doi: 10.1084/jem.20121946.

Nairz, M. *et al.* (2014) 'Iron at the interface of immunity and infection.', *Frontiers in pharmacology*. Frontiers Media SA, 5, p. 152. doi: 10.3389/fphar.2014.00152.

Nakayama, H. *et al.* (1998) 'A controllable gene-expression system for the pathogenic fungus Candida glabrata',

Microbiology. Microbiology Society, 144(9), pp. 2407–2415. doi: 10.1099/00221287-144-9-2407.

Nemeth, E., Tuttle, M. S., *et al.* (2004) 'Hepcidin regulates cellular iron efflux by binding to ferroportin and inducing its internalization.', *Science (New York, N.Y.)*. American Association for the Advancement of Science, 306(5704), pp. 2090–3. doi: 10.1126/science.1104742.

Nemeth, E., Rivera, S., *et al.* (2004) 'IL-6 mediates hypoferremia of inflammation by inducing the synthesis of the iron regulatory hormone hepcidin.', *The Journal of clinical investigation*. American Society for Clinical Investigation, 113(9), pp. 1271–6. doi: 10.1172/JCI20945.

Netea, M. G. *et al.* (2015) 'Immune defence against Candida fungal infections', *Nature Reviews Immunology*. Nature Publishing Group, 15(10), pp. 630–642. doi: 10.1038/nri3897.

Netea, M. G., Quintin, J. and van der Meer, J. W. M. (2011) 'Trained Immunity: A Memory for Innate Host Defense', *Cell Host & Microbe*. Cell Press, 9(5), pp. 355–361. doi: 10.1016/J.CHOM.2011.04.006.

Nevitt, T. and Thiele, D. J. (2011) 'Host iron withholding demands siderophore utilization for Candida glabrata to survive macrophage killing', *PLoS Pathogens*. Edited by T. L. Doering. Public Library of Science, 7(3), p. e1001322. doi: 10.1371/journal.ppat.1001322.

Nicolas, G. *et al.* (2002) 'The gene encoding the iron regulatory peptide hepcidin is regulated by anemia, hypoxia, and inflammation.', *The Journal of clinical investigation*. American Society for Clinical Investigation, 110(7), pp. 1037–44. doi: 10.1172/JCI15686.

Ogawa, K. *et al.* (2001) 'Heme mediates derepression of Maf recognition element through direct binding to transcription repressor Bach1', *The EMBO Journal*. John Wiley & Sons, Ltd, 20(11), pp. 2835–2843. doi: 10.1093/emboj/20.11.2835.

Ostrosky-Zeichner, L. *et al.* (2005) 'Multicenter Clinical Evaluation of the (1->3) -D-Glucan Assay as an Aid to Diagnosis of Fungal Infections in Humans', *Clinical Infectious Diseases*, 41(5), pp. 654–659. doi: 10.1086/432470.

Pantopoulos, K. *et al.* (2012) 'Mechanisms of mammalian iron homeostasis.', *Biochemistry*. NIH Public Access, 51(29), pp. 5705–24. doi: 10.1021/bi300752r.

Pestka, S., Krause, C. D. and Walter, M. R. (2004) 'Interferons, interferon-like cytokines, and their receptors', *Immunological Reviews*. John Wiley & Sons, Ltd (10.1111), 202(1), pp. 8–32. doi: 10.1111/j.0105-2896.2004.00204.x.

Petrat, F. *et al.* (2002) 'The Chelatable Iron Pool in Living Cells: A Methodically Defined Quantity', *Biological Chemistry*. Walter de Gruyter, 383(3–4), pp. 489–502. doi: 10.1515/BC.2002.051.

Pfaller, M. A. *et al.* (2010) 'Geographic variation in the frequency of isolation and fluconazole and voriconazole susceptibilities of Candida glabrata: an assessment from the ARTEMIS DISK Global Antifungal Surveillance Program', *Diagnostic Microbiology and Infectious Disease*. Elsevier, 67(2), pp. 162–171. doi: 10.1016/J.DIAGMICROBIO.2010.01.002.

Philpott, C. C. and Ryu, M.-S. (2014) 'Special delivery: distributing iron in the cytosol of mammalian cells.', *Frontiers in pharmacology*. Frontiers Media SA, 5, p. 173. doi: 10.3389/fphar.2014.00173.

Plüddemann, A. *et al.* (2011) *Innate immunity to intracellular pathogens: macrophage receptors and responses to microbial entry*, *Immunological Reviews*. Available at: https://onlinelibrary.wiley.com/doi/pdf/10.1111/j.1600-065X.2010.00989.x (Accessed: 23 June 2019).

Pollard, J. W. (2009) 'Trophic macrophages in development and disease', *Nature Reviews Immunology*. Nature Publishing Group, 9(4), pp. 259–270. doi: 10.1038/nri2528.

Praußе, M. T. E. *et al.* (2018) 'Predictive virtual infection modeling of fungal immune evasion in human whole blood', *Frontiers in Immunology*. Frontiers Media SA, 9(MAR), p. 560. doi: 10.3389/fimmu.2018.00560.

Read, S. A. *et al.* (2017) 'Zinc is a potent and specific inhibitor of IFN-λ3 signalling.', *Nature communications*. Nature Publishing Group, 8, p. 15245. doi: 10.1038/ncomms15245.

Recalcati, S. *et al.* (2010) 'Differential regulation of iron homeostasis during human macrophage polarized activation', *European Journal of Immunology*. John Wiley & Sons, Ltd, 40(3), pp. 824–835. doi: 10.1002/eji.200939889.

Rink, L. and Haase, H. (2007) 'Zinc homeostasis and immunity.', *Trends in immunology*. Elsevier, 28(1), pp. 1–4. doi: 10.1016/j.it.2006.11.005.

Roche, B. *et al.* (2013) 'Reprint of: Iron/sulfur proteins biogenesis in prokaryotes: Formation, regulation and diversity', *Biochimica et Biophysica Acta (BBA) - Bioenergetics*. Elsevier, 1827(8–9), pp. 923–937. doi: 10.1016/J.BBABIO.2013.05.001.

Van Rompaey, L. *et al.* (2011) *GLPG0634 J ki i hibit f th GLPG0634 a Janus kinase inhibitor for the GLPG0634, a Janus kinase inhibitor for the GLPG0634, a Janus kinase inhibitor for the f h id h i i treatment of rheumatoid arthritis treatment of rheumatoid arthritis treatment of rheuma*. Available at: www.glpg.com (Accessed: 8 July 2019).

Rusinova, I. *et al.* (2012) 'INTERFEROME v2.0: an updated database of annotated interferon-regulated genes', *Nucleic Acids Research*. Narnia, 41(D1), pp. D1040–D1046. doi: 10.1093/nar/gks1215.

Saijo, S. *et al.* (2010) 'Dectin-2 Recognition of α-Mannans and Induction of Th17 Cell Differentiation Is Essential for Host Defense against Candida albicans', *Immunity*. Cell Press, 32(5), pp. 681–691. doi: 10.1016/J.IMMUNI.2010.05.001.

Sanguinetti, M. *et al.* (2005) 'Mechanisms of azole resistance in clinical isolates of Candida glabrata collected during a hospital survey of antifungal resistance.', *Antimicrobial agents and chemotherapy*. American Society for Microbiology Journals, 49(2), pp. 668–79. doi: 10.1128/AAC.49.2.668-679.2005.

Schrettl, M. *et al.* (2004) 'Siderophore biosynthesis but not reductive iron assimilation is essential for Aspergillus fumigatus virulence.', *The Journal of experimental medicine*. The Rockefeller University Press, 200(9), pp. 1213–9. doi: 10.1084/jem.20041242.

Schroeder, B. O. and Bäckhed, F. (2016) 'Signals from the gut microbiota to distant organs in physiology and disease', *Nature Medicine*. Nature Publishing Group, 22(10), pp. 1079–1089. doi: 10.1038/nm.4185.

Seider, K. *et al.* (2011) 'The facultative intracellular pathogen Candida glabrata subverts macrophage cytokine production and phagolysosome maturation.', *Journal of immunology (Baltimore, Md. : 1950)*. American

Association of Immunologists, 187(6), pp. 3072–86. doi: 10.4049/jimmunol.1003730.

Sharma, V., Purushotham, R. and Kaur, R. (2016) 'The Phosphoinositide 3-Kinase Regulates Retrograde Trafficking of the Iron Permease CgFtr1 and Iron Homeostasis in Candida glabrata.', *The Journal of biological chemistry*. American Society for Biochemistry and Molecular Biology, 291(47), pp. 24715–24734. doi: 10.1074/jbc.M116.751529.

Shi, H. *et al.* (2008) 'A cytosolic iron chaperone that delivers iron to ferritin.', *Science (New York, N.Y.)*. American Association for the Advancement of Science, 320(5880), pp. 1207–10. doi: 10.1126/science.1157643.

Silva, B. and Faustino, P. (2015) 'An overview of molecular basis of iron metabolism regulation and the associated pathologies', *Biochimica et Biophysica Acta (BBA) - Molecular Basis of Disease*. Elsevier, 1852(7), pp. 1347–1359. doi: 10.1016/J.BBADIS.2015.03.011.

Silva, S. *et al.* (2012) '*Candida glabrata, Candida parapsilosis* and *Candida tropicalis* : biology, epidemiology, pathogenicity and antifungal resistance', *FEMS Microbiology Reviews*, 36(2), pp. 288–305. doi: 10.1111/j.1574-6976.2011.00278.x.

Singh, V., Ahmad, S. and Rao, G. S. (1994) 'Prooxidant and antioxidant properties of iron-hydroquinone and iron-1,2,4-benzenetriol complex. Implications for benzene toxicity', *Toxicology*. Elsevier, 89(1), pp. 25–33. doi: 10.1016/0300-483X(94)90130-9.

Smeekens, S. P. *et al.* (2013) 'Functional genomics identifies type I interferon pathway as central for host defense against Candida albicans', *Nature Communications*, 4(1), p. 1342. doi: 10.1038/ncomms2343.

Soares, M. P. and Hamza, I. (2016) 'Macrophages and Iron Metabolism.', *Immunity*. Elsevier, 44(3), pp. 492–504. doi: 10.1016/j.immuni.2016.02.016.

Soares, M. P. and Weiss, G. (2015) 'The Iron age of host-microbe interactions.', *EMBO reports*. EMBO Press, 16(11), pp. 1482–500. doi: 10.15252/embr.201540558.

Soe-Lin, S. *et al.* (2009) 'Nramp1 promotes efficient macrophage recycling of iron following erythrophagocytosis in vivo', *Proceedings of the National Academy of Sciences*. National Academy of Sciences, 106(14), pp. 5960–5965. doi: 10.1073/PNAS.0900808106.

Sow, F. B. *et al.* (2007) 'Expression and localization of hepcidin in macrophages: a role in host defense against tuberculosis', *Journal of Leukocyte Biology*, 82(4), pp. 934–945. doi: 10.1189/jlb.0407216.

Spellberg, B. *et al.* (2012) 'The Deferasirox-AmBisome Therapy for Mucormycosis (DEFEAT Mucor) study: a randomized, double-blinded, placebo-controlled trial.', *The Journal of antimicrobial chemotherapy*. Oxford University Press, 67(3), pp. 715–22. doi: 10.1093/jac/dkr375.

Srivastava, V. K., Suneetha, K. J. and Kaur, R. (2014) 'A systematic analysis reveals an essential role for high-affinity iron uptake system, haemolysin and CFEM domain-containing protein in iron homoeostasis and virulence in Candida glabrata', *Biochemical Journal*. Portland Press Limited, 463(1), pp. 103–114. doi: 10.1042/bj20140598.

Subramanian Vignesh, K. *et al.* (2013) 'Granulocyte Macrophage-Colony Stimulating Factor Induced Zn Sequestration Enhances Macrophage Superoxide and Limits Intracellular Pathogen Survival', *Immunity*. Cell

Press, 39(4), pp. 697–710. doi: 10.1016/J.IMMUNI.2013.09.006.

Subramanian Vignesh, K. *et al.* (2016) 'IL-4 Induces Metallothionein 3- and SLC30A4-Dependent Increase in Intracellular Zn(2+) that Promotes Pathogen Persistence in Macrophages.', *Cell reports*. NIH Public Access, 16(12), pp. 3232–3246. doi: 10.1016/j.celrep.2016.08.057.

Subramanian Vignesh, K. and Deepe, G. S. (2016) 'Immunological orchestration of zinc homeostasis: The battle between host mechanisms and pathogen defenses', *Archives of Biochemistry and Biophysics*. Academic Press, 611, pp. 66–78. doi: 10.1016/J.ABB.2016.02.020.

Sun, J. *et al.* (2004) 'Heme regulates the dynamic exchange of Bach1 and NF-E2-related factors in the Maf transcription factor network.', *Proceedings of the National Academy of Sciences of the United States of America*. National Academy of Sciences, 101(6), pp. 1461–6. doi: 10.1073/pnas.0308083100.

Taylor, K. M. *et al.* (2005) 'Structure-function analysis of a novel member of the LIV-1 subfamily of zinc transporters, ZIP14', *FEBS Letters*. John Wiley & Sons, Ltd, 579(2), pp. 427–432. doi: 10.1016/j.febslet.2004.12.006.

Tenopoulou, M. *et al.* (2007) 'Does the calcein-AM method assay the total cellular "labile iron pool" or only a fraction of it?', *The Biochemical journal*. Portland Press Ltd, 403(2), pp. 261–6. doi: 10.1042/BJ20061840.

Urban, C. F. *et al.* (2009) 'Neutrophil extracellular traps contain calprotectin, a cytosolic protein complex involved in host defense against Candida albicans.', *PLoS pathogens*. Public Library of Science, 5(10), p. e1000639. doi: 10.1371/journal.ppat.1000639.

Uzé, G. *et al.* (2007) 'The receptor of the type I interferon family.', *Current topics in microbiology and immunology*, 316, pp. 71–95. Available at: http://www.ncbi.nlm.nih.gov/pubmed/17969444 (Accessed: 5 July 2019).

Vale-Silva, L. A. and Sanglard, D. (2015) 'Tipping the balance both ways: drug resistance and virulence in Candida glabrata', *FEMS Yeast Research*. Narnia, 15(4). doi: 10.1093/femsyr/fov025.

Vidal, S. M. *et al.* (1996) 'Natural resistance to intracellular infections: Nramp1 encodes a membrane phosphoglycoprotein absent in macrophages from susceptible (Nramp1 D169) mouse strains.', *Journal of immunology (Baltimore, Md. : 1950)*. American Association of Immunologists, 157(8), pp. 3559–68. Available at: http://www.ncbi.nlm.nih.gov/pubmed/8871656 (Accessed: 3 July 2019).

Vieira, O. V, Botelho, R. J. and Grinstein, S. (2002) 'Phagosome maturation: aging gracefully.', *Biochemical Journal*. Portland Press Ltd, 366(Pt 3), p. 689. doi: 10.1042/BJ20020691.

Vignesh, K. S. *et al.* (2013) 'Zinc Sequestration: Arming Phagocyte Defense against Fungal Attack', *PLoS Pathogens*. Edited by J. Heitman. Public Library of Science, 9(12), p. e1003815. doi: 10.1371/journal.ppat.1003815.

Wagner, D. *et al.* (2005) 'Elemental analysis of Mycobacterium avium-, Mycobacterium tuberculosis-, and Mycobacterium smegmatis-containing phagosomes indicates pathogen-induced microenvironments within the host cell's endosomal system.', *Journal of immunology (Baltimore, Md. : 1950)*. American Association of Immunologists, 174(3), pp. 1491–500. doi: 10.4049/jimmunol.174.3.1491.

Wang, S.-C. *et al.* (2003) 'Severe Bacterial Infection in Transfusion-Dependent Patients with Thalassemia Major', *Clinical Infectious Diseases*. Narnia, 37(7), pp. 984–988. doi: 10.1086/378062.

Weinberg, E. D. (1975) 'Nutritional Immunity', *JAMA*. American Medical Association, 231(1), p. 39. doi: 10.1001/jama.1975.03240130021018.

White, M. F. and Dillingham, M. S. (2012) 'Iron–sulphur clusters in nucleic acid processing enzymes', *Current Opinion in Structural Biology*. Elsevier Current Trends, 22(1), pp. 94–100. doi: 10.1016/J.SBI.2011.11.004.

Winters, M. S. *et al.* (2010) 'Metallomic Analysis of Macrophages Infected with *Histoplasma capsulatum* Reveals a Fundamental Role for Zinc in Host Defenses', *The Journal of Infectious Diseases*. Narnia, 202(7), pp. 1136–1145. doi: 10.1086/656191.

Wisplinghoff, H. *et al.* (2004) 'Nosocomial Bloodstream Infections in US Hospitals: Analysis of 24,179 Cases from a Prospective Nationwide Surveillance Study', *Clinical Infectious Diseases*, 39(3), pp. 309–317. doi: 10.1086/421946.

Wrighting, D. M. and Andrews, N. C. (2006) 'Interleukin-6 induces hepcidin expression through STAT3.', *Blood*. American Society of Hematology, 108(9), pp. 3204–9. doi: 10.1182/blood-2006-06-027631.

Yamasaki, S. *et al.* (2007) 'Zinc is a novel intracellular second messenger', *The Journal of Cell Biology*. Rockefeller University Press, 177(4), pp. 637–645. doi: 10.1083/JCB.200702081.

Yang, Y., Zhu, Y. and Xi, X. (2018) 'Anti-inflammatory and antitumor action of hydrogen via reactive oxygen species', *Oncology Letters*. Spandidos Publications, pp. 2771–2776. doi: 10.3892/ol.2018.9023.

Van Zandt, K. E. *et al.* (2008) 'The iron export protein ferroportin 1 is differentially expressed in mouse macrophage populations and is present in the mycobacterial-containing phagosome.', *Journal of leukocyte biology*. The Society for Leukocyte Biology, 84(3), pp. 689–700. doi: 10.1189/jlb.1107781.

Zhang, X. *et al.* (2018) 'Bach1: Function, Regulation, and Involvement in Disease', *Oxidative Medicine and Cellular Longevity*. Hindawi Limited, 2018. doi: 10.1155/2018/1347969.